Strategies to optimize engineered tissue towards native human aortic valves

Strategies to optimize engineered tissue towards native human aortic valves

A catalogue record is available from the Eindhoven University of Technology Library

ISBN 978-90-386-1185-3

Cover design: Angelique Balguid

Printed by Universiteitsdrukkerij TU Eindhoven, Eindhoven, The Netherlands.

Strategies to optimize engineered tissue towards native human aortic valves

PROEFSCHRIFT

ter verkrijging van de graad van doctor
aan de Technische Universiteit Eindhoven,
op gezag van de Rector Magnificus, prof.dr.ir. C.J. van Duijn,
voor een commissie aangewezen door het College voor Promoties
in het openbaar te verdedigen op
dinsdag 12 februari 2008 om 16.00 uur

door

Angelique Balguid

geboren te Berkel en Rodenrijs

Dit proefschrift is goedgekeurd door de promotor:

Prof. Dr. Ir. F.P.T. Baaijens

Copromotoren:
Dr. C.V.C. Bouten
en
Dr. A. Mol

Het verschijnen van dit proefschrift werd mede mogelijk gemaakt door steun van de Nederlandse Hartstichting.

voor Jeroen
&
mijn ouders

Contents

Summary

Heart valve replacement is a common treatment of end-stage valvular diseases to restore functionality of the valve. Although conventional valve replacements by mechanical or biological prosthesis offer prosperous function, they are associated with risks that limit their success. An important shortcoming of all prosthetic valves is their inability to grow, adapt and repair, which is particularly relevant for treatment of pediatric and adolescent patients. The lack of these features in current prosthesis drives the multidisciplinary approach of tissue engineering as a promising technique to create living heart valve substitutes. The concept of tissue engineering is based on seeding autologous cells onto a carrier of biodegradable material (the scaffold). This construct of cells and scaffold is stimulated to grow and develop in a mimicked physiological environment. Implantations of tissue engineered valves have been performed successfully at the pulmonary position in animal models. However, engineered valves did not possess sufficient mechanical integrity for implantation at the aortic position. Therefore, a major challenge in tissue engineering is to create tissue structures that resemble properties of native tissues to ensure durable functioning and in-vivo survival.

For future human applications, one of the most important questions is: "How good is good enough for *in vivo* survival of tissue engineered heart valves?". The first objective of this work was to define qualitative and quantitative bench-marks for tissue engineered heart valves to determine when these valves qualify for implantation in patients. In this thesis these bench-marks were based on mechanical and structural characteristics of healthy human adult aortic valve leaflets. In native aortic valves, the collagen fiber architecture is the most prominent matrix component responsible for sustaining the load under high pressure conditions. Therefore, knowledge about the function of collagen in relation with the mechanical behavior of native heart valve tissue was an important research focus in the process to define bench-marks for tissue engineering.

The relation between mechanical properties and collagen organization was investigated on a global and local scale in human adult aortic valve leaflets. Mechanical properties obtained by tensile tests of the leaflets were correlated to the amount of collagen and cross-links. Collagen cross-links, but not the collagen amount, appeared highly correlated to tissue stiffness in human heart valve leaflets. With these findings, the relevance of collagen cross-links for the mechanical integrity of engineered tissues should be given particular attention. Furthermore, in heart valve tissue, it remained

unclear to what extent mechanical loading affects the collagen fibril morphology. To determine if local stresses affect the collagen fibril morphology (i.e. fibril diameter, its distribution, and fibril density), these parameters were investigated with transmission electron microscopy in adult human aortic valve leaflets. The mechanical behavior of human aortic valves was implemented in a computational model to predict the stress distribution in the valve leaflet during the diastolic phase of the cardiac cycle. The results showed that large tissue stress was associated with larger average fibril diameter, lower fibril density and wider fibril size distribution compared with low stress locations in the leaflets. These findings provide insight in the effect of mechanical loading on the collagen ultrastructure, and are valuable to optimize mechanical conditioning protocols for heart valve tissue engineering.

The second objective of this thesis was to improve the mechanical properties of engineered tissues towards values of healthy native human aortic valves, which was considered an objective bench-mark for tissue engineering. Two strategies were adopted in the tissue engineering protocol to achieve this. The first approach involved modification of the scaffold design to provide sufficient mechanical support to engineered tissues. The currently used scaffold material is a mesh of rapid degrading polyglycolic acid coated with poly-4-hydroxybutyrate (PGA-P4HB). This material degrades within weeks, and does not provide mechanical integrity after implantation. As some tissue engineering applications do require a prolonged period of mechanical support by the scaffold, the feasibility of a slow degrading polymer scaffold of electrospun poly-ε-caprolactone (PCL) was evaluated for cardiovascular tissue engineering, and compared with the PGA-P4HB scaffold. After optimization of the electrospun PCL scaffold, proper cell ingrowth and extracellular matrix biosynthesis were observed, while retaining elastic properties and mechanical integrity. PCL scaffolds appeared a promising alternative to PGA-P4HB scaffolds, specifically for tissue engineered blood vessels and the wall of an engineered heart valve, where prolonged mechanical support of the scaffold may be desired.

As a second approach, the growing engineered tissues were biochemically stimulated to enhance tissue formation and strengthen the tissue. After an evaluation of biochemical factors known to promote protein synthesis, hypoxia and insulin were chosen for the experiments. A physiologically relevant oxygen tension, being lower than currently used in tissue engineering approaches, and insulin supplements were applied to the growing heart valve tissues to enhance their strength. Both insulin and hypoxia were associated with enhanced matrix production and improved mechanical properties, however, a synergistic effect was not observed. Although the amount of collagen and cross-links in the engineered tissues were still lower than native adult human aortic valves, tissues cultured under hypoxic conditions reached native human aortic valve values of tissue strength and stiffness after four weeks of culture, and were up to twice the values of the normoxic controls. These results strongly indicate that oxygen tension is a key parameter to achieve native-based bench-mark values of tissue strength in engineered heart valves. Engineered tissues, based on rapid degrading scaffolds, of such strength have not been achieved up to now. These findings bring the potential use for systemic applications a step closer, and can be considered an important improvement in heart valve tissue engineering.

Chapter 1

General introduction

1.1 The aortic valve

1.1.1 Anatomy

Blood flow in the heart is controlled by four valves: the aortic valve, the pulmonary valve, the mitral valve and the tricuspid valve (figure 1.1(a)). The aortic valve is situated at the transition of the left ventricle and the aorta. It is composed of three thin half-moon shaped tissue flaps, referred to as leaflets or cusps, three sinuses and the aortic ring (figure 1.1(b)). The leaflets are passive soft tissue structures of less than a millimeter in thickness, each with a small swelling in the center called the nodule, and are attached to the aortic root at the fixed edge. Behind each leaflet the aortic wall expands to form dilated pouches, the sinuses of Valsalva. The coronary arteries that provide the heart muscle with oxygen-rich blood and nutrients, descend from two of the three sinuses. Schematics of the heart and the aortic valve are shown below.

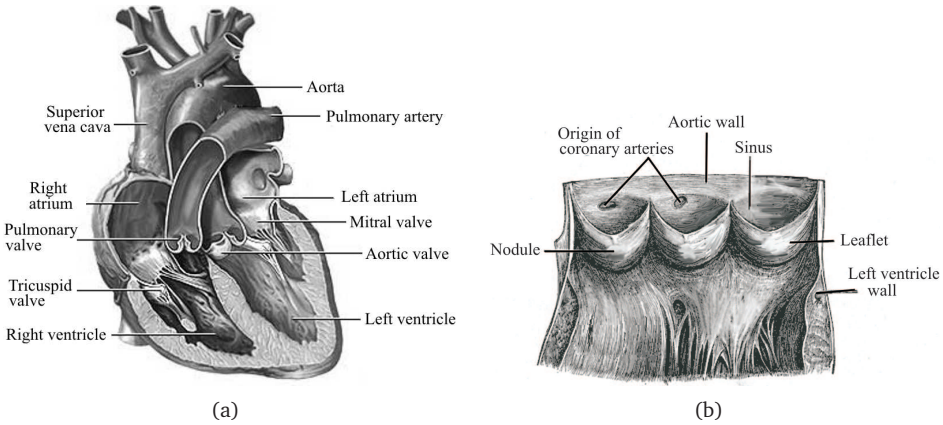

Figure 1.1: Schematics of the human heart and the aortic valve. a) Cross-section of the heart, anterior view, with the tricuspid valve and the mitral valve located at the outlets of the right, respectively, left atrium, and the pulmonary and aortic valve positioned at the outlet of the right, respectively, left ventricle (www.urac.org). b) The aortic valve, transected longitudinally, showing the three leaflets, the sinuses, the aortic and left ventricular wall. Adapted from Gray (1918)

1.1.2 Function

During the systolic phase of the cardiac cycle the left ventricle contracts, causing a rise in pressure (figure 1.2). When the pressure in the left ventricle exceeds the pressure in the aorta, the three cusps of the aortic valve are pushed aside to allow

passage of blood into the aorta. In healthy valves, the leaflets offer little impediment to flow. During diastole, relaxation occurs and the pressure in the left ventricle drops. Backflow of blood forces the valve to close and the cusps to coapt, preventing blood from flowing back into the left ventricle. During this phase, oxygen-rich blood flows into the left ventricle from the left atrium across the mitral valve, thus refilling the ventricle before the next contraction.
Two types of heart valve problems can disrupt blood flow through the valves: stenosis or regurgitation. A stenotic heart valve can not open completely, while regurgitation occurs when the valve is unable to close properly, allowing backflow of blood. Both conditions reduce the pumping efficiency of the heart, and may lead to heart failure.

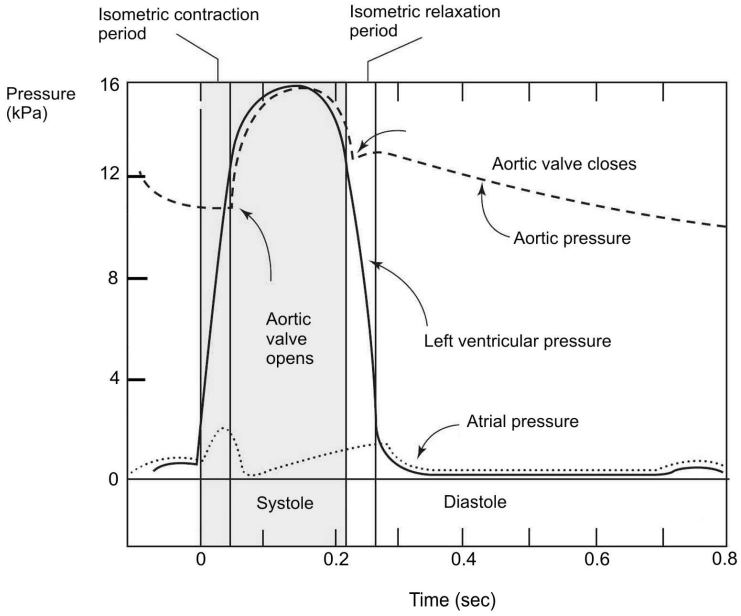

Figure 1.2: The pressure in the left ventricle rises during its contraction (systole). When the ventricular pressure exceeds the aortic pressure, the aortic valve opens and blood flows freely from the left ventricle into the aorta. Upon relaxation of the left ventricle, the ventricular pressure drops (diastole) and the backflow of blood forces the aortic valve to close.

1.1.3 Heart valve replacements

In case of heart valve disease or dysfunction, valve replacement may be necessary. Current valve prostheses include mechanical and biological valves. A mechanical heart valve is made of metal or synthetic materials, or a combination of the two. These valves can usually last a lifetime, but they have an increased risk of thrombo-

genic responses. Therefore, patients with mechanical valve prostheses need life-long anti-coagulation therapy. Even though this therapy is relatively safe, it involves increased risk of internal bleeding.
Biological valve prostheses are either of animal (xenografts) or of human origin (homografts). These valves undergo several chemical procedures, including preservative treatment and sterilization, to make them suitable for implantation in the human heart. In contrast to mechanical valves, biological valves do not require the use of anticoagulant drugs due to the improved blood flow dynamics, which results in lower thrombogenic risks. The main disadvantage of this type of valvular prosthesis is their limited lifespan. Bioprosthetic valves are prone to structural dysfunction due to tissue deterioration and calcification (Hopkins, 2005) and within 10 years of initial heart valve replacement, 50 - 60% of the patients will require re-operations (Bloomfield *et al.*, 1991; Hammermeister *et al.*, 2000).
Although conventional valve replacement therapies do offer prosperous function, they are associated with risks that limit their success (Grunkemeier and Rahimtoola, 1990; Schoen and Levy, 1999; Vara *et al.*, 2005). An important shortcoming of all prosthetic valves is their inability to grow, adapt and repair, which is particularly relevant for treatment of pediatric and adolescent patients. This drives the multidisciplinary approach of tissue engineering (TE) as a promising technique for heart valve substitutes. Up to now, TE heart valves did not possess sufficient mechanical integrity to adopt the function of a natural valve. To overcome this, a thorough understanding of the aortic valve tissue structure and its mechanical functioning is crucial.

1.1.4 Tissue structure and biomechanical behavior

Valvular tissue consists of cells embedded in a matrix of proteins and other macromolecules, the extracellular matrix (ECM). The three major types of biomolecules present in the ECM are structural proteins, specialized proteins, and proteoglycans. The structural proteins in the ECM, such as collagen and elastin, provide support and anchorage for cells. The specialized matrix proteins, such as fibrillin and fibronectin, engage interactions with cellular integrins, hence contributing to cell attachment and differentiation, cell shape and movement, and maintenance of tissue phenotype (Haralson and Hassell, 1996).
During the diastolic phase of the cardiac cycle, the transvalvular pressure across the aortic valve leaflets exceeds 11 kPa. This pressure difference generates large stresses within the leaflets. Considering this order of magnitude, it is quite remarkable that these thin flaps of delicate tissue are sufficiently strong to withstand these stresses. The complex layered tissue structure in the valve leaflet is responsible for its functionality. The aorta-facing fibrosa layer of the valve is composed predominantly of a dense network of collagen fibers (Schoen and Levy, 1999). The collagen network in the fibrosa is the strongest and stiffest portion of the leaflet (Driessen *et al.*, 2003a; Sacks *et al.*, 1997). The macroscopically visible inhomogeneous and circumferentially aligned fiber architecture in the tissue matrix (figure 1.3) is associated with the anisotropic mechanical properties of the leaflet (i.e. stiffer and stronger in circumferential, than in radial direction) (Sauren *et al.*, 1980; Billiar and Sacks, 2000a). The

collagen structure is responsible for bearing and distributing end-diastolic stresses over the leaflets and the transfer of stresses from the leaflets to the fibrous skeleton of surrounding sinuses and aortic wall (Driessen *et al.*, 2003a; Sacks *et al.*, 1997; Broom, 1988).

The movement of the aortic valve during the cardiac cycle depends on the contri-

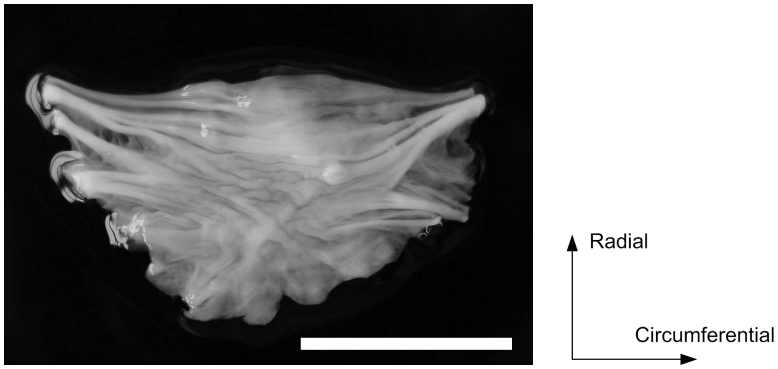

Figure 1.3: Matrix structure of an aortic valve leaflet. Originating at the commisures, connective tissue bundles run nearly parallel with the free leaflet margin. The white bar represents a scale of 1 cm.

bution of its three different layers (figure 1.4). The layers are very mobile and can easily compress and shear during leaflet flexure as the valve opens and closes. The three-layered structure assures both low flexural rigidity, necessary to allow normal valve opening and non-obstructed passage of blood in the aorta, as well as high tensile strength required to resist transvalvular pressures (Langdon, 1999; Sacks *et al.*, 1998). The central spongiosa is composed of loosely arranged collagen and an abundant amount of glycosaminoglycans (GAGs). GAGs are covalently bound to matrix proteins to form proteoglycans. Due to their high viscosity and low compressibility, GAGs in the spongiosa form a shock and shear absorbing layer. On the other hand, their rigidity provides structural integrity to the cells and allows cell migration due to providing the passageways between cells.

The ventricularis layer is situated at the ventricular side of the valve leaflet and consists mainly of elastin with radially aligned elastic fibers. Elastin is primarily responsible for generating the preload in the ventricularis. Elastin fibers maintains the collagen fibre architecture in its neutral state (Mendelson and Schoen, 2006), and are thought to function as a 'return-spring mechanism', restoring the contracted configuration after stretching of the valve leaflet. During stretching, in the first part of the diastolic phase, elastin fibers carry a fraction of the load while collagen fibers extend and uncrimp. However, near full closure, when collagen has fully unfolded, the load-bearing element shifts from elastin to collagen (Schoen, 1997). The preloaded configuration of the fibrosa and ventricularis is associated with their attachment to each other; the fibrosa under compression and the ventricularis under tension (Vesely,

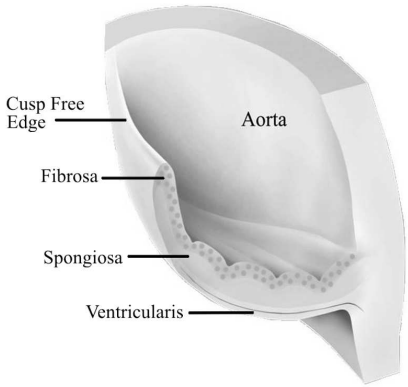

Figure 1.4: Schematic of the three layered structure in the aortic valve leaflet. These are the ventricularis, the spongiosa, and the fibrosa layer.

1998).

1.2 Collagen

In heart valves, like in many tissues, collagen is the most prominent load bearing component of the extracellular matrix. It is responsible for structural integrity and provides resistance to tensile strength (Hulmes, 2002; Kadler, 1995). The collagens are synthesized by myofibroblasts, the valvular interstitial cells (VICs). With growth, maturation and ageing, continuous remodeling and repair of the tissue matrix is essential to withstand mechanical fatigue. Collagen contents gradually increase from early to late fetal stages up to a constant level (Aikawa *et al.*, 2006). With ageing, decreasing collagen contents have been observed in adults (McDonald, 2002; Bashey *et al.*, 1967), accompanied by a decrease in the extensibility of the heart valve leaflet (Christie and Barratt-Boyes, 1995).

To understand the functioning of collagen in valvular tissue, it is necessary to investigate the collagen architecture at different microscopical levels (figure 1.5). Collagen fibers are composed of fibril bundles, which in turn consist of units of five collagen triple helical molecules staggered together; the microfibrils (Sung, 2003). The individual tropocollagen units, 1.5nm in diameter and 300nm in length are made up of three helical chains. The polypeptide chains are stabilized by intra- and intermolecular hydrogen bonds, the cross-links. Structural integrity of tissues is achieved by collaboration of all the levels in the collagen architecture.

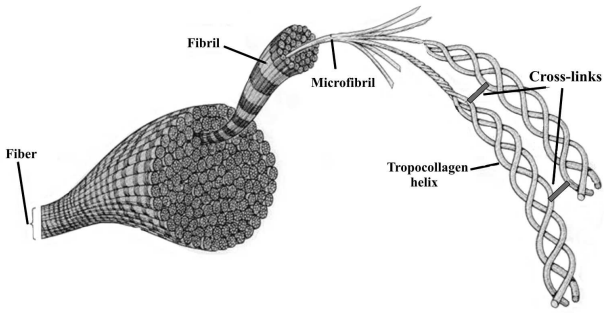

Figure 1.5: The hierarchical structure of collagen from the triple helical collagen molecule to a collagen fiber.

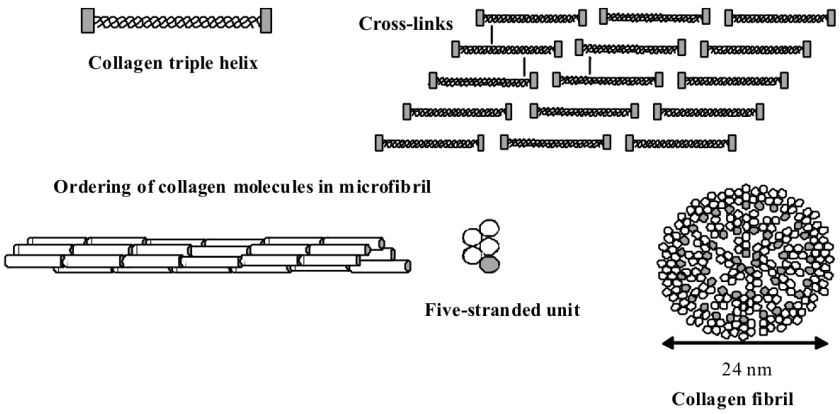

Figure 1.6: Molecular structure of the fibril. The basic unit of the fibril, the microfibril is composed of five collagen molecules. These collagen molecules aggregate into a staggered parallel array creating overlap. These microfibrils are aggregated in a distinct pattern to form collagen fibrils.

1.2.1 Molecular structure

Variations in the amino acid sequence of the α-chains result in structural components that are the same size (approximately 1000 amino acids), but with slightly different properties. These α-chains are combined to form the various types of collagen. Collagen type I and III are the most abundant types in heart valves. These collagens are classified as the fibrous collagens, along with type II, V and XI. Collagen type I

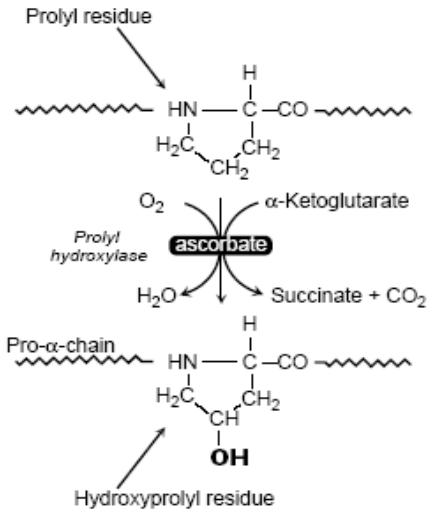

(a) Hydroxylation of prolyl residues of pro-α-chains of collagen by prolyl hydroxylase

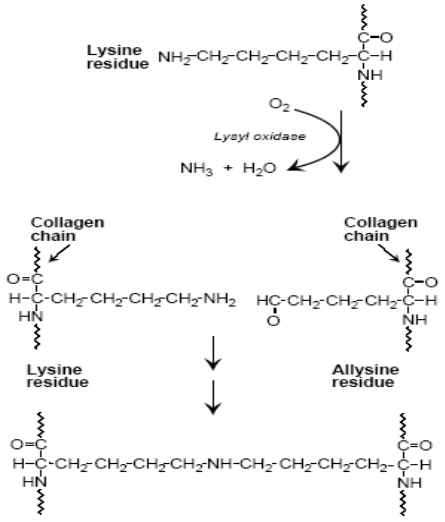

(b) Formation of cross-links in collagen.

Figure 1.7: Chemical reactions involved in fiber formation of collagen. a) Ascorbic acid, oxygen and α-ketoglutarate hydroxylate the proline and lysine residues of the α-chains, allowing triple helix formation of the α-chains. b) Lysyl oxidase oxidatively deaminates a lysine residue of a collagen triple helix. This allows the formation of a divalent enzymatic cross-link with another collagen molecule (adapted from Champe and Harvey (1994)).

consists of two identical chains (α1) and one different chain (α2) which is denoted as $[\alpha 1(I)]_2\alpha 2$ (Bailey *et al.*, 1998). It is the only heteropolymer among collagens (Hulmes, 2002). The primary structure of collagen is a repetitive sequence of a small glycine residue and an X and Y group (-Gly-X-Y-), where X is frequently proline and Y is often proline or lysine. Glycine is small enough to fit into the restricted space where the three chains of the helix come together. The α-chains are synthesized in the rough endoplasmic reticulum after which they are processed by a number of enzymic steps. The proline and lysine residues are hydroxylated to form hydroxyproline and hydroxylysine residues. These hydroxylation reactions require prolyl and lysyl hydroxylase, respectively, molecular oxygen and a reducing agent, such as ascorbic acid (figure 1.7(a)). Hydroxyproline functions as a stabilizing factor in the triple-helical structure of collagen.

After hydroxylation, pro-α-chains form procollagen, a precursor of collagen that has a central region of triple helix flanked by the non-helical amino- and carboxyl-terminal extensions called propeptides. The formation of procollagen begins with disulfide bonding between the C-terminal extensions of the pro-α-chains. This brings

the three chains into an alignment favorable for the helix formation. The procollagen molecules are translocated to the Golgi apparatus, where they are entrapped in secretory vesicles. These vesicles fuse with the cell membrane, causing a release of the procollagen molecules into the extracellular space. The N- and C-terminal of the procollagen molecules are subsequently cleaved by N- and C-procollagen peptidase to release the triple-helix collagen molecule and allow fibril formation. Construction of collagen fibrils occurs by spontaneous association of the molecules. They form an ordered, overlapping, parallel array, with adjacent collagen molecules arranged in a staggered pattern to form a five-stranded unit (figure 1.6). The five-stranded microfibril accounts for a substructure, which can then continue to grow by lateral and end-to-end aggregation (Hulmes, 1992, 2002).

1.2.2 Cross-linking between collagen molecules

The formation of covalent intramolecular and intermolecular crosslinks is the final step in collagen biosynthesis that occurs as an extracellular process after cleavage of the propeptides and fibril assembly. The conversion of lysine into a hydroxylysine is catalyzed by lysyl hydroxylase. The lysine and hydroxylysine residues in collagen molecules serve as a substrate for lysyl oxidase. This copper dependent extracellular enzyme oxidatively deaminates some of the lysyl and hydroxylysyl residues in collagen (Siegel, 1976). The resulting reactive aldehydes can condense with lysyl or hydroxylysyl residues in other collagen molecules to form di- and tri-functional covalent cross-links between the collagen molecules (figure 1.7(b)) (Champe and Harvey, 1994). These crosslinks stabilize the staggered array of the collagens in the fibril, and are essential in providing the tensile strength and mechanical stability of the collagen fibrils and other supramolecular assemblies (Hulmes, 1992). Moreover, the presence of mature cross-links makes collagen fibers less suspectible for enzymatic degradation (Paul and Bailey, 2003). Mature cross-links in collagen fibers are based on trivalent 3-hydroxypyridinium residues. Two chemical forms of this type of cross-link have been identified, hydroxylysylpyridinoline (HP), derived from three hydroxylysyl residues, and lysylpyridinoline (LP), derived from two hydroxylysyl and one lysyl residue. The ratio between these two pyridinium cross-links varies between different tissue types. HP is predominant in highly hydroxylated collagens, such as type I collagen in heart valves, LP is found primarily in calcified tissues (Bailey *et al.*, 1998).

1.2.3 Influencing collagen and cross-link synthesis

The structural development of collagen is regulated *in vivo* by a cascade of growth factors, enzymes and other biochemical compounds. Table 1.2.3 presents an overview of various bioactive factors and their mechanism of altering the collagen structure. Some of these factors are described in more detail below.
Human TGF-β1 is a dimeric protein composed of two identical chains of amino acids, which controls cell proliferation and differentiation. As a mediator in tissue repair it stimulates the production of new matrix proteins such as collagens, fibronectin, and proteoglycans. In addition, it also inhibits the synthesis of proteases and stimulates

the synthesis of protease inhibitors leading to suppression of matrix degradation (Lijnen *et al.*, 2003). TGF-β1 was reported to induce an increase in alpha-smooth muscle actin, a marker of myofibroblasts, associated with an increase in collagen deposition by higher gene transcription per cell(Kubota *et al.*, 2003). TGF-β1 further enhances the expression of lysyl hydroxylase, a cross-linking enzyme (van der Slot *et al.*, 2005). Low oxygen tension, or hypoxia, was reported to increase ECM production by various fibroblast cell types (Durmowicz *et al.*, 1994; Falanga *et al.*, 2002; Chen *et al.*, 2005). Increases were observed both at the mRNA and protein level in fibronectin, collagen I and collagen IV. Interestingly, it was demonstrated that the upregulation of Col1α mRNA levels failed to occur in fibroblasts from TGF-β1 knock-out mice (Falanga *et al.*, 1993, 2002). This suggested that low oxygen tension stimulates collagen synthesis and Col1α transcription through the action of TGF-β1. Hypoxia was also reported to increase the mRNA and protein levels of prolyl and lysyl hydroxylase, which may improve collagen cross-linking.
Insulin is a polypeptide hormone that regulates certain biological processes like protein turnover and glucose transport. Insulin is known for its upregulating effect of procollagen mRNA, as well as the stimulation of latent TGF-β1 synthesis (Neidert *et al.*, 2002). Moreover, insulin was reported to act as inhibitor for collagen degrading enzymes, collagenases, in dermal fibroblasts (Lam *et al.*, 2004).
By influencing the collagen synthesis, organization or cross-linking through direct or indirect pathways, some of the bioactive factors of table 1.2.3 are known to affect the mechanical properties of a tissue. For example, the addition of insulin and TGF-β1 in tissue culture medium was reported to enhance the tissue strength in engineered tissues (Neidert *et al.*, 2002; Ross and Tranquillo, 2003). Conversely, the inhibition of lysyl oxidase by β-aminopropionitrile is known to have a profound effect on the fragility of collagenous tissues, due to the reduction in cross-linking (Bailey *et al.*, 1998; Brightman *et al.*, 2000).

1.3 Heart valve tissue engineering

1.3.1 The tissue engineering paradigm

Tissue engineering, as stated by Langer and Vacanti (1993), is an interdisciplinary field that applies the principles of engineering and life sciences toward the development of biological substitutes that restore, maintain, or improve tissue function or a whole organ.
Figure 1.8 shows the paradigm of heart valve tissue engineering. The general concept of tissue engineering involves cell donation by the patient that will eventually receive an autologous engineered valve. For heart valve TE myofibroblast cells, originating from the saphenous vein, have shown to be a suitable cell source (Schnell *et al.*, 2001). This cell type is known for its ability to actively remodel ECM and its relatively high ECM protein expression (Merryman *et al.*, 2006). The cells are seeded onto a scaffold, a temporary artificial matrix of a natural or synthetic polymer, in the shape of a heart valve.

Factor	Influence on collagen synthesis	Influence on collagen cross-linking	References
TGF-β1	+ increased cell population with activated proα2(I) collagen promoter and accelerating gene transcription per cell	+ increases lysyl oxidase enzyme activity	Centrella *et al.* (1992); Kinbara *et al.* (2002); Shanley *et al.* (1997)
TGF-β2	+ increased cell population with activated proα2(I) collagen promoter		Kinbara *et al.* (2002)
TGF-β3	+ increased activated proa2(I) collagen promoter per cell - Reduced collagen I fiber accumulation by induced expression of MMP-9		Kinbara *et al.* (2002); Hosokawa *et al.* (2003)
Ascorbic Acid		+ increased activity of prolyl and lysyl hydroxylase	Kivirikko and Pihlajaniemi (1998); Phillips *et al.* (1994)
α-ketoglutarate		+ increased activity of prolyl and lysyl hydroxylase	Kivirikko and Pihlajaniemi (1998)
Hypoxia	+ stimulates collagen production	+ (increased activity of prolyl and lysyl hydroxylase)	Kivirikko and Pihlajaniemi (1998); Horino *et al.* (2002); Chen *et al.* (2005); Brinckmann *et al.* (2005)
Coenzym A	+ by increased gene expression of α1 chain and enhancing prolyl hydroxylase activity	- no stimulation of lysyl oxidase and hydroxylase	Mio *et al.* (2001)
Copper		+ by acting as a co-factor for the enzyme lysyl oxidase	Dahl *et al.* (2005); Harris *et al.* (1980)
β-amino-propionitrile	Increases coll. synth + fibril diameter	Inhibiting effect on lysyl oxidase and cross-linking	Wong *et al.* (2002); Beekman *et al.* (1997)
Interleukin-4	+ promotes collagen I production	Increases gene expression of LH2	Martelli-Junior *et al.* (2003); Brinckmann *et al.* (2005)
Insulin-like Growth factor 1 (IGF-1)	promotes collagen synthesis		Jenniskens *et al.* (2006)
Insulin	increases procollagen synthesis, upregulate TGF-β1		Neidert *et al.* (2002); Ross and Tranquillo (2003)

Table 1.1: Overview of collagen and collagen cross-link regulating (bio)chemical factors and their mechanisms.

The cell seeded scaffold, or construct, is placed in a bioreactor, a system that simulates the physiological environment, and promotes tissue formation and development. Tissue development can be enhanced by applying mechanical loading or biochemical stimuli to the construct in a bioreactor. After several weeks of tissue development and remodeling, the newly formed autologous TE valve can be, ideally, implanted in the patient.

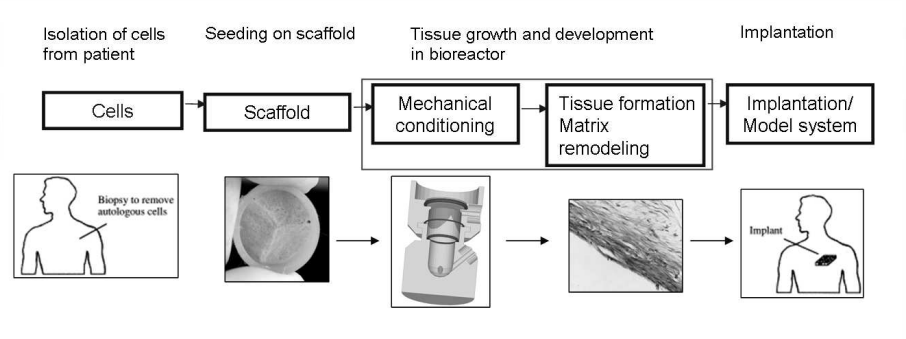

Figure 1.8: The tissue engineering paradigm. Cells are isolated from a patient, seeded on a polymer scaffold, and placed in a bioreactor to enhance tissue formation and remodeling by mechanical and biological cues. After several weeks the autologous valve can be implanted in the patient.

1.3.2 Current status and strategies

TE ovine heart valves have been successfully implanted in the pulmonary position in sheep, showing a native-resembling function and tissue composition after five months (Hoerstrup *et al.*, 2000). Mol *et al.* (2006) succeeded in fabricating human TE valves based on a rapid degrading polymer scaffold that could withstand physiological systemic pressures up to four hours in an *in vitro* setup, and showing anisotropic properties after 4 weeks of culturing in a bioreactor. Though these results are promising, tissue stiffness and strength may not be sufficient for systemic applications. To ensure durability, the quality and integrity of the tissue need further development.
During the TE process the scaffold initially provides structural integrity to the construct, while the cells produce their own natural matrix. Due to continuous changes in the constructs composition, associated with tissue growth, remodeling and scaffold degradation, the mechanical properties of the engineered valve are variable during the culture period. Initially, the scaffold is responsible for the mechanical resilience of the construct. The gradual breakdown of the scaffold decreases this resilience, while the natural ECM increasingly takes over this function. Two possible strategies to ensure sufficient mechanical integrity of the engineered tissue prior to implantation can be 1) the choice of scaffold material, or 2) enhancing tissue development during the

culture period (see figure 1.9).

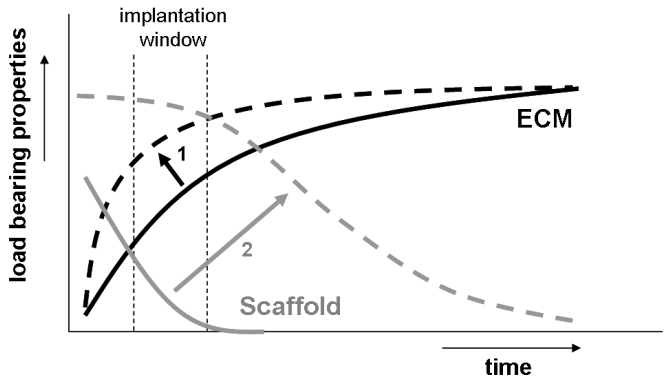

Figure 1.9: Strategies to alter the relative contributions of the scaffold and newly formed tissue to load bearing properties of TE constructs. These improvement strategies can either focus on 1) promoting tissue development by biochemical or mechanical stimuli or 2) designing a stronger and slower degrading scaffold.

The scaffold material must satisfy a number of requirements. These include biocompatibility, biodegradation to non toxic products, processability to complicated shapes, ability to support cell growth and proliferation, appropriate mechanical properties, as well as maintaining mechanical strength during the tissue regeneration process (Gunatillake and Adhikari, 2003). Furthermore, a high porosity and an adequate pore size are necessary to facilitate cell seeding throughout the whole structure. The structure of a scaffold should provide an environment where cells can easily attach, while allowing cell migration and the diffusion of biochemical factors and nutrients. The rate of scaffold degradation depends on the type of polymer used. For example, polyglycolic acid (PGA) is a rapid degrading polyester, which looses its mechanical integrity within weeks (Hoerstrup *et al.*, 2002). Poly-ε-caprolactone (PCL), on the other hand, is a slow degrading polyester, which will retain its mechanical properties for months (Hoglund *et al.*, 2007). Both scaffold materials have their advantages; PGA will be degraded by the time of implantation in patients, allowing implantation of autologous tissue. PCL, on the other hand, would remain present for a considerable time after implantation. This could be beneficial if mechanical support is needed after implantation.

Enhancing tissue development, in terms of quality and mechanical integrity, can be controlled by environmental stimuli of mechanical or biochemical nature. Mechanical loading by cyclic straining was reported to have a stimulating effect on tissue

stiffness and strength, and matrix biosynthesis of engineered constructs (Mol *et al.*, 2003). Furthermore, the effect of strain magnitude, as well as the choice for either a continuous or intermittent cyclic loading protocol is known to have an influence on the constructs' composition and mechanical properties (Boerboom, 2007).
The mechanical integrity of engineered tissue may also be improved by biochemical cues. Several growth factors, enzymes and (bio)chemical compounds are known to influence the synthesis of collagen, collagen fibril thickness or the cross-linking pathways by influencing cell metabolism, gene transcription or protein expression (table 1.2.3). A different approach is to enhance tissue stiffness by cross-linking the extracellular matrix. For example, glycation due to elevated glucose and ribose concentrations in cell culture medium was reported to stiffen and strengthen arterial tissue equivalents, by glycose-mediated pentosidine cross-links (Bailey *et al.*, 1998), and to increase their resistance to collagenolytic degradation (Girton *et al.*, 1999). Besides this non-enzymatic mechanism of cross-linking, the effectiveness of copper-dependant cross-linking enzymes in cells may be upregulated by supplementing the medium with copper. Although this method of additional cross-linking of collagen may provide collagen fibril stability and resistance to proteolysis, it was not shown to enhance global tissue strength of engineered vessels (Dahl *et al.*, 2005).

1.4 Objective and Outline

One of the main challenges in the field of heart valve tissue engineering is to approach native human tissue, in terms of mechanical integrity and tissue composition. A thorough understanding of the biomechanical behavior of the native aortic heart valve, and its relation with the tissue architecture, is therefore crucial to further progress in this field. Moreover, objective criteria and regulations for TE products are not available to determine when TE tissue qualifies for implantation in patients. These criteria should be based on native aortic valves, to serve as target values on which TE strategies can focus, either by scaffold design, or environmental cues.
The objective of this work was twofold:

- Developing bench-marks for tissue engineering by investigating the biomechanical behavior of human aortic valve leaflets, and its dependence on the collagen architecture *(Chapters 2 & 3)*.
- Aim for native valve characteristics in engineered tissues through two pathways: scaffold design *(Chapter 4)* and the application of environmental stimuli *(Chapter 5)*.

Regarding the first objective, the collagen structure in human aortic valves was investigated on a molecular and ultrastructural level. In Chapter 2 collagen parameters were correlated with mechanical characteristics of the tissue. Chapter 3 describes the use of the mechanical properties as measured in human aortic valves for a computational model to estimate local stresses in the valve leaflet. The collagen fibril morphology, in terms of fibril diameter and its distribution, was investigated in the valve leaflet and correlated to the level of stress predicted by a computational model.

Subsequently, two strategies to improve the mechanical integrity of the engineered tissue were described. Chapter 4 evaluates the implications of scaffold material and design on cell seeding efficiency and tissue development. In Chapter 5 the individual and combined potential of environmental cues (low oxygen tension and the insulin supplemented medium) on tissue development was evaluated. Chapter 6 presents a general discussion and conclusions based on the findings of the presented studies.

Chapter 2

The relation between collagen structure and biomechanical behavior of human aortic valve leaflets

The contents of this chapter are based on A. Balguid, M. P. Rubbens, A. Mol, R. A. Bank, A. J. J. C. Bogers, J. P. van Kats, B. A. J. M. de Mol, F. P. T. Baaijens and C. V. C. Bouten (2007), *The Role of Collagen Cross-Links in Biomechanical Behavior of Human Aortic Heart Valve Leaflets Relevance for Tissue Engineering*, Tissue Engineering; **13**(7): pp 1501-1511.

2.1 Introduction

Worldwide approximately 275,000 heart valve replacement surgeries are performed annually as a result of heart valve disease (Rabkin and Schoen, 2002). Although conventional valve replacement therapies do offer prosperous long-term function, they are associated with significant risks that limit their success (Harken *et al.*, 1962; Grunkemeier and Rahimtoola, 1990; Jamieson, 1993; Jr. *et al.*, 1996; Schoen and Levy, 1999; Vara *et al.*, 2005). An important shortcoming of prosthetic valves is their inability to grow, adapt and repair, which is particularly relevant for pediatric patients. This drives the multidisciplinary approach of tissue engineering (TE) as a promising technique for heart valve substitutes. In this approach, autologous cells are used to make living tissue to replace the damaged or diseased native heart valves (Schenke-Layland *et al.*, 2004; Vara *et al.*, 2005).
TE heart valves have been successfully implanted in the pulmonary position in sheep, showing a native-resembling function and tissue composition after 5 months (Hoerstrup *et al.*, 2000). Mol *et al.* (2006) succeeded in the fabrication of tissue engineered valves based on a rapid degrading polymer scaffold that could withstand physiological systemic pressures up to 4 hours in an in-vitro setup, and showing developing anisotropic properties after 4 weeks of culturing in a bioreactor. In view of these recent developments in the field of TE heart valves a comparison between TE and native valves is necessary. Criteria are needed to determine when TE tissue can be qualified as good enough for future implantations in patients. A detailed understanding of the matrix architecture and biomechanical function of the native aortic heart valve, as well as their interdependence, is therefore crucial to further progress in this field. Aortic heart valves are remarkably adapted to allow unidirectional and non-obstructed passage of blood in the aorta. The inhomogeneous matrix structure of the aortic valve leaflets is macroscopically visible in their fiber architecture (figure 2.1). The biomechanical behavior of the aortic valve during the cardiac cycle depends on the contribution of its three different layers. The ventricularis layer is situated at the ventricular side of the valve leaflet and consists mainly of collagen and elastin fibers. The middle spongiosa layer largely consists of proteoglycans, and the aorta-facing fibrosa layer of the valve is composed predominantly of a dense network of collagen fibers. This three-layered structure assures low flexural rigidity, necessary to allow normal valve opening, and high tensile strength required to resist transvalvular pressures (Sacks *et al.*, 1998). The collagen network in the fibrosa is the strongest and stiffest portion of the leaflet, and therefore largely responsible for bearing and distributing end-diastolic stresses over the leaflets (Sacks *et al.*, 1997; Driessen *et al.*, 2003a). Elastin fibers in the ventricularis are thought to function as a 'return-spring mechanism' which restores the contracted configuration following the stretch of the valve leaflet induced by diastole. During stretching, in the first part of the diastolic phase, elastin fibers carry a fraction of the load while collagen fibers extend and uncrimp. However, near full closure, when collagen has fully unfolded, the load-bearing element shifts from elastin to collagen (Schoen and Levy, 1999). The circumferentially oriented collagen network allows much higher stiffness in circumferential direction than in radial direction of the leaflets, as was demonstrated by

biaxial tensile tests on porcine aortic valves (Yacoub *et al.*, 1999). To ensure long-term function, mimicking this collagen architecture might be essential in heart valve TE, in particular when facing systemic applications. In heart valves, like in many tissues, collagens are the main structural proteins responsible for structural integrity and biomechanical strength, predominantly tensile strength (Kadler, 1995; Hulmes, 2002). How the collagen architecture contributes to biomechanical behavior of heart valves under high pressure conditions is not clear. Due to limited availability of fresh material and proper test environments, biomechanical characterization of human aortic valves has been sparsely performed (Clark, 1973; Stradins *et al.*, 2004) and the results were not correlated to structural properties. Available studies on structure-function relationships have mainly focused on the role of elastin and were performed on porcine aortic valves (Schoen, 1997; Vesely, 1998). Due to species differences, extrapolation of such results to human valves is delicate. Several studies have been conducted to investigate matrix composition and collagen architecture in healthy and diseased human and animal aortic valves. These concern histological examinations of collagen organization (Sauren *et al.*, 1980; Kunzelman *et al.*, 1993; McDonald, 2002; de Lange *et al.*, 2004; Schenke-Layland *et al.*, 2004), quantitative evaluation of the amounts and types of collagen (Bashey *et al.*, 1967; Lis *et al.*, 1987) and quantitative fiber bundle morphology (Doehring *et al.*, 2005). Interestingly, collagen architecture in heart valves seems age-dependent. With growth and maturation, collagen contents gradually increase from early to late fetal stages up to a constant level (Aikawa *et al.*, 2006). With ageing, decreasing collagen contents have been observed in adults (Bashey *et al.*, 1967; McDonald, 2002), accompanied by a decrease in the extensibility of the heart valve leaflet (Christie and Barratt-Boyes, 1995). Apart from collagen content, changes in collagen type or collagen fibril size have been proposed to influence heart valve biomechanics with age (Christie and Barratt-Boyes, 1995). Research in skin has demonstrated that with age mechanical tissue strength and stiffness increase along with an increased intermolecular collagen cross-link concentration (Avery and Bailey, 2005). Furthermore, in bone tissue a correlation was found between collagen cross-linking and biomechanical properties (Banse *et al.*, 2002). Although bone is structurally different from cardiovascular tissues, this illustrates the relevance of cross-links in enhancing collagen fibril stability and strength. A similar correlation might be expected for heart valve tissue. The objective of this study is to investigate structure-function relationships in human aortic heart valve leaflets, with special emphasis on collagen content and cross-link concentration. Correlations between these structural properties and biomechanical parameters are examined in both native and engineered leaflet tissue to further optimize tissue engineering of heart valves.

2.2 Materials and methods

2.2.1 Specimen preparation

Native human valves

Nine healthy human donor aortic valves (6 female, 3 male, mean age 48.9 $\pm$ 11.4 years) were obtained from the Rotterdam Heart Valve Bank at the Erasmus University Medical Center, Rotterdam, The Netherlands. The cause of death of the donors did not involve aortic valve disease, or other conditions known to precede aortic valve diseases. Prior to donation, none of the donors or their relatives objected to experimental use of the cardiovascular tissue following explantation. Upon dissection, the valves were stored at 4°C and biomechanical experiments were conducted at room temperature within 24 hours.

TE constructs

Scaffold preparation, cell culture, and cell seeding procedures were performed as described previously (Mol *et al.*, 2005b). Briefly, rectangular strips (5$\times$35$\times$1 mm) of rapid degrading non-woven poly-glycolic acid meshes (PGA; Cellon, Luxembourg) were coated with a thin layer of poly-4-hydroxybutyrate (P4HB; TEPHA Inc., Cambridge, USA). The strips were attached to flexible membranes in 6-well plates (Flexcell Int., McKeesport, USA) and seeded with human venous myofibroblasts using fibrin as a cell carrier (Mol *et al.*, 2005a). The cell-seeded scaffolds are further referred to as TE constructs. After five days of static culture, the TE constructs were divided into two groups to obtain a larger variance in matrix and biomechanical properties and cultured for three additional weeks. One group of constructs (*static*, n = 5) was not strained by external load. The other group (*dynamic*, n = 5) was subjected to 4% uniaxial dynamic straining at a physiologically relevant frequency of 1 Hz using a Flexcell Fx-4000T straining device (Flexcell Int. McKeesport, USA).

2.2.2 Biomechanical testing and matrix analysis

Biomechanical testing

To investigate the biomechanical characteristics of the native tissue, each valve was subjected to uniaxial tensile tests in two directions (figure 2.1b): strips of one valve leaflet in circumferential direction (each strip was 3 mm wide, n = 3-4 strips per valve) and strips of another leaflet in radial direction (n = 3-5 strips per valve). The tensile tests were performed on confined strips, meaning that the ends of the strips were clamped, not allowing translational movement between the layers of the leaflet. The thickness of the leaflet strips was measured using a Digimatic Micrometer (Mitutoyo America Corporation, Aurora, USA). Tensile tests were performed on a custom-built tensile tester, equipped with a 20 N load cell. Stress-strain curves were obtained at a strain rate of the initial length per minute (l_0/min). From the curves the ultimate tensile stress (UTS) and maximum strain at break (ε_{max}) were determined. The slope

of the linear part of the curve represented the modulus of elasticity (further referred to as modulus) of the tissue. Data were averaged per valve leaflet. Anisotropic properties were defined as differences between the moduli in the two directions.
The biomechanical properties of the tissue engineered constructs in the loading direction were determined similarly.

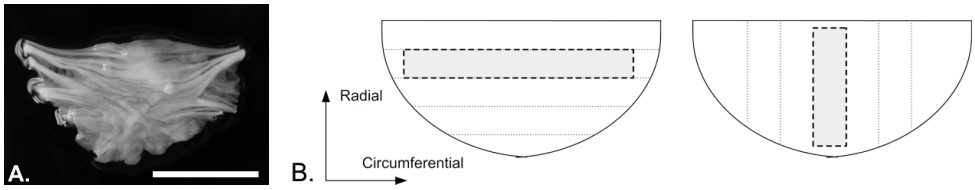

Figure 2.1: a) Anisotropic matrix structure of an aortic valve. Originating at the commisures, connective tissue bundles run nearly parallel with the free leaflet margin. The white bar represents a scale of 1 cm. b) Uniaxial tensile tests were performed on tissue strips (n = 3-5) from two leaflets in circumferential and radial direction.

Matrix analysis: collagen content and cross-links

After tensile testing, biochemical assays were performed on the valve leaflet tissue strips and TE constructs to evaluate the corresponding tissue matrix composition. The tissues were cut such that each valve leaflet strip comprised 4-6 samples, while TE strips were completely used for biochemical analyses. Lyophilized tissue samples were hydrolysed in 6 M HCl (Merck, Germany) and used for amino acid and cross-link analyses. Hydroxyproline residues were measured on the acid hydrolysates by reverse-phase high-performance liquid chromatography (RP-HPLC) after derivatisation with 9-fluorenylmethyl chloroformate (FMOC, Fluka, Switzerland) (Bank *et al.*, 1996). Collagen content was expressed as percentage relative to the specimens' dry tissue weight. The same hydrolysates were used to measure the number of the mature collagen cross-links hydroxylysyl pyridinoline (HP), which is the main type of collagen cross-links present in cardiovascular tissue, by HPLC as described previously (Robins *et al.*, 1996; Bank *et al.*, 1997). The number of HP cross-links was expressed per collagen triple helix. Data from valve leaflet strips were averaged per valve leaflet.

Histology

Tissue samples were fixed in phosphate-buffered formalin (Fluka, USA) and embedded in paraffin. Sections were cut at 5μm thickness and picrosirius red (PR) staining was used in conjunction with polarized light microscopy to assess collagen fiber organization in native valves and TE constructs under static and dynamic conditions.

2.2.3 Data analysis

Descriptive statistics (mean standard deviation) were performed for collagen content, HP cross-links, and biomechanical properties (modulus, UTS, and ε_{max}). Biomechanical properties were compared between circumferential and radial direction of leaflets strips, between statically and dynamically conditioned TE constructs, and between native and engineered tissue using student t-tests. In native valves collagen content and cross-link data were correlated to the biomechanical properties using Pearson's correlation analyses. In the two TE groups correlations between these variables, incorporating interaction effects between variables were investigated using a general linear model (GLM). The correlation coefficient was represented by r. A p-value $<$ 0.05 was considered significant. Statistical analysis was performed using SPSS 11.0 software (SPSS Inc., Chicago, USA).

2.3 Results

2.3.1 Biomechanical properties

Native human valves

In figure 2.2, typical stress-strain curves are displayed for tissue strips from the valve leaflets in circumferential and radial direction. An overview of UTS, ε_{max} and modulus for radial and circumferential direction is displayed in figure 3. The modulus (15.6 $\pm$ 6.4 MPa) and UTS (2.6 $\pm$ 1.2 MPa) of the leaflets were higher (p $<$ 0.005) in circumferential direction compared to radial direction (modulus: 2.0 $\pm$ 1.5 MPa, UTS: 0.42 $\pm$ 0.24 MPa), while ε_{max} was lower (circumferential: 21.9 $\pm$10.6 $\%$, radial: 29.8 $\pm$ 13.9 $\%$, p $<$ 0.05).

TE constructs

The biomechanical properties of the TE constructs are shown in figure 2.3. The modulus of dynamically strained constructs (5.8 $\pm$ 1.1 MPa) was higher compared to statically cultured constructs (3.0 $\pm$ 0.8 MPa, p $<$ 0.005). No significant changes were found in UTS (static: 0.73 $\pm$ 0.16 Mpa; dynamic: 0.99 $\pm$ 0.22 MPa, p = 0.07), while constructs cultured under static conditions showed a higher ε_{max} (32.3 $\pm$ 3.2 $\%$) compared to dynamically loaded constructs (24.3 $\pm$ 6.4 $\%$, p $<$ 0.05).

2.3.2 Collagen content and cross-links

Native human valves

The amount of collagen per dry weight and the number of HP cross-links per triple helix in the tested human heart valves were 0.47 $\pm$ 0.09 mg/mg dry weight and 0.52 $\pm$ 0.06, respectively (figure 4).

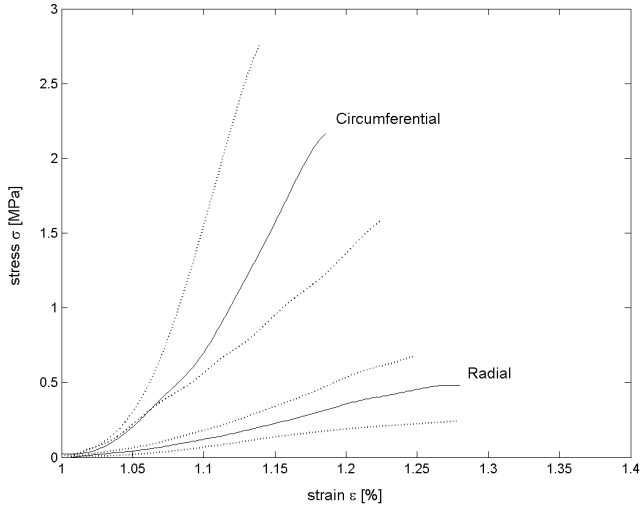

Figure 2.2: Stress-strain curves (solid lines) for human aortic valves in circumferential and radial direction. The dotted lines represent standard deviations of the modulus. The valve leaflet is much stiffer and stronger in circumferential compared with radial direction, indicating anisotropic mechanical behavior.

TE constructs

No difference in the amount of collagen per dry tissue weight between statically and dynamically loaded TE constructs was found (static: 0.09 ± 0.01 mg/mg dry weight; dynamic: 0.09 ± 0.01 mg/mg dry weight, $p = 0.46$). Interestingly, the dynamically loaded constructs contained significantly more HP cross-links per triple helix compared to the statically cultured constructs (static: 0.14 ± 0.02, dynamic: 0.28 ± 0.06, $p < 0.005$).

2.3.3 Native aortic valves versus engineered tissue

The modulus and UTS of statically as well as dynamically cultured constructs were significantly lower ($p < 0.005$) , while ε_{max} was higher in statically ($p < 0.005$), but not different in dynamically cultured constructs ($p = 0.24$), compared to native valve leaflets in circumferential direction. However, when comparing to native tissue in radial direction, statically cultured constructs had higher UTS ($p < 0.01$) and no significantly different modulus ($p = 0.13$) and ε_{max} ($p = 0.20$). Dynamically cultured constructs showed higher modulus and UTS ($p < 0.005$) and no significantly different ε_{max} ($p = 0.30$) compared to native leaflets in radial direction (figure 3). Collagen content and cross-link concentration were significantly higher in native tissue compared to TE constructs (static and dynamic, $p < 0.005$, figure 4).

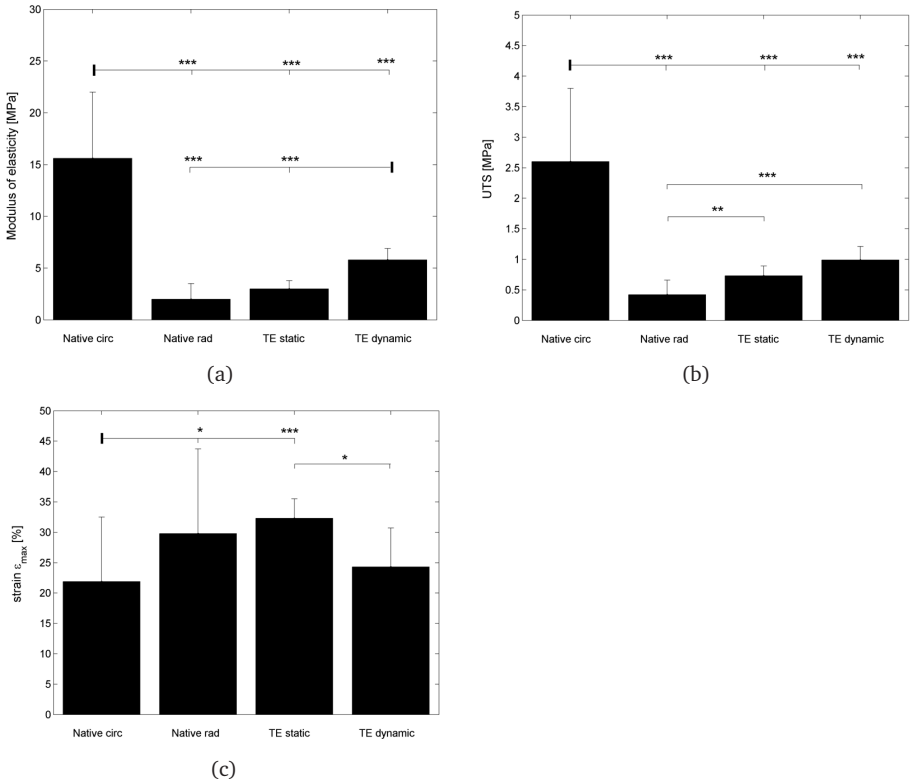

Figure 2.3: Mechanical properties of native human aortic valve leaflets and TE constructs. Modulus (a), UTS (b) and max (c) of native valve leaflets (circumferential and radial direction) and TE constructs (static and dynamic). In case of multiple comparisons, differences are compared to values under the bold stripe (* $p < 0.05$; ** $p < 0.01$; *** $p < 0.005$).

2.3.4 Correlation between collagen content, cross-links, and biomechanics

Native human valves

In circumferential direction, a significant correlation was found between the modulus and the corresponding values for HP cross-links per collagen triple helix ($r = 0.58$, $p < 0.005$). No correlation between collagen content and modulus was observed ($r = 0.05$, $p = 0.80$), as shown in figure 5. In the radial direction, no significant correlations between modulus and HP cross-links per triple helix, or between modulus and collagen content were found ($r = 0.12$, $p = 0.54$ and $r = 0.12$, $p = 0.54$, respectively, data not shown).

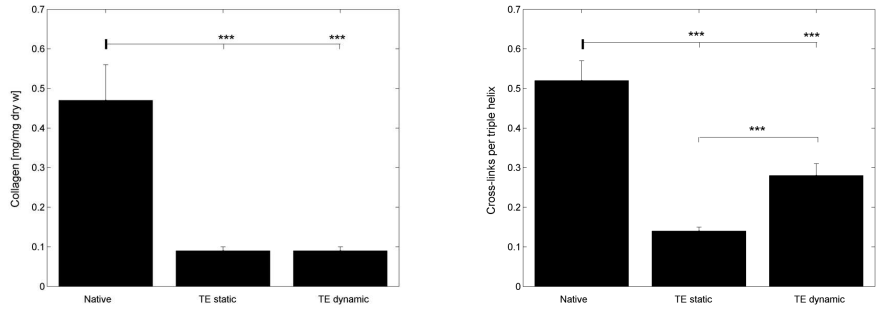

(a) (b)

Figure 2.4: Collagen content and cross-links in native human aortic valve leaflets and TE constructs (static and dynamic). In case of multiple comparisons, differences are compared to values under the bold stripe (** $p < 0.01$;***$p < 0.005$).

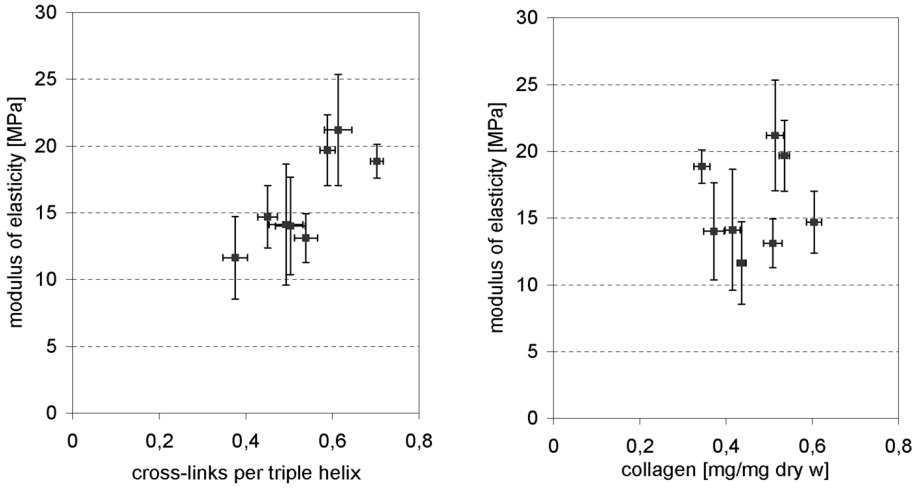

(a) (b)

Figure 2.5: Modulus and collagen data in circumferential direction of native valve leaflets. Each marker represents the average ($\pm$ SEM) of one valve (n = 4 strips). a) A significant positive linear correlation was present between modulus and cross-links per triple helix ($r = 0.58$, $p < 0.005$). b) No correlation was present between modulus and collagen content ($r = 0.05$, $p = 0.80$).

TE constructs

Statistical analysis of the two TE groups showed no significant correlation between the amount of collagen and the modulus ($r = 0.40$, $p = 0.25$), as can be observed in figure 6. However, the number of collagen cross-links per triple helix showed a significant positive linear correlation with the modulus ($r = 0.86$, $p < 0.005$). This correlation was independent of the mode of mechanical conditioning. A significant negative linear correlation of cross-links with the strain at break was observed ($r = -0.88$, $p < 0.005$).

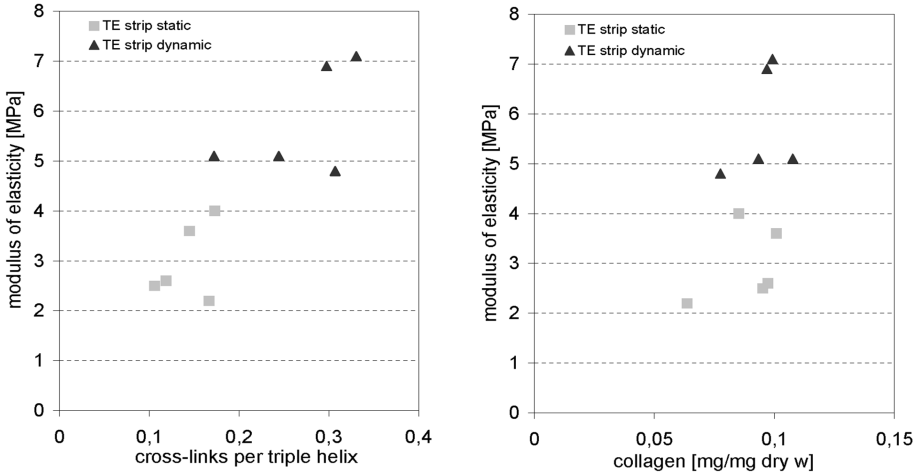

(a) (b)

Figure 2.6: Statically and dynamically conditioned tissue engineered constructs. a) A significant positive linear correlation was observed between modulus and cross-links per triple helix. ($r = 0.89$, $p < 0.005$). b) No correlation was found between modulus and collagen content. ($r = 0.40$, $p = 0.25$).

2.3.5 Histology

The tri-laminar structure of the native human valves was clearly visible in histology (figure 2.7a-d), and an alignment of collagen fibers in the circumferential direction could be observed in the fibrosa layer. In radial direction collagen bundles in the fibrosa appeared to be fragmented (figure 2.7d). Although picrosirius red stained sections of both TE groups appeared similar in transmitted light images (figure 2.7g,h), dynamically conditioned tissue engineered constructs constructs showed more brightness than statically conditioned engineered tissue (figure 2.7e,f).

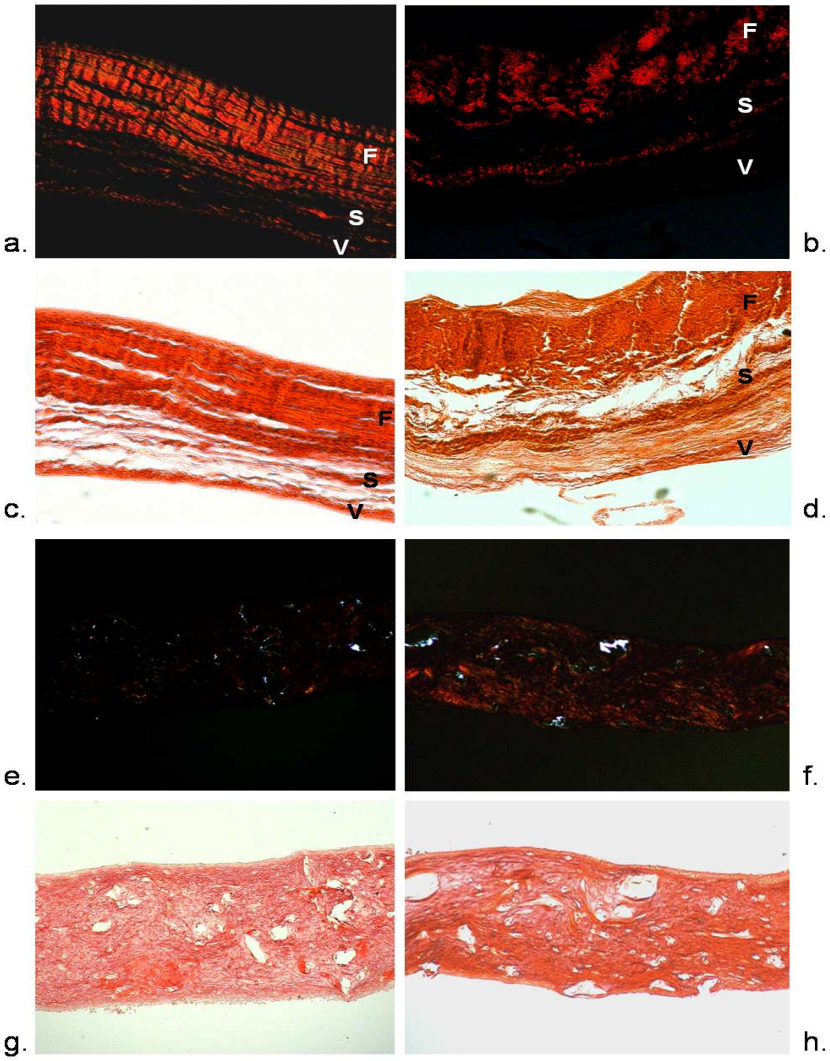

Figure 2.7: Sections of native heart valves in circumferential (a, c) and radial direction (b, d) (original magnification 100x), and statically (e,g) and dynamically strained (f,h) TE constructs (original magnification 40x). Picrosirius red stained collagen red and was viewed under polarized (a, b, e, f) and transmitted light (c, d, g, h). The tri-laminar structure in native heart valves is clearly visible in the transmitted light images, and an alignment of collagen fibers in the circumferential direction can be clearly observed in the fibrosa layer (c). In radial direction collagen bundles in the fibrosa appeared to be fragmented (d), suggesting an alignment perpendicular to the plane of sectioning. Although picrosirius red stained sections of both TE groups appeared similar in transmitted light images (g,h), dynamically conditioned tissue engineered constructs constructs showed more brightness than statically conditioned engineered tissue (e,f), suggesting a higher degree of orientation and maturation.

2.4 Discussion

A thorough insight into the functional structure of the native aortic valve related to biomechanics and matrix biology is crucial for progress in the field of heart valve tissue engineering. As a first step, this study investigated the structure-function relationship between collagen content, cross-links and biomechanical properties in human aortic heart valve leaflets and TE constructs.
Fresh native human valve leaflets were uniaxially tested in two directions, taking account of the natural anisotropy in the leaflets. The valve leaflets were much stiffer and stronger in circumferential compared with radial direction, indicating anisotropic mechanical behavior. Although uniaxial tensile tests have their limitations and do not reflect the full biaxial mechanical behavior of the valve leaflet, this method does suffice to investigate global differences in mechanical properties in the two perpendicular directions, which is defined as anisotropic behavior. The biomechanical data were consistent with values published in a recent study by Stradins *et al.* (2004), and show a high diversity possibly related to the large biological variations in gross fiber architecture observed among the mature heart valve leaflets (figure 2.1), due to age and health status of human subjects. As expected, the diversity in TE constructs was smaller, which is essential for future control and optimization of construct properties during culture protocols. Extensibility of the TE constructs was within the same range as those of the native leaflets, while the modulus and UTS of dynamically strained constructs were about one third of the leaflet properties in circumferential direction.
Interestingly, data analysis of the native leaflets showed a significant correlation of collagen cross-linking, but not the amount of collagen, with the tissue stiffness in circumferential direction (figure 2.8). Collagen was correlated to this specific mechanical parameter, since this structural protein is the main load-bearing component during the linear phase of the stress-strain curve. Similar findings were reported for bone tissue (Banse *et al.*, 2002), and in scar tissue of collateral ligaments (Frank *et al.*, 1995). Moreover, in patellar tendon the modulus was shown to be related to the amount of insoluble (cross-linked) collagen, but not to the total collagen content (Haut *et al.*, 1992).
The natural anisotropy clearly plays a large role in the biomechanical behavior of the valve leaflets, being more extensible and less stiff in radial compared to circumferential direction (figure 2.2). In radial direction, the leaflet strips failed between circumferentially running fibers. In this direction no correlation between modulus and cross-links was observed between the modulus of elasticity and the amount of collagen or cross-links. As the correlation between modulus and cross-links only holds for the circumferential direction, it is likely that collagen cross-links act in conjunction with collagen fiber orientation in providing tissue strength. The order of magnitude in the radial stress strain curves lies within the range of elastin (Vesely, 1998). The relative contribution of elastin to the mechanical behavior of a valve leaflet in radial direction may be more prominent than in circumferential direction. A more detailed correlation between other matrix components and mechanical properties would provide valuable information and will be subject of future investigations.

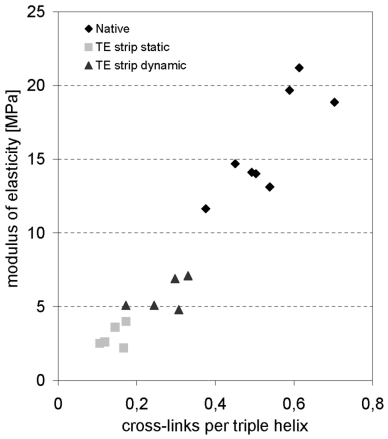

Figure 2.8: Overview of modulus versus cross-links per triple helix for native tissue and TE constructs. A positive linear trend can be observed.

In the TE experiments the modulus correlated well to the number of cross-links and not to collagen content. These data confirm the proposed relevance of cross-link stimulation to enhance tissue strength in engineered tissues (Elbjeirami *et al.*, 2003; Dahl *et al.*, 2005). Previous studies have shown mechano-induced upregulation of collagen in myofibroblasts (Kolpakov *et al.*, 1995; Engelmayr *et al.*, 2005). Interestingly, Mol *et al.* (2006) showed that collagen production in engineered tissues stabilizes to a steady state value, regardless the presence of dynamical straining. Affirming the hypothesis on mechano-induced collagen upregulation, the culture period needed to reach the steady state value did depend on strain application, and was shorter with dynamic straining. In short, collagen production rate is higher in dynamically conditioned TE valves, so the steady state value is reached earlier, but the eventual steady state value is not different from unstrained tissues. After reaching the steady state value of collagen, tissue matures further and collagen cross-links contribute increasingly more to tissue strength. Interestingly, this process is also enhanced by mechanical stimulation. We hypothesize that in the initial phase of culturing TE constructs, collagen and other ECM components are produced by cells to provide biomechanical support at an early stage. In this phase the amount of collagen increases linearly with the modulus. Hereafter, tissue maturation will play part; collagen cross-links are formed and cross-link concentration will dominate biomechanical behavior rather than the amount of collagen.
Formation of enzymatic collagen cross-links can be manipulated biochemically in tissue engineering. Elbjeirami et al. showed that transfection of cells by lysyl oxidase (a collagen cross-link enzyme involved in the formation of enzymatic/natural cross-links) increased the number of cross-links and improved mechanical properties of tis-

sue engineered constructs (Elbjeirami *et al.*, 2003). Beekman *et al.* (1997) inhibited formation of crosslinks by beta-aminopropionitrile (an inhibitor of enzymatic cross-link), resulting in less cross-links and decreased tissue stiffness. Previously published data showed that dynamic loading of tissue engineered constructs resulted in higher modulus (Mol *et al.*, 2003). It was suggested that dynamic straining might further enhance tissue organization, based on the qualitative observations by histology. Indeed our experiments show that dynamic straining increases the number of cross-links in TE constructs. Further experiments in our lab should elucidate the effect of other factors in the culturing protocol on cross-link formation, such as time, straining frequency and magnitude.

Histological examination showed highly aligned collagen fibers in the fibrosa layer of the aortic valve in circumferential direction. Due to the unstretched configuration during fixation collagen fibers were crimped and formed a wavy pattern. In radial direction cross-sections of collagen bundles were visible in the fibrosa layer, suggesting an alignment perpendicular to the plane of sectioning (figure 8a-d). Histological comparison between native and engineered tissue revealed interesting differences. Picrosirius red staining of tissue engineered constructs showed homogeneous tissue formation after 4 weeks in both groups, in contrast to the three layered structure that was observed in native tissue. Furthermore, the degree of orientation and maturation of the collagen network, which is represented by brightness in the polarized light image, was much lower in TE constructs compared to native tissue. Corresponding to higher amounts of cross-links and thus maturation, dynamically conditioned constructs were brighter than their static counterparts, suggesting that dynamic straining induces more alignment and maturation in the tissue. Interestingly, in prenatal development aortic valves initially show a homogeneous matrix distribution, mainly consisting of proteoglycans. Not until after birth a three layered structure in the valve gradually develops, together with collagen fiber alignment and maturation 28. This in-time development of the aortic valve raises the question to what extent TE valves need to resemble an adult native valve structure, as in-vivo remodeling will likely occur upon implantation (Hoerstrup *et al.*, 2000).

An outlook on the tissue engineering pathway towards functional, 'native'-approaching tissue is depicted in figure 2.8. Indeed, the number of cross-links as well as the amount of collagen in tissue engineered constructs are both still lower than that in native tissue. However, the results in this paper show that merely increased collagen contents will not improve biomechanical properties in engineered tissues, while higher cross-link concentration does. Furthermore, figure 2.8 reveals a directive role of collagen cross-links, rather than collagen content, in the biomechanical development of TE constructs towards native tissue. In conclusion, the data presented here demonstrate the importance of collagen cross-links in biomechanical tissue properties of native heart valve leaflets as well as of tissue engineered constructs. This correlation emphasizes the necessity to consider the total collagen architecture as a whole, including amount of collagen, cross-link concentration and fiber orientation, as a focus for increasing strength in engineered tissues.

Acknowledgements

The work of Angelique Balguid forms part of the research program of the Dutch Polymer Institute (project 475). This research was also supported by the Dutch Technology Foundation (STW), applied science division of NWO and the Technology Program of the Dutch Ministry of Economic Affairs. The authors would like to thank Jessica Snabel, TNO Health and Prevention Leiden, The Netherlands, for her contribution to this work.

Chapter 3

Stress related collagen ultrastructure in human aortic valves

The contents of this chapter are based on A. Balguid, N. J. B. Driessen, A. Mol, J. P. J. Schmitz, F. Verheyen, C. V. C. Bouten and F. P. T. Baaijens (2007) *Stress related collagen ultrastructure in human aortic valves*, Journal of Biomechanics; under review.

3.1 Introduction

The development of the extracellular matrix (ECM) in biological tissues is known to depend on the cellular and tissue microenvironment and biomechanical conditions. The ECM in heart valves is subjected to considerable mechanical loads during the cardiac cycle. During tissue growth and remodeling this applied load is a determining factor in the development of a functional tissue matrix structure. Heart valve leaflets are composed of three distinct layers, each with their own unique function. The biomechanical behavior of the aortic valve as a whole depends on the contribution, composition, and interaction of these layers. The aorta-facing fibrosa layer, composed predominantly of a dense network of collagen fibers, is largely responsible for bearing and distributing stresses over the leaflets during maximum loading (the end-diastolic phase) of the cardiac cycle (Sacks *et al.*, 1997; Driessen *et al.*, 2003b). The glycosaminoglycan-rich spongiosa layer is assumed to function as a shock absorber and allows shear between the ventricularis and the fibrosa (Schoen, 1997). The ventricularis layer, consisting mainly of elastin fibers, supports the recoil of the leaflet to its crimped initial state after diastolic loading. This three-layered structure assures low flexural rigidity, necessary to allow normal valve opening, and high tensile strength required to resist transvalvular pressures (Sacks *et al.*, 1998). A macroscopic view of the valve leaflet shows an anisotropic collagen structure. A highly aligned circumferential collagen fiber orientation is present at the free edge of the leaflets, while a more hammock-like structure is seen in the belly. This complex fiber architecture allows higher tissue compliance in radial direction than in circumferential direction (Schoen, 1997). The specialized collagen organization functions effectively in transferring stresses to the aortic wall. Apart from the macroscopic fiber structure, the type of collagen, the amount and type of inter- and intramolecular covalent cross-links, and the collagen fibril morphology also determine the tissue's mechanical behavior (Parry *et al.*, 1978; Beekman *et al.*, 1997; Avery and Bailey, 2005; Balguid *et al.*, 2007). Collagen fibrils, with diameters ranging from 16 to 500 nm, are the building blocks of collagen fibers. Their diameter, density and orientation are associated with the tissues requirement for tensile strength and elasticity (Parry *et al.*, 1978).

The objective of this study was to investigate the relation between the magnitude of local stress in human aortic valves, and the collagen ultrastructure, interpreted here as the collagen fibril diameter distribution and the fibril density. It is hypothesized that increased tissue stress is related to larger diameters of collagen fibrils and a broader range of fibril diameters (Parry, 1988; Bailey *et al.*, 1998). As the stress distribution in the heart valve leaflet is inhomogeneous, variations in local collagen fibril morphology may be expected.

To investigate this, the collagen ultrastructure was investigated at three representative locations in human aortic valve leaflets with transmission electron microscopy (TEM). Subsequently, a previously developed computational model of the human aortic valve was used to predict the maximum tensile stresses at these locations during diastole (Driessen *et al.*, 2005b). The relation between the collagen ultrastructure and applied stress may provide a better understanding of the mechanical function of collagen fib-

rils in heart valve leaflets. Moreover, it may promote further advances in the field of heart valve tissue engineering, where optimization of the collagen ultrastructure is essential for the creation of functional, load bearing valve replacements.

3.2 Materials and methods

3.2.1 Tissue preparation

To assess the collagen ultrastructure in valve leaflets, seven healthy human donor aortic valves (4 female, 3 male, age 47.7 $\pm$ 12.0) were obtained from the Rotterdam Heart Valve Bank at the Erasmus University Medical Center, Rotterdam, The Netherlands. Prior to donation, the donors or their relatives consented with experimental use of the cardiovascular tissue following explantation. Upon dissection, tissue samples were taken from three locations: the commissures, the belly and the fixed edge of one leaflet of each valve (figure 3.1(a)). In previous work these three locations were shown to have the most pronounced differences in stress value (Driessen *et al.*, 2005b). The valve samples were fixed in 3 $\%$ glutaraldehyde buffered to pH 7.4 with potassium phosphate. After washing in the same buffer supplemented with 7.5 $\%$ sucrose the samples were postfixed in 2 $\%$ osmium tetroxide in veronal acetate buffer (pH 7.4), rinsed in veronal buffer containing 7 $\%$ sucrose and impregnated with 1 $\%$ uranyl acetate in veronal buffer (pH 5.2). After a short rinse in the same buffer at pH 5.2 the samples were then dehydrated in a graded ethanol series and routinely embedded in Epon (LADD Research Industries Inc.). Semithin sections (2 μm) were prepared and stained with toluidine blue. Ultrathin sections were stained with uranyl acetate and lead citrate before examination in a Philips CM100 electron microscope.

3.2.2 Collagen fibril diameter measurement

A region of interest within the fibrosa layer of the toluidine blue stained sections, was selected for further EM analysis. Subsequently, transmission electron microscopical images of collagen fibril bundles in the fibrosa layer were obtained from each tissue cross-section at a fixed magnification of 21.500x. The resolution of the images was The faces of the sections were perpendicular to the main fiber direction and areas of collagen fibril cross-sections were identified. Fibrils were identified using a contrast-based edge recognition algorithm in Matlab (The MathWorks Inc., USA). The algorithm fitted ellipses on the fibril contours, and the shortest principal axis was measured to assess the fibril diameter. Considering the cylindrical shape of the fibril cross-sections, fitting ellipses rather than circles on the fibrils accounted for the three dimensional orientation of the fibril with respect to the cutting plane, and prevented an overestimation of the fiber diameter. The fibril density was calculated as the number of fibrils per unit area. For each leaflet 4 TEM images of collagen fibril bundles were taken at each location. Per location 28 images (7 leaflets) were analyzed in total.

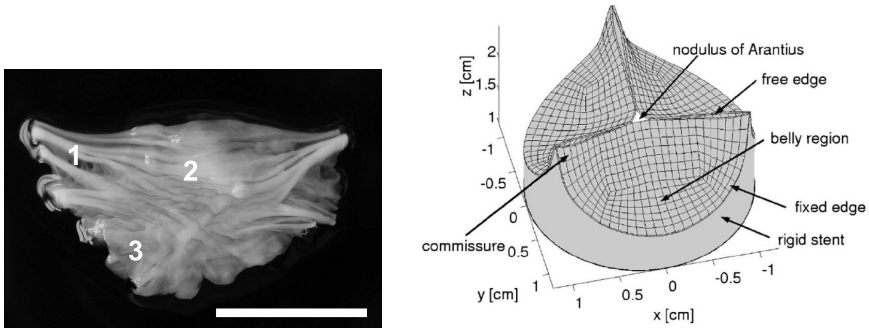

(a) (b)

Figure 3.1: a) Anisotropic matrix structure of an aortic valve leaflet. Location 1 represents the commissures. Location 2 is the belly of the leaflet, and 3 represents the fixed edge. The white bar corresponds to 1 cm. b) Finite element mesh of the stented valve geometry, adapted from Driessen *et al.* (2005b).

3.2.3 Computational simulations

To test the hypothesis of stress related collagen ultrastructure, a structurally based constitutive model for collagenous cardiovascular tissues (Driessen *et al.*, 2005b,a) was applied to describe the mechanical behavior of the human leaflets. Finite element analyses (FEA), using the mesh shown in figure 3.1(b), were performed to simulate the local mechanical response of the valve leaflets to a transvalvular aortic pressure load of 12 kPa. Uniaxial tensile tests and geometric properties previously obtained by Balguid *et al.* (2007) were used to identify the anisotropic mechanical properties of the human valve leaflets in two orthogonal orientations, the circumferential and radial direction. A detailed description of the computational simulations was described previously (Driessen *et al.*, 2007), and is briefly presented below.

3.2.4 Constitutive equations

The aortic valve leaflets were modeled as incompressible fiber-reinforced tissues (Holzapfel *et al.*, 2000; Driessen *et al.*, 2005b), as described previously (Driessen *et al.*, 2007). The total Cauchy stress $\boldsymbol{\sigma}$ consists of the hydrostatic pressure p and the extra stress $\boldsymbol{\tau}$:

$$\boldsymbol{\sigma} = -p\boldsymbol{I} + \boldsymbol{\tau} \tag{3.1}$$

The extra stress is split into an isotropic matrix part and an anisotropic fiber part, in which a fiber volume fraction (ϕ_f) is incorporated, and is written as (Driessen *et al.*,

2005b):

$$\boldsymbol{\tau} = \hat{\boldsymbol{\tau}} + \sum_{i=1}^{N_f} \phi_f^{\,i} (\psi_f^{\,i} - \vec{e}_f^{\,i} \cdot \hat{\boldsymbol{\tau}} \cdot \vec{e}_f^{\,i}) \vec{e}_f^{\,i} \vec{e}_f^{\,i} \tag{3.2}$$

where $\hat{\boldsymbol{\tau}}$ represents the matrix stress and N_f denotes the number of fiber directions. ψ_f is the fiber stress, which acts only in the direction of the fiber $\vec{e}_f$. The isotropic matrix stress is modeled as a Neo-Hookean material with a shear modulus G. The constitutive behavior of the fibers is described with an exponential relationship between the fiber stress ψ_f and the fiber stretch λ_f:

$$\psi_f = k_1 \lambda_f^2 \left[e^{k_2(\lambda_f^2 - 1)} - 1 \right] \tag{3.3}$$

where k_1 and k_2 are stress-like and dimensionless parameters, respectively, and it is assumed that the fibers cannot withstand compressive forces ($\psi_f = 0$ for $\lambda_f < 1$). The fiber stretch is defined as the ratio of lengths in the deformed and undeformed configuration (i.e., l/l_0). The relationship between the fiber direction in the deformed ($\vec{e}_f$) and undeformed configuration ($\vec{e}_{f_0}$) is given by:

$$\lambda_f \vec{e}_f = \boldsymbol{F} \cdot \vec{e}_{f_0} \tag{3.4}$$

with $\boldsymbol{F}$ the deformation gradient tensor. In order to incorporate the angular distribution of fibers in the plane of the leaflet, $\vec{e}_{f_0}$ is defined in a coordinate system spanned by the vectors $\vec{v}_1$ and $\vec{v}_2$:

$$\vec{e}_{f_0} = \cos(\gamma)\vec{v}_1 + \sin(\gamma)\vec{v}_2 \tag{3.5}$$

where the angle γ is defined with respect to $\vec{v}_1$. To specify the relative amount of fibers in each direction, a (discretized) Gaussian distribution function is used for the fiber contents:

$$\phi_f = A \exp\left[\frac{-(\gamma - \mu)^2}{2\sigma^2} \right] \tag{3.6}$$

with μ and σ the mean value and standard deviation of the distribution function, respectively. The scaling factor A is introduced to ensure that the total fiber volume fraction equals ϕ_{tot}.

3.2.5 Parameter estimation

The directions $\vec{v}_1$ and $\vec{v}_2$ are chosen to coincide with the circumferential and radial direction, respectively. Based on values in literature for native heart valves (Bashey *et al.*, 1967; Li *et al.*, 2001; Balguid *et al.*, 2007), the total fiber volume fraction ϕ_{tot} is set to 0.5. To further reduce the number of material parameters, a fixed value for the shear modulus of the matrix material G of 50 kPa is chosen. The averaged results of independent uniaxial tensile tests in the circumferential and radial directions were fit simultaneously to estimate the remaining material parameters (k_1, k_2 and σ), as described previously (Driessen *et al.*, 2007).

3.2.6 Geometry and boundary conditions

The finite element mesh of the initial, stress-free, closed configuration of the leaflets is shown in figure 3.1(b) (de Hart *et al.*, 2003). The radius of the stented valve geometry is 12 mm and the thickness of the leaflets (t) was measured with a micrometer (Mitutoyo, USA). By symmetry, only one half of a leaflet is modeled and normal displacements are suppressed at the symmetry edge. At the fixed edge all displacements are suppressed and a contact surface is defined at the free edge to model contact between the leaflets (i.e., coaptation). Subsequently, a transvalvular pressure (p_{tv}) of 12 kPa, representative for the aortic valve, is applied to the top surface to induce deformations. The directions $\vec{v}_1$ and $\vec{v}_2$ are calculated from the principal stretch directions in an isotropic leaflet (Driessen *et al.*, 2003a, 2005b).

3.2.7 Data analysis

Statistical analysis was performed using SPSS 13.0 software (SPSS, USA). Per image the fibril diameter, its distribution, and the fibril density were assessed. For each location these parameters were averaged and expressed as mean $\pm$ standard error of the mean (s.e.m.). The variation in fibril diameter was represented by the width at half peak height of the fibril diameter distribution histogram. This was defined as two times the standard deviation of the fibril diameter in the image. Differences between the locations were analyzed using univariate Analysis of Variance (ANOVA), followed by Bonferroni's multiple comparison test, with valve and location as independent and dependent variables, respectively. A p-value < 0.05 was considered significant.

3.3 Results

3.3.1 The collagen ultrastructure

Representative images of collagen fibrils at the three locations are shown in figure 3.2. The mean collagen fibril diameter and fibril density were significantly different among all three locations ($p < 0.05$, figure 3.3(a)). The smallest fibril diameters were observed at the fixed edge of the leaflet (33.8 $\pm$ 0.9 nm), larger fibrils were found in the belly of the leaflets (38.7 $\pm$ 1.2 nm) and the largest fibrils were observed at the commissures (41.6 $\pm$ 1.3 nm). Interestingly, the fibril densities at the three locations were inversely related to the fibril diameters, with lowest fibril densities in the commissures (256 $\pm$ 14 μm^{-2}), followed by the belly of the leaflet (303 $\pm$ 14 μm^{-2}), and highest at the fixed edge (352 $\pm$ 19 μm^{-2}) (figure 3.3(b)).

The fibril diameter distribution was analyzed by comparing the width at half peak height, as measured per location, and averaged over all valves (figure 5.5). The results showed that in the commissures (11.3 $\pm$ 0.70 nm) and belly (10.6 $\pm$ 0.34 nm) a significantly larger variation in fibril diameter was observed compared to the fixed edge (8.84 $\pm$ 0.33 nm, $p < 0.01$).

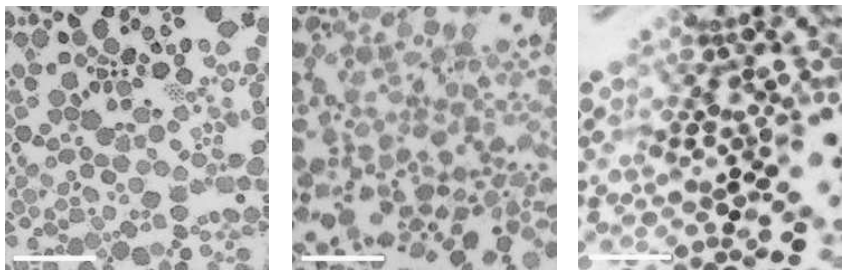

(a) Commissures (b) Belly (c) Fixed edge of leaflet

Figure 3.2: Collagen fibril bundles at three locations of the heart valve. From left to right: the commissures (a), the belly (b) and the fixed edge of the leaflet (c). The collagen fibrils in the fixed edge of the leaflet appear more uniform in size compared with the commissures and belly region. The bars indicate 200nm.

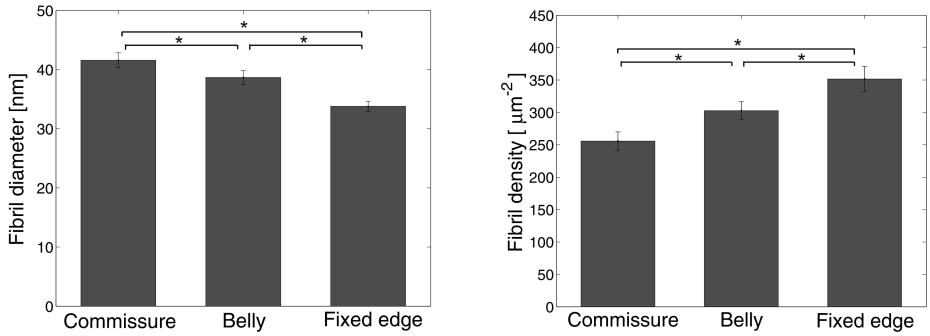

(a) (b)

Figure 3.3: a) Collagen fibril diameter ($\pm$ s.e.m.) and b) Fibril density ($\pm$ s.e.m.) measured at three locations of the valve leaflet, the commissures, belly and fixed edge (* $p < 0.05$).

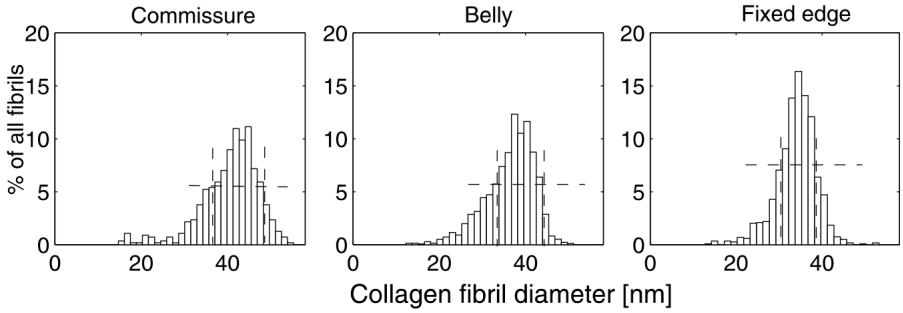

Figure 3.4: Illustrative histograms of collagen fibril diameter at the commissures, belly and fixed edge for one leaflet. The width at half peak height was significantly larger in the commissures and belly, compared with the fixed edge. This corresponds with a higher uniformity in fibril diameter at the fixed edge.

3.3.2 Constitutive model and experimental data

The first step in predicting the stress distribution in a human valve was a fit of the constitutive model to the experimental data. The fitted stress-stretch curves of the model corresponded quite well with the averaged experimental stress-stretch curves of human aortic valve leaflets (figure 3.5(a)), both in circumferential and in radial direction. The mechanical response of the native human aortic valve leaflets were obtained with the following parameters: t = 0.46 mm, G = 50 kPa, k_1 = 1877 kPa, k_2 = 4.25 and σ = 36.4° (Billiar and Sacks, 2000b; Driessen *et al.*, 2005b). The estimated parameters were used as material properties to subsequently predict the stress distribution in the aortic valve mesh.

3.3.3 Computational simulations

To link the collagen ultrastructure to local stress predictions during maximum load, the stress distribution in the human valve leaflet was simulated with FEA. An inhomogeneous stress distribution over the valve leaflets was observed during maximum loading, the end-diastolic phase of the cardiac cycle (figure 3.5(b)). The highest stresses were observed at the commissures (550-600 kPa), in the belly of the leaflet slightly lower stresses were found (400-500 kPa), and low stresses were seen at the fixed edge (0-50 kPa) of the valve leaflet. Correlating these data to the collagen ultrastructure showed that higher stress levels are associated with increased fibril diameter and decreased fibril density. Furthermore, collagen fibrils in tissue sustaining low stresses (fixed edge) have thinner and more uniform fibril diameters compared with high stress locations.

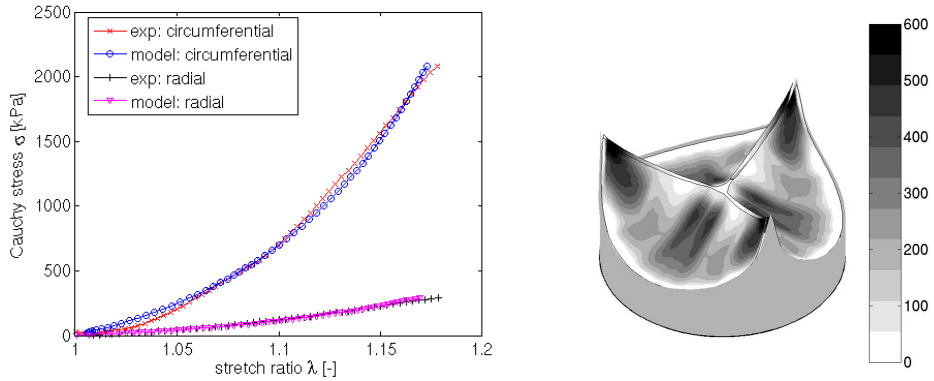

(a) (b)

Figure 3.5: a) Constitutive model fit to averaged experimental data. Both in circumferential and in radial direction the model predicted the stress-stretch curve reasonably well. b) Stress map [kPa] of aortic leaflet during end-diastole. Highest stresses were observed in the commissure (550-600 kPa), slightly lower stresses were seen in the belly (400-500 kPa) and relatively low stresses (0-150 kPa) at the fixed edge.

3.4 Discussion

The objective of this study was to investigate the relation between the local collagen ultrastructure and the level of local stress in human aortic valve leaflets. In summary, higher local stresses in valve leaflets, as predicted by the model, corresponded with larger average fibril diameter, lower fibril density and wider fibril size distribution compared with low stress locations in the leaflets. Although fibril diameters and densities were variable at the different locations, the area percentage of collagen in a cross-section was approximately equal in all locations. The data presented here indeed suggested that applied stress does affect the collagen fibril morphology. A better understanding of the impact of mechanical loading on the collagen ultrastructure is relevant for heart valve tissue engineering, where optimization of the collagen architecture is essential for clinical applications.

Several factors that were involved in the model (e.g. large biological variation between valves, the use of a stented mesh geometry) may account for a possible inaccurate representation of absolute stress values for individual valves. However, the relative differences within the leaflet are of specific interest in this study. As the model succeeded in simulating the complex nonlinear and anisotropic behavior of the aortic valve, the predicted stress distribution pattern across the leaflets can be considered similar for all the valves (Driessen *et al.*, 2005b). The fiber content in the model was homogeneously distributed over the leaflet. As the collagen cross-sectional area did not differ over the locations, this assumption seems valid.

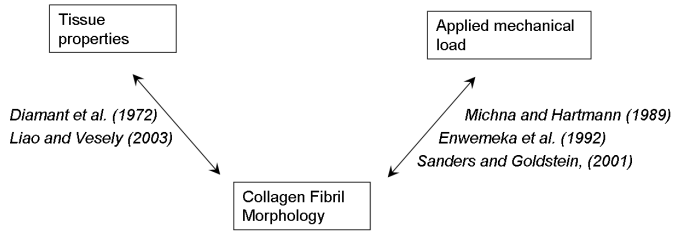

Figure 3.6: Both the applied load and the tissue mechanical properties are related to collagen fibril morphology.

Mechanical behavior of tissue is related to the collagen fibril morphology, which, in turn depends on the mechanical loading conditions of the tissue. In literature, several studies in different species and tissue types were performed to investigate the interaction between mechanics and collagen fibril morphology, resulting in different observations and proposed mechanisms relating collagen fibril size and density to biomechanics. Most of these studies can be categorized in two groups (figure 3.6); those investigating the relation between the collagen ultrastructure and the applied mechanical loading (Diamant *et al.*, 1972; Torp *et al.*, 1975; Enwemeka *et al.*, 1992; Sanders and Goldstein, 2001), and studies relating the ultrastructure to the tissues' mechanical behavior (Parry *et al.*, 1978; Liao and Vesely, 2003).

The findings here are consistent with observations in skin subjected to repetitive compressive and shear stresses (Sanders and Goldstein, 2001). Stressed skin showed larger fibril diameters, lower fibril densities, and a less unimodal distribution of fibril diameters when compared to unstressed control samples. Similar findings were reported in an exercise study in rat hindlimb tendons (Enwemeka *et al.*, 1992), where the collagen fibril diameter increased by 32% after 10 weeks of physical training, compared with an untreated control group. Mechanical stimulation is known to induce collagen remodeling (Boerboom, 2007), which may be associated with fibril thickening and formation of new fibrils, causing a wider diameter distribution. Diamant *et al.* (1972) performed mechanical tests on tail tendon of rats between the age of 2 weeks up to 29 months. With age larger collagen fibril diameters were observed, associated with an increased modulus of elasticity.
However, various studies investigating the relation between mechanics and collagen ultrastructure, do not support the reasoning above. Michna and Hartmann (1989) performed a 10-week exercise study investigating collagen fibrils in mice tendon. An initial increase in fibril diameter compared with an untreated control was observed after one week, but there was no difference between the groups after 10 weeks. Liao and Vesely (2003) studied the mechanical properties in porcine chordae tendineae

in relation with collagen fibril morphology. Higher tensile moduli were reported in chordae with smaller fibril diameters. It was postulated that thinner fibrils have more fibril-to-fibril interaction possibilities due to a larger ratio of fibril surface and cross-section, hence explaining their higher moduli.
The differences between these observations can be related to several factors, such as tissue type, species, age, loading conditions and/or training protocol. The efficiency of mechanical reinforcement of collagen fibrils and the ability of the tissue to sustain an applied load is dependent on e.g. the fibril orientation. This can vary markedly between tissues, e.g. unidirectional in tendon, laminated in cornea, random in skin (Bailey *et al.*, 1998). In heart valve leaflets the fibril orientation differs over the leaflet (figure 3.1(a)). Based on the findings in this study, one might expect that the fibril orientation varies locally within the fibrosa layer, due to inhomogeneous mechanical demands across the leaflet. Other factors that may influence the mechanical behavior of collagenous tissues are the types of collagen present and the waviness of the collagen fibrils (Baer *et al.*, 1975). Evidence from immunoelectron microscopy and biochemical studies suggests that collagen fibrils consist of several collagen types. During tissue development the structural composition and ratio of collagen types in collagen fibrils changes, causing changing fibril diameters (Kadler *et al.*, 1996). Unfortunately, how this is related with the mechanical properties of a tissue is still unclear. An extended study of the composition of the fibrils (e.g. collagen types) will be topic of further research.
In an extensive review Bailey *et al.* (1998) stated that the ability to withstand high stress levels is related to the proportion of large diameter fibrils. The reasoning behind this statement is the following: when tissue contains large diameter fibrils, the percentage of lateral intrafibrillar covalent cross-links is higher than that in small diameter fibrils. Previous work indeed showed a linear correlation between the number of collagen cross-link and the modulus of human aortic valve leaflets (Balguid *et al.*, 2007), thus supporting Baileys arguments. Since covalent cross-links cannot be made between different fibrils, the tensile strength of a fibril is predicted to increase with diameter. Therefore, large diameter fibrils may be predominantly found in tissues sustaining high tensile loading, while small diameter fibrils are likely found in tissue subject to low stresses (Parry, 1988). In light of this it could be speculated that locations in the valve leaflet sustaining higher mechanical loading comprise stronger tissue than under low stress. This has not been verified through mechanical testing yet. Cox *et al.* (2006) recently developed an indentation test method to locally determine mechanical properties of a tissue. This would be an elegant method to verify this statement and would give valuable insight in the mutual interactions between collagen architecture, applied load, and mechanical behavior (figure 3.6).
The presented data confirm the hypothesis that higher local stresses, i.e. due to applied loading, are associated with larger collagen fibrils. This structure-function relation may be used for further development of the collagen contribution in the computational aortic valve model. In addition, an important focus in the field of heart valve tissue engineering is optimization of the collagen architecture to ensure long term functioning. The findings here give a better insight into the impact of mechanical loading on the collagen ultrastructure, and may be valuable to improve loading

protocols for tissue engineering.

Acknowledgements

The work of Angelique Balguid forms part of the research program of the Dutch Polymer Institute (project 475). The authors would like to acknowledge Sjors P. van Kats and Ad J. J. C. Bogers from the Erasmus University Medical Center, Rotterdam, The Netherlands, for their contribution to this work.

Chapter 4

Tailoring fiber diameter in electrospun PCL scaffolds for optimal cellular infiltration in cardiovascular tissue engineering

The contents of this chapter are based on A. Balguid, A. Mol, M. H. van Marion, R. A. Bank, C. V. C. Bouten, F. P. T. Baaijens (2007) *Tailoring fiber diameter in electrospun PCL scaffolds for optimal cellular infiltration in cardiovascular tissue engineering*, Tissue Engineering; under review.

4.1 Introduction

Scaffold design in tissue engineering (TE) plays an important role in modulating tissue growth and development. Various scaffold fabrication techniques, including rapid prototyping, solvent casting, salt leaching and electrospinning, are used to construct a broad range of scaffold geometries. Using electrospinning, highly porous, nonwoven, three-dimensional fiber structures can be made, of which the fiber diameter can range from nano- to microscale (Yoshimoto *et al.*, 2003; Subbiah *et al.*, 2005; Li *et al.*, 2006). The basis of this technique is to produce thin fibers by electrically charging a polymer solution flowing through a needle (Reneker and Chun, 1996). The geometry of the collector determines the gross shape of the fiber mesh, this can be adapted to suit its purpose, e.g. a blood vessel or heart valve geometry (Vaz *et al.*, 2005; van Lieshout *et al.*, 2006). The morphology of fibers can be controlled with various parameters in the electrospinning process, such as solution properties (e.g. viscosity, conductivity, polymer molecular weight), controlled variables (e.g. flow rate, electric field strength), and ambient parameters (e.g. temperature, humidity) (Pham *et al.*, 2006a).
One advantage of electrospun scaffolds is that their fiber structure, particularly when in nanoscale, is associated with high surface-to-volume ratios, providing a large area for cell attachment. Furthermore, the physical form of the nanofibrillar matrices provides high porosity and high spatial interconnectivity. The use of nanofibrous structures was postulated to bear a close resemblance to the dimensions of natural extracellular matrix (ECM) (Li *et al.*, 2002). Though this resemblance may apply to the fiber thickness and the porosity of the nanofibrous scaffold, the spatial characteristics of ECM are not attained (Li *et al.*, 2002; Pham *et al.*, 2006b). In fact, the pore size of the scaffold reduces with decreasing fiber diameter and can be as small as 100nm (Kwon *et al.*, 2005). Such small pore sizes may interfere with cellular infiltration in the scaffold, thus undoing the advantages of nanofibrous scaffolds for use in TE. However, this feature may be beneficial when the nanofiber mesh is used as a membrane, separating cell types, yet allowing communication through interconnected pores (Zhu *et al.*, 2007).
Microfiber scaffolds, on the other hand, consist of a more spatious, coarser geometry with fiber diameters up to 10μm and corresponding pore sizes of up to 45μm (Pham *et al.*, 2006b). Although the geometry of a microfiber scaffold appears more suitable for TE purposes with regard to cell ingrowth, the majority of electrospinning research has focused on nanofibers. Pham *et al.* (2006b) demonstrated the reproducibility and uniformity of electrospun poly-ε-caprolactone (PCL) microfiber scaffolds with fiber diameters ranging from 2 up to 10μm. Subsequently, they constructed a bilayered electrospun structure of a 5μm scaffold with a nanofiber top layer, to evaluate the combined potential of both scaffold geometries. Rat marrow stromal cells could succesfully infiltrate the structure (Pham *et al.*, 2006b). van Lieshout *et al.* (2006) compared a large pore-sized knitted PCL scaffold with an electrospun PCL scaffold. Although human myofibroblast cells penetrated easily in the knitted scaffold, retaining the cells within the scaffold matrix was a problem due to the excessively large pores (+200 μm). Oppositely, in the electrospun scaffold, cell ingrowth was limited,

despite its microscale fiber diameter. To ensure successful use of electrospun scaffolds, the advantage of a high surface-to-volume ratio, as well as a sufficient pore size should be maintained. Therefore, the ideal scaffold environment for cells should be a cell-specific trade-off between complete cell ingrowth and minimal pore size. Clearly, the potential of electrospun scaffolds for TE depends on cell type, and more importantly, on cell size. In this study human myofibroblasts of approximately 10μm in diameter were used. The minimal pore size should hence have at least similar dimensions.
The objective of this study was to investigate the optimal fiber diameter of electrospun PCL scaffolds for human myofibroblasts. This was determined by comparing cell penetration in 5 different scaffold groups. Electrospun PCL scaffolds with fiber diameters ranging from 3.4 to 12.1μm were evaluated for their potential in cardiovascular TE. Subsequently, the scaffold that complied with the requirements of complete cell penetration, was used in a 4 week TE experiment, using a porous non-woven fiber mesh of poly-glycolic acid coated with poly-4-hydroxybutyrate (PGA-P4HB) as reference scaffold. This scaffold has been successfully used in cardiovascular TE (Hoerstrup *et al.*, 2000; Mol *et al.*, 2006). Both scaffold materials are FDA approved (Li *et al.*, 2006). Tissue formation was analyzed in PCL scaffolds seeded with human myofibroblasts after 4 weeks of culture.

4.2 Materials and methods

4.2.1 Materials

Chemicals were obtained from Sigma-Aldrich (Zwijndrecht, Netherlands) unless otherwise stated. PCL (Mn 8×10^4) was dissolved at 13.7 and 17.5 w/v% in chloroform (99.9% HPLC grade). Non-woven PGA meshes (Cellon, Luxembourg) were dip-coated in a solution of P4HB (Mn 1×10^6; TEPHA Inc., USA) in tetrahydrofuran, as described previously (Mol, 2005).

4.2.2 PCL electrospinning

The custom-built electrospinning set-up existed of a high voltage power supply, an infusion pump (Kd Scientific, USA), a 10 ml plastic syringe (Terumo, Belgium), a stainless steel blunt needle (inner diameter 0.6 mm) and a stagnant grounded collector. The syringe was horizontally fixed in the infusion pump. The polymer solution was led through a plastic tube to the needle, which was vertically fixed 15 cm above the collector. The polymer solution was electrostatically drawn from the tip of the needle by high voltage between the needle and the collector. Five sheet-like scaffolds (group A to E) with increasing fiber diameters were produced by varying the spinning parameters: flow rate (Q), the applied voltage (V) and the concentration of the polymer solution (table 4.1). The thickness of all electrospun sheets was approximately 1 mm.

Group	Q_{PCL} [μL/min]	V [kV]	Concentration [w/v%]	Fiber diameter [μm]
A	8	20	13.7	3.40 ± 0.29
B	12	15	13,7	4.97 ± 0.29
C	20	15	13.7	6.73 ± 0.56
D	35	15	13.7	8.71 ± 0.57
E	60	15	17.5	12.09 ± 1.21

Table 4.1: Parameters for electrospinning PCL scaffolds and the resulting fiber diameters. Q_{PCL}: the flow of the PCL solution through the needle, V: the voltage difference over the needle and the collector, concentration: polymer weight/volume percentage in solution.

4.2.3 Measurement of fiber diameters

Recent work by Eichhorn and Sampson (2005) elegantly described a theoretical model of the fibrous network structure produced by electrospinning. The model demonstrated the mutual dependence of fiber width and mean pore radius, more specifically, a direct relation between fiber diameter and pore size. Based on this relation, fiber diameter can be interpreted as a reliable predictor of pore size, which is difficult to accurately measure in thin sheets of electrospun scaffolds. The fiber diameters of the electrospun scaffolds were imaged with ESEM (Philips XL30 ESEM-FEG), and fiber diameter was assessed on 5 samples per group, 10 measurements per sample. Quantitative image analysis of fiber diameters were performed in MATLAB (The MathWorks Inc., USA).

4.2.4 Culture of human venous myofibroblasts

Myofibroblast cells, harvested from the human vena saphena magna and expanded using regular cell culture methods, were used as described previously (Schnell *et al.*, 2001). As culture medium DMEM advanced (Gibco, USA) supplemented with 10% fetal bovine serum (Biochrom, Germany), 1% glutamax (Gibco), and 0.1% gentamycin (Biochrom) was used. Every 3-4 days the medium was replaced and cultures were maintained in a humidified incubator at 37°C with 5% CO_2.

4.2.5 Cell seeding and tissue culture

Cells of passage 7 were enzymatically detached by adding trypsin-EDTA (Cambrex, USA) to the monolayer cultures. After a centrifuging step, the cells were resuspended in a fibrin gel, serving as cell carrier (Mol *et al.*, 2005a), and evenly distributed over rectangular scaffold strips (5×35×1mm). The cell-seeded scaffolds will be further referred to as TE constructs. In the first study, cell ingrowth was investigated in the electrospun PCL scaffolds with increasing fiber diameter after 3 days of culture (n = 4 per group). In the second study, tissue development was investigated in PCL constructs and compared with PGA-P4HB constructs after 4 weeks of culture (n = 6

per group). PCL group E was chosen based on the results of the cell infiltration experiment. Electrospun PCL scaffolds without cells served as controls. To create static strain conditions, which has shown to be beneficial for tissue development (Mol *et al.*, 2006), the scaffolds were attached at the ends, using a polyurethane-tetrahydrofuran glue (20 w/v%). The medium for tissue culture was supplemented with extra gentamycin (0.3%) and L-ascorbic acid 2-phosphate (0.25 mg/ml) to promote extracellular matrix production.

4.2.6 Quantification of cell ingrowth

The TE constructs were fixed in 3.7% formaldehyde (Merck, Germany) after 3 days of culture and embedded in Technovit 7100 (Heraeus Kulzer, Germany). 5 μm sections were cut and cells were fluorescently stained with 4'-6-Diamidino-2-phenylindole (DAPI). In each scaffold group, 12 fluorescence and corresponding light microscopy images (to distinguish the edges of the scaffold) were acquired with a Nikon TE300 fluorescence camera. Cell ingrowth in the scaffold was analyzed in three layers of equal size: the seeding side, middle and bottom layer. The layers were divided after selecting the total cross-sectional area in the light microscopy images. Cells were counted in each layer and expressed as a percentage of the total number of cells in the image, using image analysis in MATLAB.

4.2.7 Mechanical properties of TE constructs

After 4 weeks of culture the mechanical properties of the TE constructs and the unseeded scaffold material were measured using a uniaxial tensile tester equipped with a 20-N load cell (Kammrath & Weiss, Germany). The dimensions of the rectangular shaped constructs were measured with an optical imaging profiler (SensoFar PLμ 2300, Sensofar-Tech, Spain) and each sample was tested at a speed of the initial length (l_0) per minute. The Young's modulus, defined as the slope at the linear part of the curve, and Cauchy stresses at fixed strain values (5, 10, and 15% strain) were assessed from the stress-strain curves. This way of presenting the data was preferred over presenting the strain at break as the rupture mode was different among the groups.

4.2.8 Quantitative tissue analysis

After tensile testing, biochemical assays were performed on the TE constructs to evaluate the ECM composition. For DNA and glycosaminoglycan (GAG) analyses, lyophilized tissue samples were digested in papain solution (phosphate buffer, L-cysteine, ethylenediaminetetraacetic acid (EDTA), and papain) at 60°C for 16 hours. The DNA content was determined using the Hoechst dye method (Cesarone *et al.*, 1979) and a standard curve from calf thymus DNA. The GAG content was determined using a modification of the assay described by Farndale *et al.* (1986) and a standard curve from chondroitin sulfate from shark cartilage. For collagen analysis, the digested samples were hydrolysed in 6 M HCl (Merck, Germany). Hydroxyproline (Hyp)

residues were measured on the acid hydrolysates by reverse-phase high-performance liquid chromatography (RP-HPLC) after derivatisation with 9-fluorenylmethyl chloroformate (FMOC, Fluka, Switzerland) (Bank *et al.*, 1996). The same hydrolysates were used to measure the number of the mature collagen cross-links hydroxylysyl pyridinoline (HP) by HPLC as described previously (Bank *et al.*, 1997; Robins *et al.*, 1996). HP is the main type of collagen cross-links present in cardiovascular tissue. The number of HP cross-links was expressed per collagen triple helix. Hyp and GAG content were normalized to the amount of DNA to obtain a measure for the amount of matrix components produced per cell. The amount of DNA was not normalized to dry weight, but expressed as absolute values, since the scaffold contribution to the constructs weight after 4 weeks was considerably different for PGA-P4HB and PCL.

4.2.9 Qualitative tissue analysis

After 4 weeks of culture the TE constructs were fixed with 3.7% formaldehyde and embedded in Technovit 7100 (Heraeus Kulzer, Germany). Sections of 5 μm thickness were cut and stained with toluidine blue (Klinipath, Netherlands) to evaluate tissue formation.

4.2.10 Statistics

Statistical analysis was performed using SPSS 13.0 software (SPSS, USA). Values are presented as mean $\pm$ standard deviation. Differences between groups were determined with Univariate ANOVA, followed by Bonferroni post-hoc tests. Differences with a p-value smaller than 0.05 were considered significant.

4.3 Results

4.3.1 Scaffold morphology

The spinning parameters were optimized to obtain smooth regular shaped fibers in all scaffold groups. Using the parameters shown in table 1, the electrospun scaffolds consisted of randomly oriented uniform meshes of smooth regular shaped fibers. The fiber diameters increased from 3.4 $\pm$ 0.29 μm (group A), 5.0 $\pm$ 0.29 μm (group B), 6.7 $\pm$ 0.56 μm (group C), 8.7 $\pm$ 0.57 μm (group D), to 12.1 $\pm$ 1.21 μm (group E). Small standard deviations in the fiber diameter and uniform fibers, as visible in ESEM images (Figure 4.1a-e), suggested that all groups consisted of meshes with constant fiber thickness.

4.3.2 Cell ingrowth

Fluorescent images of the constructs with DAPI stained cells clearly showed differences in cell ingrowth between the 5 groups (figure 4.1f-j). Scaffold A, having the smallest fiber diameter, showed barely any cell ingrowth, while with increasing fiber

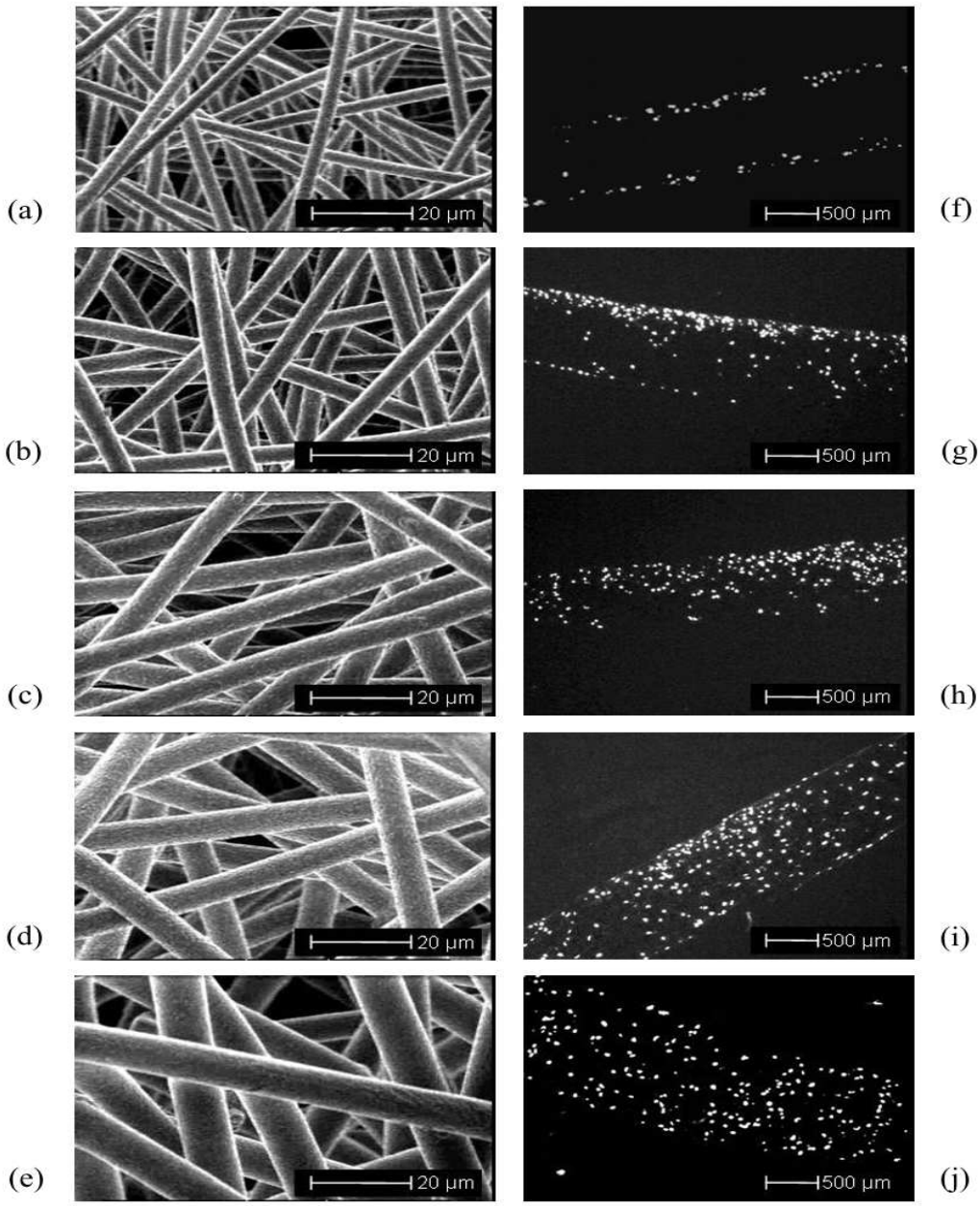

Figure 4.1: a-e) ESEM images of scaffolds A-E without cells. All electrospun scaffolds consist of randomly oriented uniform meshes of smooth regular shaped fibers with increasing fiber diameter. f-j) Fluorescent images of cross-sections of the scaffold groups A-E with DAPI stained cells after 3 days of culture. Clear differences in cell ingrowth between the 5 groups can be observed. With increasing fiber diameter, the number of intruded cells in the scaffold increased gradually (f-i) to a homogeneous cell distribution in group E (j).

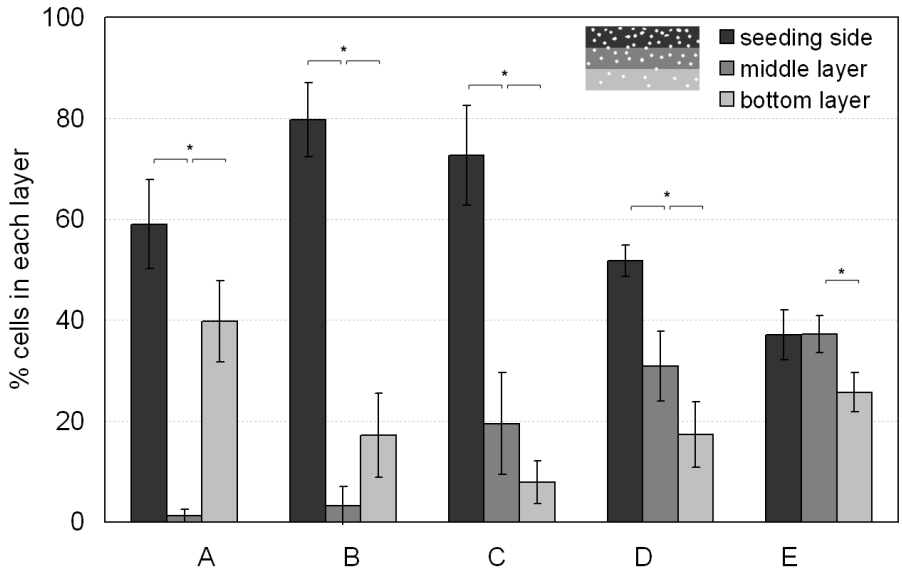

Figure 4.2: Quantified cell ingrowth, expressed as a percentage of the total number of cells per cross-section in PCL scaffold groups A-E. The number of cells in the middle layer of the scaffold increases with increasing fiber diameter. * indicates a difference with $p < 0.05$.

diameter the number of intruded cells in the scaffold increased to a homogeneous cell distribution in group E. Quantification of the number of cells in each of the three layers by image analysis is shown in figure 4.2. The graph shows increasing percentages of cells in the middle layer of the scaffold with increasing PCL fiber diameter. Remarkably, only in the largest fiber diameter mesh (group E) cellular infiltration did not appear impeded by the scaffold structure. Although the number of cells in the bottom layer was lower than in the two layers above, the equal amounts of cells in the two upper layers indicate that cell penetration was not obstructed. Interestingly, cells in the thinner fiber meshes (A and B) rather surrounded the scaffold than penetrating it, represented by the large amounts of cells in both the seeding and the bottom layer. These data suggest that from the tested scaffolds the 12.1μm fiber group has the least fiber size to obtain sufficiently large pores, which allow complete cellular infiltration.

4.3.3 TE experiment

A morphological comparison of the two scaffolds types (PGA-P4HB and PCL group E) before cell seeding is shown in figure 4.3. A strong resemblance in fiber morphology could be observed between the two scaffold types. After 4 weeks of culture, the PCL

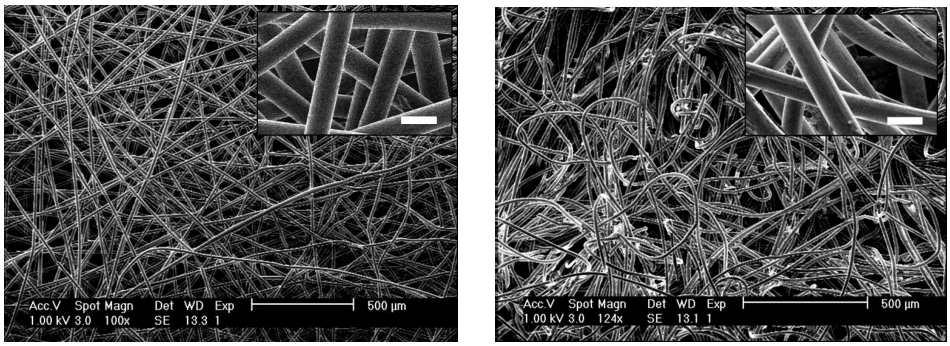

(a) (b)

Figure 4.3: ESEM images of PCL group E (a) and PGA-P4HB (b) scaffolds before cell seeding (100x, bar indicates 500 μm). Higher magnifications (1800x) of the scaffolds are shown in the upper right corner of both images (white bar = 20 μm). The porosity of both scaffolds appeared similar. At a high magnification strong resemblance in fiber morphology could be observed between the two scaffold types.

group E scaffold was still completely intact, in contrast to the largely degraded PGA-P4HB scaffold.

Mechanical properties

Stress-strain curves were obtained from uniaxial tensile tests to assess the mechanical properties of the constructs after 4 weeks of culture. Representative curves of each group are shown in figure 4.4 and averaged values are displayed in table 4.2. PCL constructs with and without cells were stiffer (higher modulus) and stronger (higher tensile stress at fixed strains) compared with PGA-P4HB constructs with cells. As PCL was not degraded after 4 weeks, the polymer dictated the constructs' mechanical response, hence the difference between the PCL and PGA-P4HB constructs. Significantly higher values of the modulus and the stress at fixed strains (at 5, 10, and 15% strain) were found in the PCL scaffolds with cells, compared to scaffolds without cells, indicating that the presence of cells significantly improved both stiffness and strength.

Quantitative tissue analysis

Tissue composition (collagen, collagen cross-links, GAGs and DNA) of all scaffolds was quantified after 4 weeks and presented in table 4.3. No difference was observed in the amount of DNA between the constructs from the PCL and PGA-P4HB scaffold groups. The amount of GAG per DNA and Hyp per DNA were about 20% higher in the PCL constructs, compared with the PGA-P4HB constructs, indicating slightly

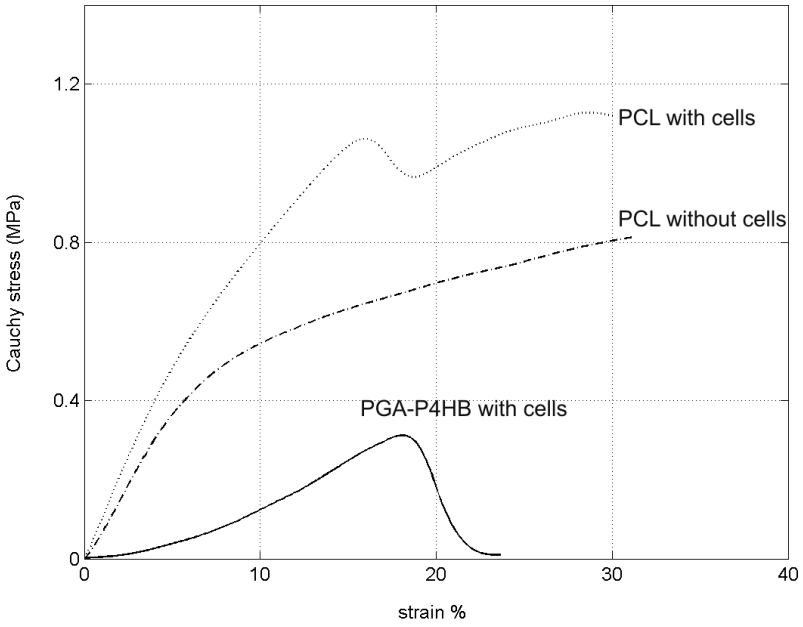

Figure 4.4: Representative stress-strain curves of TE constructs after 4 weeks of culture. The PCL scaffold was stiffer and stronger compared with the PGA-P4HB construct. The presence of cells clearly improved the stiffness and strength of the PCL scaffold.

		PCL with cells	**PCL w/o cells**	**PGA-P4HB**
Modulus [MPa]		10.36 ± 1.41	7.97 ± 1.07 *	2.28 ± 0.57 * ‡
Stress [MPa] at:	5% strain	0.53 ± 0.07	0.40 ± 0.05 *	0.06 ± 0.03 * ‡
	10% strain	0.86 ± 0.13	0.54 ± 0.07 *	0.14 ± 0.06 * ‡
	15% strain	1.09 ± 0.20	0.61 ± 0.08 *	0.24 ± 0.12 * ‡

Table 4.2: Mechanical properties of PGA-P4HB and PCL constructs (with and without cells) after 4 weeks of culture. * is significantly different compared with PCL with cells ($p < 0.01$), ‡ is significantly different from PCL without cells ($p < 0.01$).

	PCL constructs	**PGA-P4HB constructs**
GAG/DNA [$\mu g/\mu g$]	7.40 ± 0.36	6.23 ± 0.59 *
Hyp/DNA [$\mu g/\mu g$]	8.90 ± 0.89	6.90 ± 0.40 *
DNA [μg]	8.05 ± 0.96	8.93 ± 1.11
HP cross-links/ collagen molecule	0.27 ± 0.01	0.43 ± 0.02 *

Table 4.3: Tissue composition (DNA, GAG, Hyp, collagen crosslinks HP) of PGA-P4HB and PCL constructs after 4 weeks of culture. * indicates significantly different compared with PCL ($p < 0.01$).

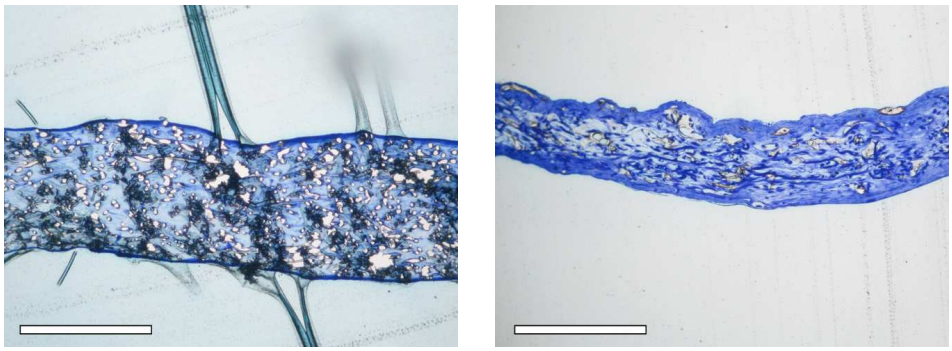

(a) (b)

Figure 4.5: Histological images of toluidine blue stained slides of PCL group E (a) and PGA-P4HB (b). Homogeneous tissue throughout the whole scaffold was observed in the PCL construct, while in the PGA-P4HB construct the tissue structure was more compact at the edges. Scale bar indicates 1mm.

increased matrix synthesis per cell in the PCL group. However, the number of cross-links per collagen molecule was lower in the PCL constructs, compared with the PGA-P4HB group.

Qualitative tissue analysis

Images of toluidine blue stained histological sections of the PCL and PGA-P4HB groups are shown in figure 5.5. In the PGA-P4HB group, the strongest proliferation and ECM deposition was observed at the edges of the constructs, while more homogeneous tissue was seen in the PCL group. Additionally, substantial compaction of PGA-P4HB constructs was observed due to scaffold degradation, in contrast to the unaffected dimensions of PCL constructs.

4.4 Discussion

The objective of this study was to investigate the optimal fiber diameter of electrospun PCL scaffolds for cardiovascular TE purposes with human venous myofibroblasts. The data presented in this study show that an average fiber diameter of 12.1μm is the minimal fiber size in an electrospun scaffold that allows unobstructed cellular infiltration. Quantification of cell ingrowth in 5 scaffold groups, with fiber diameters ranging from 3.4 up to 12.1μm, showed a relation between fiber diameter and cellular infiltration. Cell ingrowth of human myofibroblasts increased with increasing fiber diameter.
The results of the cell infiltration study validated the theoretical predictions of Eichhorn's model (Eichhorn and Sampson, 2005) that pore size increases with increasing fiber diameter. Pham *et al.* (2006b) demonstrated a high reproducibility and uniformity of electrospun microfiber scaffolds in the same diameter range as were used in the present study. Although cell ingrowth was not investigated in different sized microfiber scaffolds, it was suggested that smaller fibers can inhibit cellular infiltration. The data presented here confirm this suggestion, and showed that even a small change in average fiber diameter can have a significant effect on cellular infiltration. This emphasizes that fiber thickness is an essential parameter for 3D TE applications. As cell size differs between cell types and species (Krombach *et al.*, 1997), the optimal electrospun scaffold structure is not a uniform geometry, but should be cell-specific.
In the second part of this study the PCL electrospun scaffold with average fiber diameter of 12.1μm was evaluated for tissue development and compared with a PGA-P4HB scaffold. The PGA-P4HB model system has produced strong and functional engineered tissues (Hoerstrup *et al.*, 2002; Mol *et al.*, 2006). As PGA-P4HB is degraded before implantation in patients, implantation of completely autologous tissue is possible. The choice for PCL as scaffold material arose from a shortcoming of the current status of cardiovascular engineered tissues: the lack of elastin. Proper *in vivo* functioning of vascular TE grafts has up to now been unsuccessful due to the lack of elastin biosynthesis in the tissue equivalents (Patel *et al.*, 2006). PCL exhibits elastic behaviour with only minor permanent deformation (Klouda *et al.*, 2007). Therefore, PCL could function as an elastic substitute while natural elastin is gradually produced to take over this role. It appears a promising material for cardiovascular tissue engineering, especially when prolonged periods of mechanical support are desired.
With SEM, a high morphological resemblance was observed between the PCL scaffold and the reference PGA-P4HB scaffold prior to seeding, supporting the potential of the PCL scaffold for TE. After 4 weeks of culture, PGA-P4HB constructs showed a denser tissue structure and more compact dimensions compared with PCL constructs. PCL obviously served as a support structure, maintaining its initial dimensions, while the PGA-P4HB scaffold degraded and lost its mechanical support, allowing compaction of the construct. Mechanical testing showed that the PCL construct could sustain higher tensile stresses and was stiffer compared to the PGA-P4HB construct. The PCL scaffold remained fully intact during the 4 weeks of culture, while the PGA-P4HB scaffold lost mechanical integrity. The amount of DNA was equal in both groups, however, GAG and collagen production of the cells was approximately 20% higher in the PCL constructs compared with PGA-P4HB.

It could be argued that the cells in the two scaffold groups experienced different environmental stimuli, which could account for the difference in ECM production. In the stiff PCL fiber mesh, the cells are surrounded by a rigid environment, which imposes mechanical restraints. Contrarily, the PGA-P4HB is degraded after 4 weeks of culture, leaving the cells with little mechanical support and no mechanical restraints. As a mechanically restrained environment can induce myofibroblast differentiation (Hinz, 2006), which is characterized by increased biosynthesis of ECM components (Merryman *et al.*, 2006), this might explain the moderately higher levels of matrix components in PCL compared with PGA-P4HB. Additionally, scaffold degradation products diffuse into the medium during culture. Therefore, the rapid degrading PGA-P4HB scaffold produces a considerably higher concentration of acidic degradation products than the slow degrading PCL scaffold. It has been reported that extracellular pH influences matrix synthesis of GAGs as well as collagen in chondrocytes (Wu *et al.*, 2007). Furthermore, it was demonstrated that high levels of PGA degradation products altered cellular function in terms of proliferation and differentiation (Higgins *et al.*, 2003). This could account for lower matrix production, which in turn may have promoted collagen cross-linking in the PGA-P4HB constructs, compared with the PCL constructs.

In summary, despite the attractive features of nanofibrous structures for cell attachment, the data presented here encourage a shift from nano to micro fiber meshes for use in 3D TE applications. Electrospun PCL scaffolds appear a promising alternative to PGA-P4HB scaffolds for cardiovascular tissue engineering. The scaffold allows for sufficient cell ingrowth and proper ECM biosynthesis, provided that the fiber diameter in the mesh is adapted to the size of the cells to be seeded. An electrospun PCL scaffold would be particularly advantageous when a tissue engineered implant should retain elastic properties and mechanical integrity. After implantation the cells could gradually form elastin and a strong tissue matrix to eventually function without the support of a polymer structure.

Acknowledgements

The work of Angelique Balguid forms part of the research program of the Dutch Polymer Institute (project 475). The authors would like to acknowledge Jessica Snabel from TNO Health and Prevention, Leiden, The Netherlands, and Anita van de Loo from Eindhoven University of Technology, Eindhoven, The Netherlands, for their contribution to this work.

Chapter 5

The use of biochemical factors and oxygen level to improve mechanical properties of engineered heart valve tissue

The contents of this chapter are based on A. Balguid, A. Mol, C. V. C. Bouten and F. P. T. Baaijens (2007) *Hypoxia induced near-native mechanical properties of engineered heart valve tissue*, Circulation; under review.

5.1 Introduction

Tissue engineered (TE) heart valve replacements appear promising autologous valvular substitutes that possess the ability to grow, adapt and remodel *in vivo*, which is in particular relevant for pediatric and young adult patients. These attractive features distinguish TE valves from currently used valvular prostheses, which consist of foreign body material and are nonviable. TE heart valves have been successfully implanted in the pulmonary position in sheep, showing a native-resembling function and tissue composition after five months (Sodian *et al.*, 2000; Hoerstrup *et al.*, 2000). However, the valves did not show sufficient mechanical strength for systemic pressure applications, such as the aortic valve.
In native human aortic valves, the features responsible for maintaining the mechanical integrity and functionality of the tissue are the anisotropic mechanical and structural properties, and the mature, well-developed collagen architecture present in the valve leaflets (Bashey *et al.*, 1967; Rabkin and Schoen, 2002; Balguid *et al.*, 2007). The maturity of collagen is determined by the presence of collagen cross-links, which were shown to directly influence the stiffness of human native aortic valve leaflets (Balguid *et al.*, 2007). So far, these critical features have not been sufficiently mimicked in engineered heart valves. Recently, a novel *in vitro* conditioning strategy was developed, which mimics the diastolic phase of the cardiac cycle. This resulted in the fabrication of tissue engineered valves, based on a rapid degrading polymer scaffold, that could withstand physiological systemic pressures during four hours in an *in vitro* setup (Mol *et al.*, 2006). The dynamically conditioned valves were associated with considerable improvement of tissue quality and developing anisotropic mechanical properties after 4 weeks of culture in a bioreactor, compared with a static control. Though these results are promising, native values of tissue strength were not achieved in the engineered heart valves. Besides dynamic conditioning, altering the cellular niche by environmental and biochemical cues may also enhance tissue strength.
The aim of this study was to improve the mechanical properties of TE valves by external stimuli during the culture period. An environmental factor of interest is the level of oxygen supplied during culture. Up to now, the growing valves were exposed to atmospheric air, providing the engineered tissue with considerably more oxygen than under *in vivo* conditions (Fournier, 1999). Various studies in 2D and 3D cell cultures have demonstrated an upregulation of collagen on mRNA and protein expression level, associated with hypoxia, i.e. low oxygen tension (Horino *et al.*, 2002; Saini and Wick, 2004). From a biochemical perspective, insulin is considered an interesting stimulus for its enhancing effect on collagen production (Neidert *et al.*, 2002; Ross and Tranquillo, 2003; Tokudome *et al.*, 2004).
In this study, the separate and combined contribution of hypoxia and insulin were evaluated for their potential to promote tissue development in heart valve tissue equivalents. Human saphenous vein cells and a non-woven rapid degrading polymer fiber scaffold were used as an *in vitro* model system for engineered heart valve tissue, as described previously (Balguid *et al.*, 2007). The mechanical behavior and tissue properties were studied in the engineered tissues, and subsequently compared

with those of adult human aortic valves.

5.2 Materials and methods

5.2.1 Tissue engineering of heart valve constructs

Myofibroblasts, harvested from the human vena saphena magna and expanded using regular cell culture methods, were used as described previously (Schnell *et al.*, 2001). The culture medium consisted of DMEM advanced (Gibco, USA) supplemented with 10% fetal bovine serum (Biochrom, Germany), 1% glutamax (Gibco), and 0.1% gentamycin (Biochrom). Cultures were maintained in a humidified incubator at 37°C and 5% CO_2, and the medium was replaced every 3-4 days. Before seeding, the cells (passage 6-8) were enzymatically detached by adding trypsin-EDTA (Cambrex, USA) to the monolayer cultures. Scaffold preparation was performed as described previously (Mol *et al.*, 2005b). Briefly, rectangular strips (5×35×1 mm) of rapid degrading non-woven polyglycolic acid meshes (PGA; Cellon, Luxembourg) were coated with a thin layer of poly-4-hydroxybutyrate (P4HB; TEPHA Inc., Cambridge, USA). After a centrifuging step the cells were resuspended in a fibrin gel- serving as cell carrier (Mol *et al.*, 2005a)- and evenly distributed over rectangular scaffold strips. To create static strain conditions, which has shown to be beneficial for tissue development (Mol *et al.*, 2006), the scaffolds were attached at the ends, using a polyurethane-tetrahydrofuran glue (20 w/v%). The medium for tissue culture was supplemented with additional gentamycin (0.3%) and L-ascorbic acid 2-phosphate (0.25 mg/ml) to promote extracellular matrix production. The cell-seeded scaffolds will be further referred to as TE constructs.

5.2.2 Experimental design

Four experimental groups were studied (table 5.1); the *control* and *insulin* group, both cultured under atmospheric air conditions (normoxia). The *insulin + hypoxia* and *hypoxia* group were cultured under low oxygen tension, or hypoxia. As aortic valve leaflets are avascular tissue structures, oxygen transport to valvular cells occur primarily through oxygen diffusion from the aortic blood (Charest *et al.*, 2006). The oxygen concentration in arterial blood, which is 130 μM (Fournier, 1999), was therefore considered physiologically representative in the culture medium. The conversion of oxygen concentration (mM) to partial oxygen pressure (mmHg) in medium, which is very close to water, was calculated with Henry's law (5.1), using the coefficient of oxygen solubility in water (α) (Fournier, 1999):

$$C_{O_2,medium}[mM] = \alpha \cdot P_{O2}[mmHg] \tag{5.1}$$

where α = 1.39·10^{-3}mmol·L^{-1}·(mmHg)$^{-1}$.
Using the formula, the oxygen tension (mmHg) in culture medium can be calculated

Treatment	Time of Analysis	
	2 weeks	4 weeks
Control	n = 5	n = 5
Insulin	n = 5	n = 5
Hypoxia	n = 5	n = 5
Insulin + Hypoxia	n = 5	n = 5

Table 5.1: Four groups were studied in the experimental design, a control and insulin group under normoxic conditions, and two hypoxic groups with and without insulin. Upon sacrifice after 14 and 28 days, quantitative assessment of matrix components (DNA, GAG, Hyp, cross-links), mechanical testing (modulus, UTS), and histological examination (Masson Trichrome) were performed.

from the oxygen concentration (130 μM), and was 93 mmHg. Previously, Anderson *et al.* (1991) investigated the diffusion of oxygen from gas to culture media at various partial pressures. From these data the oxygen pressure in air, required to obtain an oxygen tension of 93 mmHg in the medium, was estimated 53-57 mmHg, which corresponds with 7-7.5% O_2 (0.07-0.075 bar). Therefore, a gas mixture consisting of 7 % O_2, 5 % CO_2, and 88 % N_2 was supplied to the *hypoxia* groups. Despite the claim that this oxygen concentration may be more representative of physiological conditions, in this study 7% O_2 levels are termed hypoxic and 20% O_2, normoxic, for consistency with conventional terminology in cell culture studies.
The *control* group was cultured with normal tissue culture medium, the culture medium for the *insulin* groups were supplemented with insulin (2.5 μg/ml). The insulin concentration was determined from literature (Neidert *et al.*, 2002; Ross and Tranquillo, 2003) and confirmed by metabolic activity tests of a range of concentrations (data not shown). The *hypoxia* groups were placed in a closed bell jar (figure 5.1), which was flushed with the hypoxic gas mixture daily. In all groups, constructs were sacrificed for analysis at two time points, at 2 and 4 weeks (n = 5 per group at each time point, table 5.1). During culture the constructs were placed on a shaking table, to promote gas exchange and diffusion.

5.2.3 Mechanical behavior

After 2 and 4 weeks of culture, the mechanical properties of the TE constructs were measured using a uniaxial tensile tester equipped with a 20-N load cell (Kammrath & Weiss, Germany). The dimensions of the rectangular shaped constructs were measured with an optical imaging profiler (SensoFar PLμ 2300, Sensofar-Tech, Spain) and each sample was tested at a speed of the initial length (l_0) per minute. The ultimate tensile stress (UTS), indicative for tissue strength, was assessed from the stress-strain curves. The slope of the linear part of the curve represented the Young's modulus of elasticity (indicative for tissue stiffness). These parameters were compared with averaged tensile data in circumferential direction of native adult human aortic valve

Figure 5.1: Experimental setup for groups under hypoxic conditions. The glass bell was flushed with gas mixture consisting of 7 % O_2, 5 % CO_2, and 88 % N_2, and was continuously shaken to promote gas exchange and diffusion.

leaflets from previous work (Balguid *et al.*, 2007).

5.2.4 Tissue composition of TE constructs

After tensile testing biochemical assays were performed on the TE constructs to evaluate the ECM composition. For DNA and glycosaminoglycan (GAG) analyses, lyophilized tissue samples were digested in papain solution (phosphate buffer, L-cysteine, ethylenediaminetetraacetic acid (EDTA), and papain) at 60°C for 16 hours. The DNA content was determined using the Hoechst dye method (Cesarone *et al.*, 1979) and a standard curve from calf thymus DNA. The GAG content was determined using a modification of the assay described by Farndale *et al.* (1986) and a standard curve from chondroitin sulfate from shark cartilage. For collagen analysis, the digested samples were hydrolysed in 6 M HCl (Merck, Germany). Hydroxyproline (Hyp) residues were measured on the acid hydrolysates by reverse-phase high-performance liquid chromatography (RP-HPLC) after derivatisation with 9-fluorenylmethyl chloroformate (FMOC, Fluka, Switzerland) (Bank *et al.*, 1996). The same hydrolysates were used to measure the number of the mature collagen cross-links hydroxylysyl pyridinoline (HP) by HPLC as described previously (Bank *et al.*, 1997; Robins *et al.*, 1996). HP is the main type of collagen cross-links present in cardiovascular tissue. The number of HP cross-links was expressed per collagen triple helix. Hyp and GAG content were normalized to the amount of DNA to obtain a measure for the amount of matrix components produced per cell. The tissue properties of the engineered constructs were compared with native tissue. Native values were obtained from human adult aortic valves, previously used for mechanical testing (Balguid *et al.*, 2007).

5.2.5 Histology

To evaluate the development of tissue formation in time in the engineered tissue samples, histology was performed. The constructs were fixed with 3.7% formaldehyde (Merck, Germany) and embedded in parafin. Tissue sections of 10 μm thickness were cut, and stained with Masson Trichrome.

5.2.6 Statistics

Descriptive statistics (mean $\pm$ standard deviation) were performed for collagen content, cross-links, and mechanical properties (modulus and UTS). Statistical differences between the groups were determined for both time points using univariate ANOVA, followed by Bonferroni post-hoc tests. Differences with a p-value smaller than 0.05 were considered significant. Statistical analysis was performed using SPSS 13.0 software (SPSS Inc., USA).

5.3 Results

5.3.1 The effect of insulin and hypoxia on tissue composition

The addition of insulin in the medium under normoxic conditions resulted in significantly higher GAG and collagen production per cell and more collagen cross-linking in the constructs after 2 weeks of culture, when compared with the control group (table 5.2). This difference in collagen production per DNA and cross-linking disappeared after 4 weeks, however, the weight percentage of collagen remained higher. Culturing under hypoxic conditions induced an increase in collagen per DNA as well as cross-link production after 2 and 4 weeks, when compared with the control group. In the combined hypoxia and insulin group, more collagen and cross-links were observed after 2 and 4 weeks, and the GAG production had increased after 4 weeks, compared with the control group. Both hypoxic groups showed less collagen and GAG (per DNA and per dry weight), compared with the insulin group after 2 weeks. This difference was absent after 4 weeks. The number of cells in all treated groups had increased compared with the control group after 4 weeks of culture.

5.3.2 The effect of insulin and hypoxia on mechanical behavior

The tissue stiffness (modulus) and strength (UTS) for all groups are shown in figures 5.2 and 5.3, respectively. The insulin group showed an initial increase in tissue stiffness and strength after 2 weeks of culture. Remarkably, after 4 weeks these parameters did not differ from the control group anymore. The hypoxia group showed no difference in stiffness or strength after 2 weeks compared with the normoxic control group. However, after 4 weeks substantially higher tissue stiffness and strength were found. The addition of insulin under hypoxic conditions resulted in stiffer tissue already after 2 weeks compared with the control and hypoxia group. After 4 weeks

	Treatment group					
Tissue properties	**Control**	**Insulin**	**Hypoxia**	**Insulin + Hypoxia**		**Native tissue**
Culture period: 2 weeks						
DNA [μg/mg]	2.78 $\pm$ 0.14	2.81 $\pm$ 0.27	2.84 $\pm$ 0.35	2.87 $\pm$ 0.34		
GAG/DNA [-]	3.29 $\pm$ 0.22	4.66 $\pm$ 0.68**	3.60 $\pm$ 0.30††	3.62 $\pm$ 0.42†		
Hyp/DNA [-]	2.08 $\pm$ 0.13	4.64 $\pm$ 0.20**	3.22 $\pm$ 0.56** ††	2.81 $\pm$ 0.40* ††		
HP/TH [-]	0.02 $\pm$ 0.02	0.07 $\pm$ 0.01**	0.09 $\pm$ 0.02**	0.09 $\pm$ 0.02**		
GAG/dw [μg/mg]	9.13 $\pm$ 0.68	13.01 $\pm$ 1.66**	10.28 $\pm$ 0.78†	10.20 $\pm$ 1.58†		
HYP/dw [μg/mg]	6.48 $\pm$ 0.65	13.13 $\pm$ 1.55**	6.83 $\pm$ 1.17††	7.95 $\pm$ 1.55††		
Modulus [MPa]	2.75 $\pm$ 0.22	4.76 $\pm$ 1.24*	3.16 $\pm$ 0.63	6.00 $\pm$ 1.43** ‡‡		
UTS [MPa]	0.55 $\pm$ 0.11	0.56 $\pm$ 0.14	0.59 $\pm$ 0.22	0.37 $\pm$ 0.10		
Culture period: 4 weeks						
DNA [μg/mg]	3.32 $\pm$ 0.32	4.36 $\pm$ 0.29**	4.33 $\pm$ 0.31**	4.20 $\pm$ 0.48**		5.66 $\pm$ 3.00
GAG/DNA [-]	4.75 $\pm$ 0.41	5.68 $\pm$ 0.25*	5.22 $\pm$ 0.69	5.77 $\pm$ 0.46*		6.05 $\pm$ 1.87
Hyp/DNA [-]	4.04 $\pm$ 0.52§§	5.23 $\pm$ 0.56§§	5.54 $\pm$ 0.57** §§	5.78 $\pm$ 0.82** §§		12.9 $\pm$ 3.84
HP/TH [-]	0.05 $\pm$ 0.01§§	0.08 $\pm$ 0.03§§	0.11 $\pm$ 0.01** §§	0.11 $\pm$ 0.01** §§		0.52 $\pm$ 0.06
GAG/dw [μg/mg]	15.68 $\pm$ 1.16§§	24.72 $\pm$ 1.65**	24.07 $\pm$ 1.14**	22.49 $\pm$ 1.77**		31.0 $\pm$ 6.71
HYP/dw [μg/mg]	20.11 $\pm$ 2.03§§	25.94 $\pm$ 3.55* §§	27.69 $\pm$ 2.68* §§	26.25 $\pm$ 2.22** §§		63.0 $\pm$ 12.1
Modulus [MPa]	9.63 $\pm$ 0.86§§ ♯♯	10.74 $\pm$ 1.32§ ♯♯	19.02 $\pm$ 1.06** †† ♯♯	21.54 $\pm$ 5.32** †† § ♯♯	circumferential radial	15.6 $\pm$ 6.4 ♯♯ 2.6 $\pm$ 1.2
UTS [MPa]	1.29 $\pm$ 0.20§§ ♯	1.58 $\pm$ 0.10§§ ♯♯	2.43 $\pm$ 0.24** † ♯♯	2.64 $\pm$ 0.65** †† ♯♯	circumferential radial	2.0 $\pm$ 1.5 ♯♯ 0.42 $\pm$ 0.24

Table 5.2: Tissue composition and mechanical properties of engineered tissues in different treatment groups, and native values (mechanical properties from Balguid *et al.* (2007), n = 9). * indicates a difference compared with the *control* group , † is indicative for a difference with the *insulin* group, ‡ represents a difference with the hypoxia group. Differences compared with native tissue was indicated with §, in general for tissue composition and with respect to circumferential direction for mechanical properties. Differences with native radial direction was indicated by ♯. Single or double symbols indicate $p < 0.05$, and $p < 0.01$, respectively.

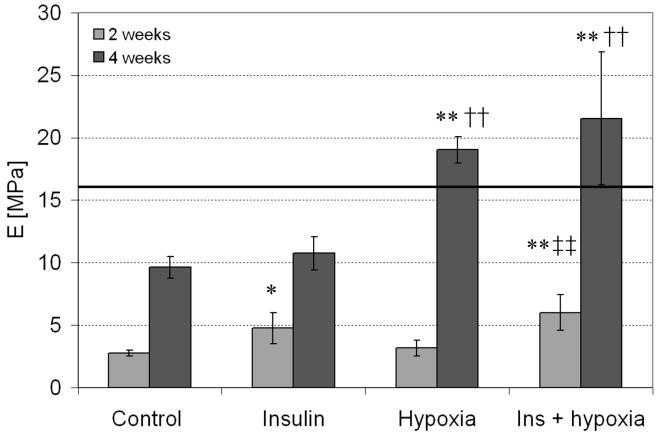

Figure 5.2: Tissue stiffness (E) in the engineered constructs after 2 and 4 weeks of culture. After 2 weeks both insulin treated groups, under normal and hypoxic conditions, showed a significant increase in tissue stiffness compared with the control group. After 4 weeks both groups cultured under hypoxic conditions showed a distinct increase in tissue stiffness compared with the untreated control, in contrast with the insulin group. The bold black line indicates the average stiffness of human native aortic valve leaflets in the circumferential direction. Statistical comparisons were performed only between groups of the same culture period. * and ** indicate a difference compared with the *control* group ($p < 0.05$, and $p < 0.01$, respectively), † and †† is indicative for a difference with the *insulin* group ($p < 0.05$, and $p < 0.01$, respectively), ‡ and ‡‡ represent differences with the hypoxia group ($p < 0.05$, and $p < 0.01$, respectively).

the tissue stiffness and strength were distinctly higher than in the control group, but were not different from the hypoxia group.

5.3.3 Comparison of engineered tissue with native human aortic valves

Averaged stress-strain data obtained from human aortic valve leaflets were obtained from previous work (Balguid *et al.*, 2007). The stress-strain curves of the engineered tissue strips and native aortic valve leaflets, in circumferential direction, are shown in figure 5.4. The modulus, UTS and tissue properties of engineered, as well as native tissue are shown in table 5.2. The tissue equivalents cultured under normoxic conditions failed to achieve native values of tissue stiffness and strength, despite the addition of insulin. Remarkably, the groups cultured under hypoxic conditions, with and without the addition of insulin, both showed comparable mechanical behavior

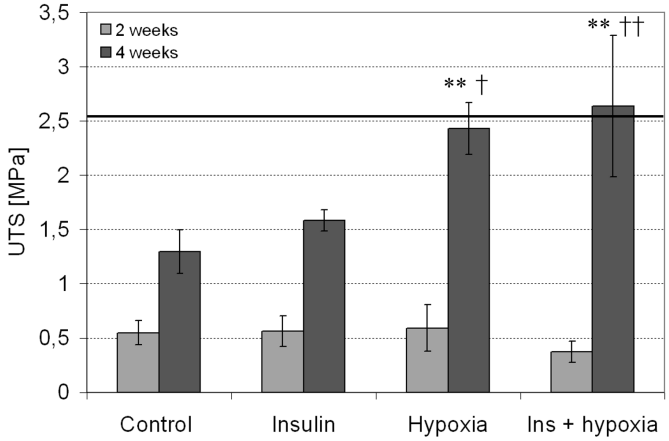

Figure 5.3: Ultimate tensile strength (UTS) in the engineered constructs after 2 and 4 weeks of culture. After 2 weeks the UTS was not different among the groups. A dramatic increase in tissue strength was observed in the hypoxic groups after 4 weeks, in comparison with the normoxic control. The bold black line indicates the average UTS of human native aortic valve leaflets in the circumferential direction. Statistical comparisons were performed only between groups of the same culture period. * and ** indicate a difference compared with the *control* group ($p < 0.05$, and $p < 0.01$, respectively), † and †† is indicative for a difference with the *insulin* group ($p < 0.05$, and $p < 0.01$, respectively), ‡ and ‡‡ represent differences with the hypoxia group ($p < 0.05$, and $p < 0.01$, respectively).

after 4 weeks compared with native valve leaflets in circumferential direction (figure 5.4). The *hypoxia* group showed similar stiffness, and in the *hypoxia + insulin* group the stiffness was even higher than average native values (table 5.2). The anisotropic collagen organization and mechanical properties in native valve leaflets clearly shown in the tissue stiffness and strength in radial, compared with circumferential direction. All engineered tissues are significantly stronger and stiffer, compared with the radial direction of native valve leaflets. The amount of GAGs per cell and per dry weight in the engineered tissues approached native values in the treated groups, however, the amount of collagen and cross-linking remained significantly lower in the engineered tissues.

5.3.4 Histology

Histological examination of the engineered tissues showed homogeneous tissue formation after 2 weeks in all groups figure 5.5. After 4 weeks of culture the tissue composition is very dense and contains considerably more collagen than after 2 weeks. Interestingly, the groups cultured under hypoxic conditions showed denser and more compact tissue, in comparison with the normoxic control and insulin groups.

5.4 Discussion

Living autologous valve replacements contain many attractive and promising perspectives, such as the ability to grow and remodel, which is especially relevant for pediatric and adolescent patients. However, such valvular substitutes, when based on biodegradable synthetic scaffolds, have not yet reached sufficient tissue properties and mechanical integrity for systemic applications (Hoerstrup *et al.*, 2000; Sodian *et al.*, 2000). To ensure durable functioning of TE valves the complex anisotropic mechanical behavior of native aortic valves should be realized (i.e. much stiffer and stronger in circumferential, than in radial direction of the valve leaflet), associated with a highly organized collagen matrix. Therefore, it is proposed to set the benchmark for engineered valves predominantly on the mechanical characteristics of human native aortic valves. Although mechanical anisotropic behavior was shown to be achieved in TE valves by mechanical conditioning during culture, the tissue stiffness and strength needed additional improvement (Mol *et al.*, 2006). Both insulin and hypoxia have previously shown stimulatory effects on engineered tissue equivalent in terms of matrix production (Neidert *et al.*, 2002; Horino *et al.*, 2002; Saini and Wick, 2004; Tokudome *et al.*, 2004), and may be a key factor in attaining native properties in TE heart valves. The aim of this study was to enhance tissue development during culture by the addition of insulin to the culture medium and reducing the oxygen level to physiologically relevant values.
Hypoxia induced increased mechanical properties, associated with improved extracellular matrix biosynthesis. These responses were observed moderately after 2 weeks of culture, but the major effect of hypoxia occurred between 2 and 4 weeks of culture. Remarkably, the addition of insulin during culture under normoxic conditions

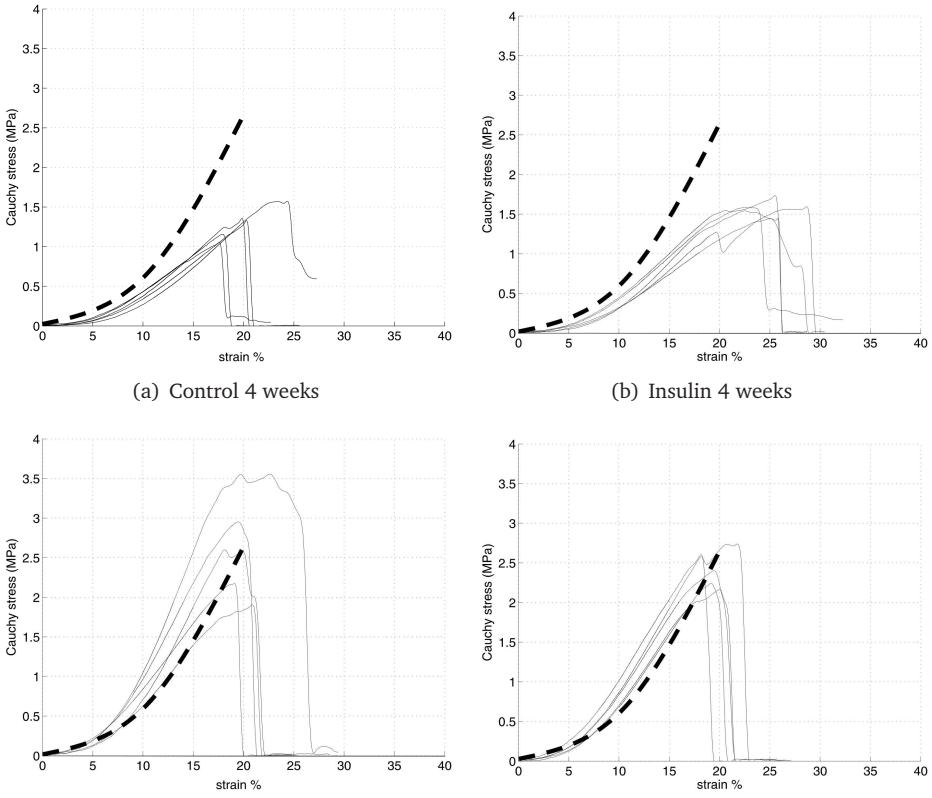

(a) Control 4 weeks

(b) Insulin 4 weeks

(c) Insulin + Hypoxia 4 weeks

(d) Hypoxia 4 weeks

Figure 5.4: Stress-strain curves of engineered tissue strips after 4 weeks of culture. The control group (a) and the insulin group (b) were both cultured under normoxic conditions. The hypoxic groups, cultured with (c) and without (d) the addition of insulin, showed improved tissue stiffness and strength. The bold, dashed line overlaid in each graph indicates the stress-strain curve of human aortic valve leaflets in the circumferential direction (obtained from Balguid *et al.* (2007)).

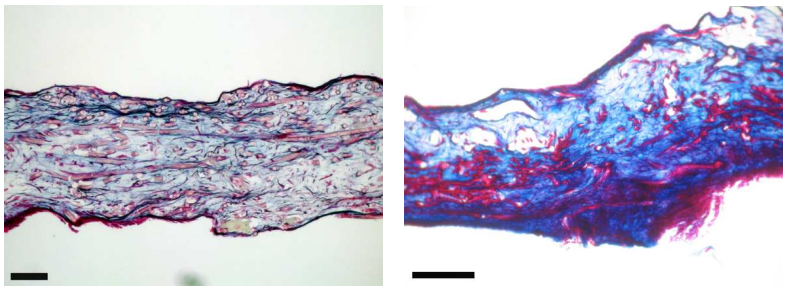

(a) Control 2 weeks

(b) Control 4 weeks

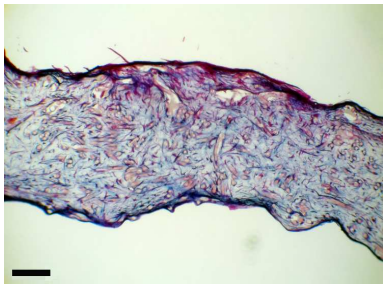

(c) Insulin 2 weeks

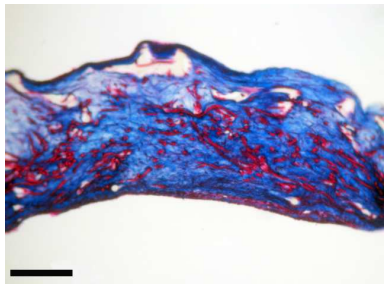

(d) Insulin 4 weeks

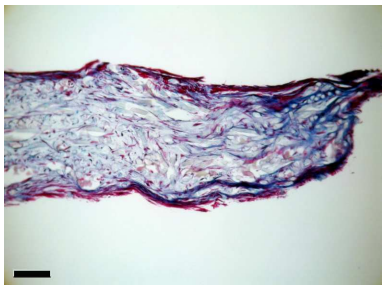

(e) Hypoxia 2 weeks

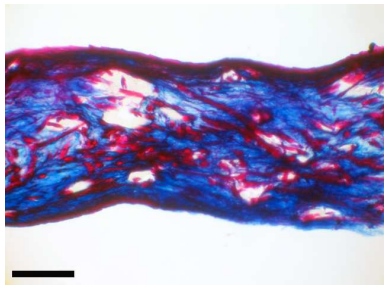

(f) Hypoxia 4 weeks

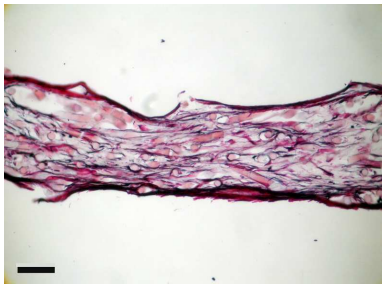

(g) Insulin + Hypoxia 2 weeks

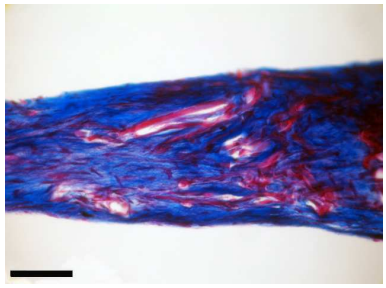

(h) Insulin + Hypoxia 4 weeks

Figure 5.5: Masson trichrome staining of tissue sections. Homogeneous tissue formation was present after 2 weeks in all groups, and differences were not observed between the groups at this point of evaluation. After 4 weeks, compact and homogeneous tissue was observed in all groups, which appeared more dense in the two groups cultured under hypoxic conditions (f, h), compared with the normoxic groups (b, d). Bars indicate 200 μm.

appeared to enhance the tissue matrix and mechanical properties particularly during the first 2 weeks of culture. This effect of insulin on extracellular matrix biosynthesis was previously demonstrated in various cell types (Neidert *et al.*, 2002; Ross and Tranquillo, 2003; Tokudome *et al.*, 2004; Naito *et al.*, 2006; Williams *et al.*, 2006). Interestingly, besides an increase in collagen production, insulin was reported to enhance synthesis of elastic fibers (Long and Tranquillo, 2003), an essential matrix component in native heart valves. Although elastin was not investigated in the present study, it is considered important in further progress in heart valve TE, and will be a focus in future research. The addition of insulin induced a substantial increase in GAG production by the cells. A possible explanation is that the gel-like GAG molecules may help retaining matrix proteins in the tissue matrix, thus adopting the function of fibrin in this system (Mol *et al.*, 2005a). This could account for the improvement in tissue stiffness after 2 weeks compared with the control group. Measurement of the matrix proteins in the culture medium of the insulin and control group would clarify this matter, and will be subject for further investigation.

Interestingly, the hypoxic insulin group did not show this increase in GAG production. This discrepancy may be explained by the impact of scaffold degradation on cell metabolism. Under normal culture conditions the scaffold would degrade within 2 to 4 weeks. The hypoxic environment may have induced a moderately higher acidity in the culture medium (Gawlitta, 2005), which could result in accelerated scaffold degradation, leading to an even lower pH. An acidic environment has been reported to suppress cell metabolism and negatively affect GAG and collagen biosynthesis, thus interfering with tissue development (Reipschlager and Portner, 1996; Wu *et al.*, 2007). This degradation effect is expected to predominantly occur within the first 2 weeks, as the major part of the PGA scaffold degrades during this time frame. Therefore, this effect on the tissue properties was not observed after 4 weeks of culture. Despite the argument that hypoxia enhanced collagen cross-linking already within 2 weeks, one might speculate that hypoxic conditions should be postponed until a significant part of the scaffold has degraded. Hypoxia induced variable effects on tissue composition and mechanical properties after different culture periods. Evident correlations between collagen, cross-linking and mechanical properties were not observed (data not shown). Clearly, the mechanical properties and structural integrity of a tissue are determined by the combined contribution of cross-linking, collagen alignment, amount and type, and these factors may vary during culture.

The present study demonstrated that by culturing under low oxygen tension, engineered heart valve tissue reached mechanical characteristics of native adult aortic valves. It should be noted that these results were achieved in a model system of rectangular tissue strips. Obviously, caution is in order to extrapolate these data to a heart valve geometry. However, tissues of such strength have not been achieved previously, hence these findings are a major step forward in heart valve tissue engineering.

The tissue stiffness and ultimate tensile strength of these groups were comparable with native values. Native valve leaflets appeared slightly more flexible compared with the hypoxic engineered tissues in the lower strain range (0-10%). The matrix structure of native aortic valve leaflets are composed such that they allow movement and extension of the tissue (up to 10%) at minimal load. Above 10% strain, collagen

fibers lock up and the tissue becomes stiffer to carry the high pressure difference over the valve (Schoen and Levy, 1999). This combined flexibility and rigidity is necessary for proper functioning of the valve. Higher flexibility of the engineered tissues in the lower strain range may therefore be desirable. Dynamic conditioning in a strain-based bioreactor previously demonstrated to result in anisotropic mechanical behavior. As this system imposes constant movement to the engineered valve, it may additionally result in improved flexibility.
Lower concentrations of matrix proteins were measured in the engineered tissues compared with human native valves. Yet, the mechanical properties of the engineered tissues were similar to those of adult native tissue. This discrepancy may be explained by the difference in structure between the engineered and native tissues. Native aortic valves consist of a three-layered tissue matrix, of which only one layer, the fibrosa, bears the largest part of the load during the cardiac. In the engineered tissues the collagen distribution in the tissue matrix is more homogeneous, allowing a relatively homogeneous stress distribution over the tissue. This may account for the differences in the ratios of matrix components and mechanical behavior between engineered and native tissue.
In this study, engineered tissues were compared with adult native aortic valves. In prenatal development, aortic valves initially show a homogeneous matrix distribution, mainly consisting of proteoglycans. Not until after birth a three-layered structure in the valve gradually develops, together with collagen fiber alignment and maturation (Aikawa *et al.*, 2006). This in-time development of the aortic valve raises the question of to what extent TE valves need to resemble adult native valve structure, because *in vivo* remodeling is expected to occur upon implantation (Hoerstrup *et al.*, 2000).
Further studies are required to determine how variations in cell source, scaffold geometry and mechanical conditioning protocol will affect the ECM expression and physiological properties of the engineered tissue cultured under hypoxic conditions. Moreover, ultrastructural, immunochemical and gene expression studies will be performed as a next step to elucidate the mechanism behind hypoxia-induced strengthening of the tissues. Yet, the results presented here strongly indicate that oxygen tension is a key parameter that promotes the development of human venous myofibroblasts into heart valve tissue equivalents. The combination of hypoxia with mechanical conditioning of TE heart valves will be topic of further research, to improve anisotropic mechanical behavior of the valve leaflets and enhance the tissues' flexibility in the lower strain range.

5.5 Conclusion

The results presented in this study demonstrated that the use of hypoxic culture conditions resulted in the mechanical characteristics of native aortic valve tissue. To our knowledge, this has not been demonstrated previously. These findings bring the potential use for systemic applications a step closer, and can be considered an important improvement in heart valve tissue engineering.

Acknowledgements

The work of Angelique Balguid forms part of the research program of the Dutch Polymer Institute (project 475). The authors would like to thank Anita van de Loo, Eindhoven University of Technology, Eindhoven, The Netherlands, and Jessica Snabel, TNO Health and Prevention, Leiden, The Netherlands for their contribution to this work.

Chapter 6

General discussion

6.1 Introductory remarks

Tissue engineered heart valves present many attractive and promising perspectives. Especially for pediatric and adolescent patients, the implantation of autologous, living and adapting valvular substitutes would be a valuable option. Up to now, these patient groups commonly receive non-living valvular prosthesis, and are often subjected to multiple re-operations, with all risks and consequences involved. This has been an important motivation for researchers in the field of heart valve tissue engineering.
One of the main challenges in this field is to create valvular leaflets, that despite their minimal thickness, are sufficiently strong to bear the physiological loads in the aortic position. Furthermore, to ensure durable functioning of TE valves the complex anisotropic mechanical behavior of native aortic valves should be realized (i.e. stiffer and stronger in circumferential, than in radial direction of the valve leaflet), associated with a highly organized collagen matrix.
TE heart valves of ovine origin have been successfully implanted in the pulmonary position in sheep, showing a native-resembling function and tissue composition after five months (Sodian *et al.*, 2000; Hoerstrup *et al.*, 2000). However, the valves did not show sufficient mechanical strength for systemic pressure applications, such as the aortic valve. The application of dynamical conditioning during culture in the bioreactor resulted in the fabrication of human tissue engineered valves that could withstand physiological systemic pressures for 4 hours in an *in vitro* setup (Mol *et al.*, 2006). Excitingly, after 4 weeks of culture the TE valves showed developing anisotropic mechanical properties. Though these results are promising, native values of tissue strength or composition were not yet attained in the engineered heart valves.
This raises the question whether native properties are a necessary requirement for clinical applications, or can durable functioning also be achieved by *in vivo* remodeling and adaptation? For future *in vivo* applications one of the most important questions is: How good is good enough for *in vivo* survival of TE heart valves? Criteria are necessary to determine when TE tissue qualifies for implantation in patients. In this thesis, bench-marks were chosen based on mechanical properties and corresponding tissue composition (in particular the collagen architecture) of healthy human adult aortic valve leaflets.
To reach mechanical characteristics and tissue composition of native aortic valves, the stiffness and strength of engineered tissues needed additional improvement. Two main approaches were employed to enhance these parameters. First, it was attempted to improve the mechanical properties by enhancing matrix biosynthesis in tissue-equivalents using environmental and biochemical stimuli during culture (section 6.3.2). Secondly, a slow degrading scaffold material was chosen to provide durable support to the newly formed tissue (section 6.3.3).
Future perspectives of heart valve tissue engineering, in terms of optimization of the culturing protocol and future clinical applications are discussed in section 6.4.

6.2 Native heart valves as bench-mark

In terms of eventual clinical applications and risk assessment, it is necessary to define qualitative and quantitative criteria for TE heart valves. A list of requirements for clinically used non-living cardiac valve prosthesis, which may also apply to TE valves, were formulated as ISO standards (ISO 5840:2005). These are:

- to allow forward flow with acceptably small mean pressure difference
- to prevent retrograde flow with acceptably small regurgitation
- to resist embolization and haemolysis
- biocompatibility
- compatibility with *in vivo* diagnostics
- deliverable and implantable in the target population
- to remain fixed once placed
- to maintain its functionality for a reasonable lifetime
- to maintain its functionality and sterility for a reasonable time prior to implantation

Whether these criteria are sufficient for TE heart valves remains to be discussed, as objective criteria and regulations are not available for TE products. In terms of future clinical applications and risk assessment, these should be defined in consultation with clinical specialists.
Some of the above requirements were already evaluated to determine the functionality of TE valves. In an *in vitro* setup Mol *et al.* (2006) demonstrated functional opening and closing behavior of a TE heart valve, as well as the capability of bearing physiological systemic loading, by monitoring the mean pressure gradient, regurgitation and effective orifice area under conditions. Additionally, the mechanical characteristics of a TE valve were used to predict the functioning of the valve by simulating the mechanical response to physiological loading in a previously developed computational model (Driessen *et al.*, 2007). Several *in vivo* studies evaluated the functioning of autologous TE valves in sheep models (Shinoka *et al.*, 1995; Sodian *et al.*, 2000; Hoerstrup *et al.*, 2000). The opening and closing behavior of the valve was monitored with Doppler echocardiography, the pressure gradient was assessed as a measure for the resistance to forward flow. Additionally, the surface morphology, endothelialization, *in vivo* tissue remodeling, inflammation responses, and cell phenotype characterization macroscopic may be investigated to evaluate the TE implant. Optimization of TE protocols in order to obtain stronger tissue, requires systematic and fundamental research, which is often performed with simplified, instead of heart valve, scaffold geometries. Although functionality measurements are not feasible for these geometries, qualitative or quantitative bench-marks for these TE experiments

are necessary for mutual comparisons and reproducibility. In this thesis mechanical properties were considered adequate testing characteristics as they represent the tissues' quality and integrity. The mechanical properties of healthy native human aortic valves were considered objective bench-marks for engineered tissues, and were used to develop TE strategies (section 6.2 and 6.3.1). In this thesis, adult human heart valves were analyzed to obtain bench-marks for tissue engineering. However, to what extent are adult human valve characteristics, in terms of mechanical properties and tissue composition, a fair and reasonable comparison for engineered tissue after merely 4 weeks of culture?
Even though the mechanical characteristics of engineered tissues approached native values, the tissue composition was considerably different (Chapter 5). Homogeneous tissue matrices were observed in the engineered tissues after 4 weeks of culture, in contrast with the highly organized layered structure present in adult native valve leaflets (Chapter 2). In the development from the prenatal to adult phase, the human aortic valve is subjected to and must adapt to continuous changes of mechanical stress. In the prenatal phase, aortic valves initially show a homogeneous matrix distribution, mainly consisting of proteoglycans. Not until after birth a three-layered structure in the valve gradually develops, together with collagen fiber alignment and maturation (Aikawa *et al.*, 2006). Maturation and remodeling of the tissue structure clearly takes time, therefore, a comparison with fetal or pediatric heart valves may be more valid. Due to the highly limited availability of healthy pediatric donor tissue, these were not studied, and only adult valves were investigated in the present work.

6.3 Main findings and implications

6.3.1 Structure-function relation in native aortic valves

Tissue mechanical behavior is strongly related to the collagen organization, which, in turn, is related to the mechanical loading conditions of the tissue (Boerboom, 2007), (This thesis, Chapter 2 and 3). In Chapters 2 and 3 the role of collagen on mechanical behavior, and mechano-induced collagen morphology in native human aortic valves was investigated. The results demonstrated a dominant role for collagen cross-links, and not for collagen content, with respect to tissue stiffness in human heart valve leaflets. However, collagen cross-links do not exclusively determine the mechanical behavior of heart valve tissue. The efficiency of mechanical reinforcement of collagen fibrils and the ability of the tissue to sustain an applied load also depends on the collagen fibril morphology, the fiber orientation, the types of collagen present and the waviness of the collagen fibrils. Reversely, it was demonstrated that the level of tissue stress influences the collagen fibril morphology, suggesting a counteracting mechanism. This stress-related collagen structure may be of interest in collagen remodeling studies and computational models. The mechanical behavior of the native aortic valve leaflets, obtained from Chapter 2, was used to define objective requirements for tissue engineering.
One step in satisfying these requirements may be mechanical stimulation. Previous

studies have shown mechano-induced upregulation of collagen and cross-links and collagen fibril orientation in myofibroblasts (Kolpakov *et al.*, 1995; Engelmayr *et al.*, 2005; Boerboom, 2007). Moreover, dynamic conditioning of engineered valves during culture improved collagen architecture, leading to anisotropic tissue behavior (Mol *et al.*, 2006). Despite these promising results, the tissue-engineered cardiovascular tissues did not attain the strength or stiffness of their native adult counterparts. Therefore, it was attempted to improve these parameters by employing two approaches (figure 1.9), namely 1) applying biochemical and environmental stimuli to enhance tissue development (Chapter 5), and 2) using a slow degrading polymer scaffold to provide mechanical integrity for several months, while *in vivo* tissue development gradually takes over this function (Chapter 4).

6.3.2 Environmental cues

Cells can be stimulated to produce more extracellular matrix (ECM) proteins and enhance tissue quality and integrity by the use of biochemical and environmental cues. In Chapter 5 the separate and combined effect of insulin and low oxygen tension, or hypoxia, on tissue composition and mechanical behavior were evaluated. Remarkably, exposing the cells and ECM to hypoxia in a 3D environment considerably improved the strength and stiffness of engineered heart valve tissue, and was associated with higher collagen and cross-linking values. Similar effects were observed in different cell types of various 2D and 3D studies. In previous *in vitro* monolayer studies (2D), hypoxia was reported to increased cellular proliferation, and upregulate collagen I/III mRNA expression (Moussavi-Harami *et al.*, 2004; Scherer *et al.*, 2004). In human adipose derived and mesenchymal stem cells, hypoxia induced significant increases in protein synthesis, and higher expression of differentiation markers compared with normal oxygen conditions in 2D and 3D environments (Wang *et al.*, 2005; Grayson *et al.*, 2006). Furthermore, fibroblast cells from various sources showed increases at the mRNA and protein level in fibronectin, collagen I and collagen IV under hypoxic conditions (Durmowicz *et al.*, 1994; Chen *et al.*, 2005).
To elucidate the underlying mechanism of hypoxia related protein expression, Falanga *et al.* (1993, 2002) investigated the role of transforming growth factor β1 (TGF-β1) in collagen expression pathways. Interestingly, it was demonstrated that the upregulation of Col1α mRNA levels failed to occur in fibroblasts from TGF-β1 knock-out mice. It was postulated that low oxygen tension stimulates collagen synthesis and Col1α transcription through the action of TGF-β1. Although TGF-β1 is naturally present *in vivo*, and it may appear an interesting additive, it may not be a suitable supplement for TE, as it is known for its potentially oncogenic effect (Leivonen and Kahari, 2007). The addition of insulin resulted in an upregulation of collagen and GAGs, in particular during the first two weeks of culture (This thesis, Chapter 5). Increased protein synthesis upon addition of insulin were also reported in cardiac myocytes, cardiac fibroblasts, and aortic smooth muscle cells (Zimmermann *et al.*, 2002; Neidert *et al.*, 2002; Tokudome *et al.*, 2004; Naito *et al.*, 2006). Apart from the increase in protein synthesis, the enhancing effect of insulin on tissue development may be related to

the abundant presence of GAGs in the insulin constructs. As GAGs possess gel-like properties, they might entrap the newly synthesized collagen fibrils, hereby accelerating tissue formation. This feature may be valuable in the initial culture phase to maximally retain the newly produced structural proteins, after which remodeling and maturation can be enhanced by mechanical stimuli or hypoxia.
It can be concluded that hypoxia is a useful tool in tissue engineering, perhaps because it provides a better representation of *in vivo* oxygen supply to the cells. The next step towards functional TE heart valves for systemic applications would be to develop a protocol that combines the favorable effects of insulin and hypoxia with dynamic conditioning of the tissue, successively or simultaneously. This combination of mechanical and environmental cues may lead to both improved tissue strength, and anisotropic mechanical properties.

6.3.3 Scaffold design

Scaffold design is crucial for successful tissue engineering. In chapter 4 the feasibility of a slow degrading polymer scaffold, electrospun poly-ε-caprolactone, was evaluated for cardiovascular TE, and compared with the currently used rapid degrading polyglycolic acid/poly-4-hydroxybutyrate (PGA-P4HB) scaffold. Optimization of the spinning parameters was necessary, as fiber thickness of the PCL scaffold appeared highly correlated with cellular infiltration. Despite the attractive features of nanofiber scaffolds, cellular infiltration was impeded in thin fiber scaffolds (Chapter 4). These findings argue for a shift from nano to micro fiber meshes for use in 3D TE applications.
After optimization of the electrospun PCL scaffold, it allowed for proper cell ingrowth and ECM biosynthesis, while retaining elastic properties and mechanical integrity. Slow degrading PCL scaffolds appear a promising alternative to PGA-P4HB scaffolds, specifically for TE blood vessels and the outer wall of a TE heart valve, where external mechanical support is desired over a longer time. For applications such as TE heart valve leaflets, where the scaffold is prone to constant movement, the relatively large stiffness of the scaffold material may obstruct blood flow to a certain degree. By way of comparison, the native heart valve leaflets are quite flexible as a whole, allowing blood flow through the valve with minor resistance. Only when the stresses in the leaflet exceed certain threshold values, the collagen structure in the leaflet locks, and the valve becomes stiffer. This non-linear material behavior may be difficult to capture in a scaffold material, however, improvement of the scaffold design (e.g. native-like layered structure) may enhance its functionality. All things considered, electrospinning allows the relatively easy fabrication of tailor-made scaffold geometries and structures, which will be valuable for future patient-specific TE applications.

In conclusion, both strategies have led to interesting prospects for different applications in TE. For heart valve TE, the scaffold may be constructed of a combination of PGA-P4HB leaflets and an electrospun PCL aortic root to profit from both polymers,

while cultured under hypoxic conditions to promote tissue strength. This may provide an interesting approach towards systemic application of autologous non-stented heart valves.

6.4 Future perspectives and recommendations

6.4.1 Standardization of the culturing protocol

During tissue culture, specific factors and stimuli are required to simulate the physiological environment and to induce functionality of cells and tissue. Low oxygen tension in the medium, equivalent to that in arterial blood, is one example that resulted in significant improvement of tissue strength during culture (Chapter 5). Besides hypoxia, a variety of external and cell-associated conditions may influence the outcome of TE experiments.
Various factors that may contribute to discrepancies between TE experiments are cell source, seeding density, frequency of medium change, batch-variability of additives, cell passage number, etcetera. This may explain the high variability in tissue characteristics that were observed between different experiments. For example, in Chapter 4 and 5 the same model system was used, however, large variations in mechanical properties were present between the experimental groups after 4 weeks. These variations may be attributed to the cell seeding density, as this was the only obvious difference between the experiments. Similar findings were reported previously by Mol (2005). To limit the discrepancies between experiments, standardization of culturing methods is crucial.

6.4.2 Optimization towards clinical applications

Although clinical applications of TE heart valves is not yet in order, results from *in vitro* experiments and animal models offer promising prospects. The translation of animal models to humans, as well as patient-specificity are crucial items that should be investigated prior to future clinical applications in humans. Various improvements that may be introduced in the culturing protocol, are described in this section.

Elastin

To achieve improved tissue strength for the systemic application of TE heart valves, the collagen architecture was the primary focus of attention. In native heart valves, elastin is another critical structural and regulatory matrix protein, responsible for the tissues flexibility and returning to the undeformed state (Schoen, 1997). This protein was not investigated in the present study. The presence of elastin may optimize the tissue structure and contribute to the functional behavior of the valve. Therefore, the possibilities to promote elastin production, by growth factors or other stimuli, will be

investigated in future TE research.

Patient specificity and cell source

Differentiation markers may be used as an indicative tool to predict the synthetic or proliferative capacities of a cell source. Some myofibroblast differentiation markers are α-smooth muscle actin, vimentin, calponin, desmin, and caldesmon (Zalewski *et al.*, 2002; Opitz *et al.*, 2004; Schmidt *et al.*, 2005). The expression level of these differentiation markers in human venous myofibroblasts can be influenced with external factors, such as environmental and mechanical stimuli (Zalewski *et al.*, 2002; Hinz, 2006). However, the diversity of these cells, in terms of morphology, growth and protein synthesis may be high among different cell donors, and varying expression of growth regulatory genes may be expected. Therefore, mapping the fenotype markers for each cell source prior to tissue culture, may provide an insight in the cell-specific requirements to optimize the outcome of a TE product. Additionally, cells from each patient could be screened for gene expression (e.g. for collagen, various enzymes), to predict the protein expression level of the cells in tissue culture. Based on these predictions the culturing protocol may be adapted to patient-specific requirements. For example, cells with low collagen I or α-SMA expression may be stimulated with additional growth factors or mechanical stimuli (Hinz, 2006).
Furthermore, patients may provide autologous serum to be used during cell and tissue culture. Currently, culturing human cells occurs with medium supplemented with the fetal bovine serum. Animal-derived products should ideally be omitted regarding their association with zoonoses (Knight and Collins, 2001). The use of autologous human serum and fibrin would reduce the amount of foreign body substances in the cultured tissue, hence decrease the risk of immunological responses after implantation.
The optimal cell source for TE purposes may be patient specific. Constructs from saphenous vein derived myofibroblasts were reported to show excellent *in vitro* tissue generation, in terms of collagen formation and the tissues' mechanical properties (Schnell *et al.*, 2001; Mol *et al.*, 2006). Saphenous vein is easy to access for adult and pediatric patients, however for neonatal patients with congenital heart valve disorders this is hardly an option. Schmidt *et al.* (2005, 2006, 2007) demonstrated the feasibility to generate living autologous heart valve leaflets using umbilical cord stem cells, as well as amniotic fluid derived progenitor cells as single cell sources. Both cell types possessed the ability to differentiate into myofibroblasts- like cells and endothelial cells. Although similar mechanical conditioning protocols, as described by Mol *et al.* (2006), were used, tissue strength and collagen synthesis were considerably below native values. In view of the different physiological cellular niche compared with the adult saphenous vein myofibroblasts used by Mol *et al.* (2006), these cell types may require different mechanical or environmental stimuli to improve their *in vitro* development. Nevertheless, these cell sources have promising prospects for neonatal patients, as they can be harvested amply before birth, enabling the prenatal fabrication of autologous heart valves.

Translations from bench to bed-side

Geometrical differences between scaffolds (rectangular strips, heart valve geometries) may be associated with different cellular responses. The cells in a rectangular tissue strip, as described in this thesis, may respond differently to environmental or mechanical stimuli, than those in a heart valve geometry. Therefore, the effects of these stimuli should additionally be evaluated in TE heart valves, preferably cultured in a bioreactor with controlled mechanical loading (Kortsmit *et al.*, 2006). Furthermore, the translation from a adult-sized valve to a neonatal or pediatric valve may also require adaptations of the culturing protocol. This specifically regards the magnitude of applied loading and the dynamical conditioning frequency, as changes in mechanical loading occur during *in vivo* development of the valve.
Finally, it remains to be questioned whether the bench-marks developed from adult native human tissue may be used universally. As mentioned previously, neonatal or pediatric TE heart valves may not need to approach adult native tissue to function adequately. Oppositely, for a patient with severe hypertension a TE heart valve may require higher strength and stiffness than the bench-mark values obtained from healthy individuals. The reasoning above argues for a patient-specific approach in the fabrication of TE heart valves.

6.5 General conclusions

One of the main challenges in this thesis was to create heart valve tissue equivalents that approach native tissue characteristics. As a first step, quantitative bench-marks based on mechanical characteristics of native human aortic valves were defined. Two approaches, based on scaffold design and environmental cues, were successfully adopted to create stronger engineered tissues.
In this thesis it was demonstrated that engineered heart valve tissue could reach mechanical characteristics of native adult aortic valves by culturing under hypoxic conditions. Engineered tissues, based on rapid degrading polymers, of such strength have not been achieved up to now, therefore, oxygen tension may be considered a key parameter to promote tissue formation by human venous myofibroblasts. This development brings the potential use for systemic applications a step closer, and can be considered an important improvement in heart valve tissue engineering.

Bibliography

Aikawa, E., Whittaker, P., Farber, M., Mendelson, K., Padera, R., Aikawa, M., and Schoen, F. (2006). Human semilunar cardiac valve remodeling by activated cells from fetus to adult: implications for postnatal adaptation, pathology, and tissue engineering. *Circulation*, **113**(10), 1344–1352.

Anderson, L. H., Roberts, F. J., Wilson, B., and Mehm, W. J. (1991). Altering the dissolved oxygen tension in tissue culture media. *Journal of tissue culture methods*, **13**(4), 241–246.

Avery, N. C. and Bailey, A. J. (2005). Enzymic and non-enzymic cross-linking mechanisms in relation to turnover of collagen: relevance to aging and exercise. *Scandinavian journal of medicine and science in sports*, **15**, 231–240.

Baer, E., Hiltner, A., and Friedman, B. (1975). Relationship of the ultrastructure and mechanical properties in tendinous collagen, a highly ordered macromolecular composite. *Journal Mechanics of Composite Materials*, **11**(6), 896–904.

Bailey, A. J., Paul, R., and Knott, L. (1998). Mechanisms of maturation and ageing of collagen. *Mechanisms of Ageing and Development*, **106**, 1–56.

Balguid, A., Rubbens, M., Mol, A., Bank, R., Bogers, A., van Kats, J., de Mol F.P. Baaijens, B., and Bouten, C. (2007). The role of collagen cross-links in biomechanical behavior of human aortic heart valve leaflets-relevance for tissue engineering. *Tissue Engineering*, **13**(7), 1501–1511.

Bank, R. A., Jansen, E. J., Beekman, B., and TeKoppele, J. M. (1996). Amino acid analysis by reverse-phase high-performance liquid chromatography: improved derivatization and detection conditions with 9-fluorenylmethyl chloroformate. *Analytical Biochemistry*, **240**, 167–176.

Bank, R. A., Beekman, B., Verzijl, N., de Roos, J. A., Sakkee, A. N., and TeKoppele, J. M. (1997). Sensitive fluorimetric quantitation of pyridinium and pentosidine crosslinks in biological samples in a single high-performance liquid chromatographic run. *J.Chromatogr.B Biomed.Sci.Appl.*, **703**, 37–44.

Banse, X., Sims, T. J., and Bailey, A. J. (2002). Mechanical properties of adult vertebral cancellous bone: correlation with collagen intermolecular cross-links. *J. Bone Miner. Res.*, **17**(9), 1621–1628.

Bashey, R. I., Torii, S., and Angrist, A. (1967). Age-related collagen and elastin content of human heart valves. *Journal of gerontology*, **22**, 203–208.

Beekman, B., Verzijl, N., Bank, R. A., von der, M. K., and TeKoppele, J. M. (1997). Synthesis of collagen by bovine chondrocytes cultured in alginate; posttranslational modifications and cell-matrix interaction. *Experimental Cell Research*, **237**(1), 135–141.

Billiar, K. L. and Sacks, M. S. (2000a). Biaxial mechanical properties of the natural and glutaraldehyde treated aortic valve cusp - part I: experimental results. *Journal of biomechanical engineering*, **122**, 23–30.

Billiar, K. L. and Sacks, M. S. (2000b). Biaxial mechanical properties of the natural and glutaraldehyde treated aortic valve cusp - part II: a structural constitutive model. *Journal of biomechanical engineering*, **122**, 327–335.

Bloomfield, P., Wheatley, D. J., Prescott, R. J., and Miller, H. C. (1991). Twelve-year comparison of a bjork-shiley mechanical heart valve with porcine bioprostheses. *N. Engl. J. Med.*, **324**(9), 573–579.

Boerboom, R. A. (2007). *Mechano-control of tissue properties in engineered cardiovascular constructs*. Ph.D. thesis, Eindhoven University of Technology.

Brightman, A. O., Rajwa, B. P., Sturgis, J. E., McCallister, M. E., Robinson, J. P., and Voytik-Harbin, S. L. (2000). Time-laps confocal reflection microscopy of collagen fibrillogenesis and extracellular matrix assembly in vitro. *Biopolymers*, **54**, 222–234.

Brinckmann, J., Kim, S., Wu, J., Reinhardt, D., Batmunkh, C., and Metzen, E. (2005). Interleukin 4 and prolonged hypoxia induce a higher gene expression of lysyl hydroxylase 2 and an altered cross-link pattern: important pathogenetic steps in early and late stage of systemic scleroderma? *Matrix Biol*, **24**(7), 459–468.

Broom, N. (1988). Connective tissue function and malfunction: a biomechanical perspective. *Pathology*, **20**(2), 93–104.

Centrella, M., Casinghino, S., Ignotz, R., and McCarthy, T. L. (1992). Multiple regulatory effects by transforming growth factor-beta on type i collagen levels in osteoblast-enriched cultures from fetal rat bone. *Endocrinology*, **131**(6), 2863–2872.

Cesarone, C. F., Bolognesi, C., and Santi, L. (1979). Improved microfluorometric dna determination in biological material using 33258 hoechst. *Analytical Biochemistry*, **100**, 188–197.

Champe, P. and Harvey, R. (1994). *Biochemistry*, chapter 3. Globular and Fibrous Proteins, pages 25–53. Wilkins Publishers, 2nd edition edition.

Charest, A., Pepin, A., Shetty, R., Cote, C., Voisine, P., Dagenais, F., Pibarot, P., and Mathieu, P. (2006). Distribution of sparc during neovascularisation of degenerative aortic stenosis. *Heart*, **92**(12), 1844–1849.

Chen, C., Yang, Y., Su, T., Chen, C., and Aplin, J. (2005). Hypoxia and transforming growth factor-beta 1 act independently to increase extracellular matrix production by placental fibroblasts. *J Clin Endocrinol Metab*, **90**(2), 1083–1090.

Christie, G. and Barratt-Boyes, B. (1995). Age-dependent changes in the radial stretch of human aortic valve leaflets determined by biaxial testing. *Ann Thorac Surg*, **60**(2 Suppl), S156–S158.

Clark, R. E. (1973). Stress-strain characteristics of fresh and frozen human aortic and mitral leaflets and chordae tendineae. implications for clinical use. *J. Thorac. Cardiovasc. Surg.*, **66**(2), 202–208.

Cox, M. A. J., Driessen, N. J. B., Bouten, C. V. C., and Baaijens, F. P. T. (2006). Mechanical characterization of anisotropic planar biological soft tissues using large indentation: A computational feasibility study. *Journal of biomechanical engineering*, **128**, 428–436.

Dahl, S. L., Rucker, R. B., and Niklason, L. E. (2005). Effects of copper and cross-linking on the extracellular matrix of tissue-engineered arteries. *Cell transplantation*, **14**, 861–868.

de Hart, J., Baaijens, F. P. T., Peters, G. W. M., and Schreurs, P. J. G. (2003). A computational fluid-structure interaction analysis of a fiber-reinforced stentless aortic valve. *Journal of biomechanics*, **36**, 699–712.

de Lange, F. J., Moorman, A. F., Anderson, R. H., Manner, J., Soufan, A. T., de Vries, C. G., Schneider, M. D., Webb, S., van den Hoff, M. J., and Christoffels, V. M. (2004). Lineage and morphogenetic analysis of the cardiac valves. *Circ. Res.*, **95**(6), 645–654.

Diamant, J., Keller, A., Baer, E., Litt, M., and Arridge, R. G. C. (1972). Collagen; ultrastructure and its relation to mechanical properties as a function of ageing. *Proceedings of the Royal Society of London. Series B, Biological Sciences*, **180**(1060), 293–315.

Doehring, T. C., Kahelin, M., and Vesely, I. (2005). Mesostructures of the aortic valve. *Journal of heart valve disease*, **14**, 679–686.

Driessen, N. J. B., Boerboom, R. A., Huyghe, J. M., Bouten, C. V. C., and Baaijens, F. P. T. (2003a). Computational analyses of mechanically induced collagen fiber remodeling in the aortic heart valve. *Journal of biomechanical engineering*, **125**, 549–557.

Driessen, N. J. B., Peters, G. W. M., Huyghe, J. M. R. J., Bouten, C. V. C., and Baaijens, F. P. T. (2003b). Remodelling of continuously distributed collagen fibres in soft connective tissues. *Journal of biomechanics*, **36**, 1151–1158.

Driessen, N. J. B., Bouten, C. V. C., and Baaijens, F. P. T. (2005a). Improved prediction of the collagen fiber architecture in the aortic heart valve. *Journal of biomechanical engineering*, **127**, 329–336.

Driessen, N. J. B., Bouten, C. V. C., and Baaijens, F. P. T. (2005b). A structural constitutive model for collagenous cardiovascular tissue incorporating the angular fiber distribution. *Journal of biomechanical engineering*, **127**, 494–503.

Driessen, N. J. B., Mol, A., Bouten, C. V. C., and Baaijens, F. P. T. (2007). Modeling the mechanics of tissue-engineered human heart valve leaflets. *Journal of biomechanics*, **40**(2), 325–334.

Durmowicz, A. G., Parks, W. C., Hyde, D. M., Mecham, R. P., and Stenmark, K. R. (1994). Persistence, re-expression, and induction of pulmonary arterial fibronectin, tropoelastin, and type i procollagen mrna expression in neonatal hypoxic pulmonary hypertension. *Am. J. Pathol.*, **145**(6), 1411–1420.

Eichhorn, S. J. and Sampson, W. W. (2005). Statistical geometry of pores and statistics of porous nanofibrous assemblies. *J.R Soc.Interface*, pages 309–318.

Elbjeirami, W. M., Yonter, E. O., Starcher, B. C., and West, J. L. (2003). Enhancing mechanical properties of tissue-engineered constructs via lysyl oxidase crosslinking activity. *Journal of biomedical materials research*, **66**, 513–521.

Engelmayr, G. C., Rabkin, E., Sutherland, F. W. H., Schoen, F. J., Mayer, J. E., and Sacks, M. S. (2005). The independent role of cyclic flexure in the early in vitro development of an engineered heart valve tissue. *Biomaterials*, **26**, 175–187.

Enwemeka, C., Maxwell, L., and Fernandes, G. (1992). Ultrastructural morphometry of matrical changes induced by exercise and food restriction in the rat calcaneal tendon. *Tissue Cell*, **24**(4), 499–510.

Falanga, V., Martin, T. A., Takagi, H., Kirsner, R. S., Helfman, T., Pardes, J., and Ochoa, M. S. (1993). Low oxygen tension increases mrna levels of alpha 1 (i) procollagen in human dermal fibroblasts. *J. Cell Physiol*, **157**(2), 408–412.

Falanga, V., Zhou, L., and Yufit, T. (2002). Low oxygen tension stimulates collagen synthesis and col1a1 transcription through the action of tgf-beta1. *J. Cell Physiol*, **191**(1), 42–50.

Farndale, R. W., Buttle, D. J., and Barrett, A. J. (1986). Improved quantitation and discrimination of sulphated glycosaminoglycans by use of dimethylmethylene blue. *Biochim. Biophys. Acta*, **883**, 173–177.

Fournier, R. L. (1999). *Basic Transport Phenomena in Biomedical Engineering*. Taylor and Francis, Philadelphia, USA.

Frank, C., McDonald, D., Wilson, J., Eyre, D., and Shrive, N. (1995). Rabbit medial collateral ligament scar weakness is associated with decreased collagen pyridinoline crosslink density. *J. Orthop. Res.*, **13**(2), 157–165.

Gawlitta, D. (2005). *Compression-induced factors influencing the damage of engineered skeletal muscle*. PhD thesis, Technische Universiteit Eindhoven.

Girton, T. S., Oegema, T. R., and Tranquillo, R. T. (1999). Exploiting glycation to stiffen and strengthen tissue equivalents for tissue engineering. *Journal of biomedical materials research*, **46**, 87–92.

Gray, H. (1918). *Anatomy of the Human Body*. Philadelphia: Lea and Febiger.

Grayson, W. L., Zhao, F., Izadpanah, R., Bunnell, B., and Ma, T. (2006). Effects of hypoxia on human mesenchymal stem cell expansion and plasticity in 3d constructs. *J. Cell Physiol*, **207**(2), 331–339.

Grunkemeier, G. L. and Rahimtoola, S. H. (1990). Artificial heart valves. *Annu. Rev. Med.*, **41**, 251–263.

Gunatillake, P. A. and Adhikari, R. (2003). Biodegradable synthetic polymers for tissue engineering. *European Cells and Materials*, **5**, 1–16.

Hammermeister, K., Sethi, G. K., Henderson, W. G., Grover, F. L., Oprian, C., and Rahimtoola, S. H. (2000). Outcomes 15 years after valve replacement with a mechanical versus a bioprosthetic valve: final report of the veterans affairs randomized trial. *J. Am. Coll. Cardiol.*, **36**(4), 1152–1158.

Haralson, M. and Hassell, J. R. (1996). *Extracellular Matrix: A Practical Approach*. Oxford University Press, USA.

Harken, D. E., Taylor, W. J., Lefemine, A. A., Lunzer, S., Low, H. B., Cohen, M. L., and Jacobey, J. A. (1962). Aortic valve replacement with a caged ball valve. *Am. J. Cardiol.*, **9**, 292–299.

Harris, E. D., Rayton, J. K., Balthrop, J. E., DiSilvestro, R. A., and de Quevedo, M. G. (1980). Copper and the synthesis of elastin and collagen. *Ciba Found. Symp.*, **79**, 163–182.

Haut, R. C., Lancaster, R. L., and DeCamp, C. E. (1992). Mechanical properties of the canine patellar tendon: some correlations with age and the content of collagen. *J. Biomech.*, **25**(2), 163–173.

Higgins, S. P., Solan, A. K., and Niklason, L. E. (2003). Effects of polyglycolic acid on porcine smooth muscle cell growth and differentiation. *J. Biomedical Material Research A*, **67**, 295–302.

Hinz, B. (2006). Masters and servants of the force: the role of matrix adhesions in myofibroblast force perception and transmission. *Eur. J. Cell Biology*, **85**, 175–181.

Hoerstrup, S. P., Sodian, R., Daebritz, S., Wang, J., Bacha, E. A., Martin, D. P., Moran, A. M., Guleresian, J., Sperling, J. S., Kaushal, S., Vacanti, J. P., Schoen, F. J., and Mayer, J. E. (2000). Functional living trileaflet heart valves grown in vitro. *Circulation*, **102**, III49–III49.

Hoerstrup, S. P., Kadner, A., Melnitchouk, S., Trojan, A., Eid, K., Tracy, J., Sodian, R., Visjager, J. F., Kolb, S. A., Grunenfelder, J., Zund, G., and Turina, M. I. (2002). Tissue engineering of functional trileaflet heart valves from human marrow stromal cells. *Circulation*, **106**, I143–I150.

Hoglund, A., Hakkarainen, M., and Albertsson, A. (2007). Degradation profile of poly(-caprolactone)-the influence of macroscopic and macromolecular biomaterial design. *Journal of Macromolecular Science, Part A*, **44**(9), 1041–1046.

Holzapfel, G. A., Gasser, T. C., and Ogden, R. W. (2000). A new constitutive framework for arterial wall mechanics and a comparative study of material models. *Journal of elasticity*, **61**, 1–48.

Hopkins, R. A. (2005). Tissue engineering of heart valves: decellularized valve scaffolds. *Circulation*, **111**(21), 2712–2714.

Horino, Y., Takahashi, S., Miura, T., and Takahashi, Y. (2002). Prolonged hypoxia accelerates the posttranscriptional process of collagen synthesis in cultured fibroblasts. *Life Sciences*, **71**(26), 3031–3045.

Hosokawa, R., Nonaka, K., Morifuji, M., Shum, L., and Ohishi, M. (2003). Tgf-beta 3 decreases type i collagen and scarring after labioplasty. *J. Dent. Res.*, **82**(7), 558–564.

Hulmes, D. (1992). The collagen superfamily–diverse structures and assemblies. *Essays Biochemistry*, **27**, 49–67.

Hulmes, D. (2002). Building collagen molecules, fibrils, and suprafibrillar structures. a review. *Journal of Structural Biology*, **137**(1-2), 2–10.

Jamieson, W. R. (1993). Modern cardiac valve devices–bioprostheses and mechanical prostheses: state of the art. *J. Card Surg.*, **8**(1), 89–98.

Jenniskens, Y., Koevoet, W., de Bart, A., Weinans, H., Jahr, H., and Verhaar, J. (2006). Biochemical and functional modulation of the cartilage collagen network by igf1, tgfbeta2 and fgf2. *Osteoarthritis Cartilage*, **14**(11), 1136–1146.

Jr., E. L. H., E., C. R., H., C. L., L., G. G., C., M. D., and D., W. R. (1996). Guidelines for reporting morbidity and mortality after cardiac valvular operations. ad hoc liaison committee for standardizing definitions of prosthetic heart valve morbidity of the american association for thoracic surgery and the society of thoracic surgeons. *J. Thorac. Cardiovasc. Surg.*, **112**(3), 708–711.

Kadler, K. (1995). Extracellular matrix 1: Fibril-forming collagens. *Protein Profile.*, **2**(5), 491–619.

Kadler, K. E., Holmes, D. F., Trotter, J. A., and Chapman, J. A. (1996). Collagen fibril formation. *Biochem J.*, **316**(Pt 1), 1–11.

Kinbara, T., Shirasaki, F., Kawara, S., Inagaki, Y., de Crombrugghe, B., and Takehara, K. (2002). Transforming growth factor-beta isoforms differently stimulate proalpha2 (i) collagen gene expression during wound healing process in transgenic mice. *J. Cell Physiol*, **190**(3), 375–381.

Kivirikko, K. I. and Pihlajaniemi, T. (1998). Collagen hydroxylases and the protein disulfide isomerase subunit of prolyl 4-hydroxylases. *Adv. Enzymol. Relat Areas Mol. Biol.*, **72**, 325–398.

Klouda, L., Vaz, C. M., Mol, A., Baaijens, F. P. T., and Bouten, C. V. C. (2007). Effect or biomimetic conditions on mechanical and structural integrity of pga/p4hb and electrospun pcl scaffolds. *Journal of Material Science: Materials in Medicine*, **In press**.

Knight, R. and Collins, S. (2001). Human prion diseases: cause, clinical and diagnostic aspects. *Contrib. Microbiol.*, **7**, 68–92.

Kolpakov, V., Rekhter, M. D., Gordon, D., Wang, W. H., and Kulik, T. J. (1995). Effect of mechanical forces on growth and matrix protein synthesis in the in-vitro pulmonary artery. analysis of the role of individual cell types. *Circulation research*, **77**, 823–831.

Kortsmit, J., Rutten, M. C. M., and Baaijens, F. P. T. (2006). *Non-invasive assessment of leaflet deformation in heart valve tissue engineering*. Proceedings of the 5th World Congress of Biomechanics 2006, Munich, Germany.

Krombach, F., Munzing, S., Allmeling, A. M., Gerlach, J. T., Behr, J., and Dorger, M. (1997). Cell size of alveolar macrophages: an interspecies comparison. *Environ. Health Perspect.*, **105 Suppl 5**, 1261–1263.

Kubota, K., Okazaki, J., Louie, O., Kent, K. C., and Liu, B. (2003). Tgf-beta stimulates collagen (i) in vascular smooth muscle cells via a short element in the proximal collagen promoter. *J. Surg. Res.*, **109**(1), 43–50.

Kunzelman, K. S., Cochran, R. P., Murphree, S. S., Ring, W. S., Verrier, E. D., and Eberhart, R. C. (1993). Differential collagen distribution in the mitral valve and its influence on biomechanical behaviour. *J. Heart Valve Dis.*, **2**(2), 236–244.

Kwon, I. K., Kidoaki, S., and Matsuda, T. (2005). Electrospun nano- to microfiber fabrics made of biodegradable copolyesters: structural characteristics, mechanical properties and cell adhesion potential. *Biomaterials*, **26**(18), 3929–3939.

Lam, E., Tredget, E. E., Marcoux, Y., Li, Y., and Ghahary, A. (2004). Insulin suppresses collagenase stimulatory effect of stratifin in dermal fibroblasts. *Mol. Cell Biochem.*, **266**(1-2), 167–174.

Langdon, S. (1999). Biaxial mechanical/structural effects of equibiaxial strain during crosslinking of bovine pericardial xenograft materials. *Biomaterials*, **20**(2), 137–153.

Langer, R. and Vacanti, J. (1993). Tissue engineering. *Science*, **260**, 920–926.

Leivonen, S. K. and Kahari, V. M. (2007). Transforming growth factor-beta signaling in cancer invasion and metastasis. *Int. J. Cancer*, **121**(10), 2119–2124.

Li, J., Luo, X. Y., and Kuang, Z. B. (2001). A nonlinear anisotropic model for porcine aortic heart valves. *Journal of biomechanics*, **34**, 1279–1289.

Li, W. J., Laurencin, C. T., Caterson, E. J., Tuan, R. S., and Ko, F. K. (2002). Electrospun nanofibrous structure: a novel scaffold for tissue engineering. *Journal of Biomedial Materials Research*, **60**, 613621.

Li, W. J., J. A. Cooper, J., Mauck, R. L., and Tuan, R. S. (2006). Fabrication and characterization of six electrospun poly(alpha-hydroxy ester)-based fibrous scaffolds for tissue engineering applications. *Acta Biomateralia*, **2**(4), 377–385.

Liao, J. and Vesely, I. (2003). A structural basis for the size-related mechanical properties of mitral valve chordae tendineae. *Journal of biomechanics*, **36**, 1125–1133.

Lijnen, P., Petrov, V., Rumilla, K., and Fagard, R. (2003). Transforming growth factor-beta 1 promotes contraction of collagen gel by cardiac fibroblasts through their differentiation into myofibroblasts. *Methods Find. Exp. Clin. Pharmacol.*, **25**(2), 79–86.

Lis, Y., Burleigh, M. C., Parker, D. J., Child, A. H., Hogg, J., and Davies, M. J. (1987). Biochemical characterization of individual normal, floppy and rheumatic human mitral valves. *Biochem. J.*, **244**(3), 597–603.

Long, J. L. and Tranquillo, R. T. (2003). Elastic fiber production in cardiovascular tissue-equivalents. *Matrix Biology*, **22**(4), 339–350.

Martelli-Junior, H., Cotrim, P., Graner, E., Sauk, J. J., and Coletta, R. D. (2003). Effect of transforming growth factor-beta1, interleukin-6, and interferon-gamma on the expression of type i collagen, heat shock protein 47, matrix metalloproteinase (mmp)-1 and mmp-2 by fibroblasts from normal gingiva and hereditary gingival fibromatosis. *J. Periodontol.*, **74**(3), 296–306.

McDonald, P. (2002). The challenge of defining normality for human mitral and aortic valves. geometrical and compositional analysis. *Cardiovascular Pathology*, **11**(4), 193–209.

Mendelson, K. and Schoen, F. (2006). Heart valve tissue engineering: Concepts, approaches, progress, and challenges. *Annals of Biomedical Engineering*, **34**(12), 1799–1819.

Merryman, W., Youn, I., Lukoff, H., Krueger, P., Guilak, F., Hopkins, R., and Sacks, M. (2006). Correlation between heart valve interstitial cell stiffness and transvalvular pressure: implications for collagen biosynthesis. *Am J Physiol Heart Circ Physiol.*, **290**(1), H224–H231.

Michna, H. and Hartmann, G. (1989). Adaptation of tendon collagen to exercise. *International Orthopaedics*, **13**(3), 161–165.

Mio, K., Yamashita, M., Odake, Y., Tamai, H., and Takada, K. (2001). Coenzyme a stimulates collagen production in cultured fibroblasts; possible mechanisms in enzymatic and gene expression. *Arch. Dermatol. Res.*, **293**(10), 522–531.

Mol, A. (2005). *Functional tissue engineering of human heart valve leaflets*. Ph-D thesis, Technische Universiteit Eindhoven.

Mol, A., Bouten, C. V. C., Zund, G., Guenter, C. I., Visjager, J. F., Turina, M., Baaijens, F. P. T., and Hoerstrup, S. P. (2003). The relevance of large strains in functional tissue engineering of heart valves. *Thoracic and cardiovascular surgeon*, **51**, 78–83.

Mol, A., van Lieshout, M. I., de Veen, G. C. D., Neuenschwander, S., Hoerstrup, S. P., Baaijens, F. P. T., and Bouten, C. V. C. (2005a). Fibrin as a cell carrier in cardiovascular tissue engineering applications. *Biomaterials*, **26**, 3113–3121.

Mol, A., Driessen, N. J. B., Rutten, M. C. M., Hoerstrup, S. P., Bouten, C. V. C., and Baaijens, F. P. T. (2005b). Tissue engineering of human heart valve leaflets: a novel bioreactor for a strain-based conditioning approach. *Annals of biomedical engineering*, **33**, 1778–1788.

Mol, A., Rutten, M. C. M., Driessen, N. J. B., Bouten, C. V. C., Zund, G., Baaijens, F. P. T., and Hoerstrup, S. P. (2006). Autologous human tissue-engineered heart valves: prospects for systemic applications. *Circulation*, **114**, I152–I160.

Moussavi-Harami, F., Duwayri, Y., Martin, J. A., Moussavi-Harami, F., and Buckwalter, J. A. (2004). Oxygen effects on senescence in chondrocytes and mesenchymal stem cells: consequences for tissue engineering. *Iowa Orthop. J.*, **24**, 15–20.

Naito, H., Melnychenko, I., Didie, M., Schneiderbanger, K., Schubert, P., Rosenkranz, S., Eschenhagen, T., and Zimmermann, W. H. (2006). Optimizing engineered heart tissue for therapeutic applications as surrogate heart muscle. *Circulation*, **114**(1 Suppl), I72–I78.

Neidert, M. R., Lee, E. S., Oegema, T. R., and Tranquillo, R. T. (2002). Enhanced fibrin remodeling in vitro with tgf-beta1, insulin and plasmin for improved tissue-equivalents. *Biomaterials*, **23**, 3717–3731.

Opitz, F., Schenke-Layland, K., Richter, W., Martin, D. P., Degenkolbe, I., Wahlers, T., and Stock, U. A. (2004). Tissue engineering of ovine aortic blood vessel substitutes using applied shear stress and enzymatically derived vascular smooth muscle cells. *Ann. Biomed. Eng*, **32**(2), 212–222.

Parry, D. (1988). The molecular fibrillar structure of collagen and its relationship to the mechanical properties of connective tissue. *Biophysical Chemistry*, **29**(1), 195–209.

Parry, D., Barnes, G., and Craig, A. (1978). A comparison of the size distribution of collagen fibrils in connective tissues as a function of age and a possible relation between fibril size distribution and mechanical properties. *Proc R Soc Lond B Biol Sci*, **203**(1152), 305–321.

Patel, A., Fine, B., Sandig, M., and Mequanint, K. (2006). Elastin biosynthesis: The missing link in tissue-engineered blood vessels. *Cardiovascular Research*, **71**(1), 40–49.

Paul, R. and Bailey, A. (2003). Chemical stabilisation of collagen as a biomimetic. *TheScientificWorldJournal*, **3**, 138–155.

Pham, Q. P., Sharma, U., and Mikos, A. G. (2006a). Electrospinning of polymeric nanofibers for tissue engineering applications: a review. *Tissue Engineering*, **12**(5), 1197–1211.

Pham, Q. P., Sharma, U., and Mikos, A. G. (2006b). Electrospun poly(-caprolactone) microfiber and multilayer nanofiber/microfiber scaffolds: Characterization of scaffolds and measurement of cellular infiltration. *Biomacromolecules*, **7**(10), 2796 – 2805.

Phillips, C. L., Combs, S. B., and Pinnell, S. R. (1994). Effects of ascorbic acid on proliferation and collagen synthesis in relation to the donor age of human dermal fibroblasts. *J. Invest Dermatol.*, **103**(2), 228–232.

Rabkin, E. and Schoen, F. J. (2002). Cardiovascular tissue engineering. *Cardiovascular pathology*, **11**, 305–317.

Reipschlager, A. and Portner, H. O. (1996). Metabolic depression during environmental stress: the role of extracellular versus intracellular ph in sipunculus nudus. *Journal of Experimental Biology*, **199**(Pt 8), 1801–1807.

Reneker, D. H. and Chun, I. (1996). Nanometre diameter of polymer, produced by electrospinning. *Nanotechnology*, **7**, 216223.

Robins, S. P., Duncan, A., Wilson, N., and Evans, B. J. (1996). Standardization of pyridinium crosslinks, pyridinoline and deoxypyridinoline, for use as biochemical markers of collagen degradation. *Clinical Chemistry*, **42**(10), 1621–1626.

Ross, J. J. and Tranquillo, R. T. (2003). Ecm gene expression correlates with in vitro tissue growth and development in fibrin gel remodeled by neonatal smooth muscle cells. *Matrix Biology*, **22**(6), 477–490.

Sacks, M. S., Smith, D. B., and Hiester, E. D. (1997). A small angle light scattering device for planar connective tissue microstructural analysis. *Annals of biomedical engineering*, **25**, 678–689.

Sacks, M. S., Smith, D. B., and Hiester, E. D. (1998). The aortic valve microstructure: effects of transvalvular pressure. *Journal of biomedical materials research*, **41**, 131–141.

Saini, S. and Wick, T. M. (2004). Effect of low oxygen tension on tissue-engineered cartilage construct development in the concentric cylinder bioreactor. *Tissue Engineering*, **10**(5-6), 825–832.

Sanders, J. and Goldstein, B. (2001). Collagen fibril diameters increase and fibril densities decrease in skin subjected to repetitive compressive and shear stresses. *J Biomech*, **34**(12), 1581–1587.

Sauren, A. A. H. J., Kuijpers, W., van Steenhoven, A. A., and Veldpaus, F. E. (1980). Aortic valve histology and its relation with mechanics - preliminary report. *Journal of biomechanics*, **13**, 97–104.

Schenke-Layland, K., Riemann, I., Opitz, F., Konig, K., Halbhuber, K. J., and Stock, U. A. (2004). Comparative study of cellular and extracellular matrix composition of native and tissue engineered heart valves. *Matrix Biol.*, **23**(2), 113–125.

Scherer, K., Schunke, M., Sellckau, R., Hassenpflug, J., and Kurz, B. (2004). The influence of oxygen and hydrostatic pressure on articular chondrocytes and adherent bone marrow cells in vitro. *Biorheology*, **41**(3-4), 323–333.

Schmidt, D., Mol, A., Neuenschwander, S., Breymann, C., Gossi, M., Zund, G., Turina, M., and Hoerstrup, S. P. (2005). Living patches engineered from human umbilical cord derived fibroblasts and endothelial progenitor cells. *Eur. J. Cardiothorac. Surg.*, **27**(5), 795–800.

Schmidt, D., Mol, A., Breymann, C., Achermann, J., Odermatt, B., Gossi, M., Neuenschwander, S., Pretre, R., Genoni, M., Zund, G., and Hoerstrup, S. P. (2006). Living autologous heart valves engineered from human prenatally harvested progenitors. *Circulation*, **114**(1 Suppl), I125–I131.

Schmidt, D., Achermann, J., Odermatt, B., Breymann, C., Mol, A., Genoni, M., Zund, G., and Hoerstrup, S. P. (2007). Prenatally fabricated autologous human living heart valves based on amniotic fluid derived progenitor cells as single cell source. *Circulation*, **116**(11 Suppl), I64–I70.

Schnell, A. M., Hoerstrup, S. P., Zund, G., Kolb, S., Sodian, R., Visjager, J. F., Grunenfelder, J., Suter, A., and Turina, M. (2001). Optimal cell source for cardiovascular tissue engineering: venous vs. aortic human myofibroblasts. *Thoracic and Cardiovascular Surgery*, **49**(4), 221–225.

Schoen, F. J. (1997). Aortic valve structure-function correlations: role of elastic fibers no longer a stretch of the imagination. *Journal of heart valve disease*, **6**, 1–6.

Schoen, F. J. and Levy, R. J. (1999). Tissue heart valves: current challenges and future research perspectives. *Journal of biomedical materials research*, **47**, 439–465.

Shanley, C. J., Gharaee-Kermani, M., Sarkar, R., Welling, T. H., Kriegel, A., Ford, J. W., Stanley, J. C., and Phan, S. H. (1997). Transforming growth factor-beta 1 increases lysyl oxidase enzyme activity and mrna in rat aortic smooth muscle cells. *J. Vasc. Surg.*, **25**(3), 446–452.

Shinoka, T., Breuer, C. K., Tanel, R. E., Zund, G., Miura, T., Ma, P. X., Langer, R., Vacanti, J. P., and Mayer, J. E. (1995). Tissue engineering of heart valves: valve replacement study in a lamb model. *Annals of thoracic surgery*, **60**, S513–516.

Siegel, R. (1976). Collagen cross-linking; synthesis of collagen cross-links in vitro with highly purified lysyl oxidase. *Journal of Biological Chemistry*, **251**(18), 5786–5792.

Sodian, R., Hoerstrup, S. P., Sperling, J. S., Daebritz, S., Martin, D. P., Moran, A. M., Kim, B. S., Schoen, F. J., Vacanti, J. P., and Mayer, J. E. (2000). Early in-vivo experience with tissue-engineered trileaflet heart valves. *Circulation*, **102**, III22–III29.

Stradins, P., Lacis, R., Ozolanta, I., Purina, B., Ose, V., Feldmane, L., and Kasyanov, V. (2004). Comparison of biomechanical properties and structural properties between human aortic and pulmonary valve. *European journal of cardiothoracic surgery*, **26**, 634–639.

Subbiah, T., Bhat, G., Tock, R., Parameswaran, S., and Ramkumar, S. (2005). Electrospinning of nanofibers. *Journal of Applied Polymer Science*, **96**, 557–569.

Sung, H. (2003). Cross-linking of biological tissues using genipin and/or carbodiimide. *Journal of Biomedical Material Research*, **64A**(3), 427–438.

Tokudome, T., Horio, T., Yoshihara, F., Suga, S., Kawano, Y., Kohno, M., and Kangawa, K. (2004). Direct effects of high glucose and insulin on protein synthesis in cultured cardiac myocytes and dna and collagen synthesis in cardiac fibroblasts. *Metabolism*, **53**(6), 710–715.

Torp, S., Baer, E., and Friedman, B. (1975). Effects of age and of mechanical deformation on the ultrastructure of tendon. *Structure of fibrous biopolymers*, **26**, 223–250.

van der Slot, A. J., van Dura, E. A., de Wit, E. C., Groot, J. D., Huizinga, T. W., Bank, R. A., and Zuurmond, A. M. (2005). Elevated formation of pyridinoline cross-links by profibrotic cytokines is associated with enhanced lysyl hydroxylase 2b levels. *Biochim. Biophys. Acta*, **1741**(1-2), 95–102.

van Lieshout, M. I., Vaz, C. M., Rutten, M. C., Peters, G. W., and Baaijens, F. P. (2006). Electrospinning versus knitting: two scaffolds for tissue engineering of the aortic valve. *Journal of Biomaterial Science Polymer Edition*, **17**(1-2), 77–89.

Vara, D., Salacinski, H., Kannan, R., Bordenave, L., Hamilton, G., and Seifalian, A. (2005). Cardiovascular tissue engineering: state of the art. *Pathol Biol*, **53**, 599–612.

Vaz, C. M., van Tuijl, S., Bouten, C. V. C., and Baaijens, F. P. T. (2005). Design of scaffolds for blood vessel tissue engineering using a multi-layering electrospinning technique. *Acta Biomaterialia*, **1**(5), 575–582.

Vesely, I. (1998). The role of elastin in aortic valve mechanics. *Journal of biomechanics*, **31**, 115–123.

Wang, D. W., Fermor, B., Gimble, J. M., Awad, H. A., and Guilak, F. (2005). Influence of oxygen on the proliferation and metabolism of adipose derived adult stem cells. *J. Cell Physiol*, **204**(1), 184–191.

Williams, C., Johnson, S. L., Robinson, P. S., and Tranquillo, R. T. (2006). Cell sourcing and culture conditions for fibrin-based valve constructs. *Tissue Engineering*, **12**(6), 1489–1502.

Wong, M., Siegrist, M., Gaschen, V., Park, Y., Graber, W., and Studer, D. (2002). Collagen fibrillogenesis by chondrocytes in alginate. *Tissue Engineering*, **8**(6), 979–987.

Wu, M. H., Urban, J. P., Cui, Z. F., Cui, Z., and Xu, X. (2007). Effect of extracellular ph on matrix synthesis by chondrocytes in 3d agarose gel. *Biotechnol. Prog.*, **23**(2), 430–434.

Yacoub, M. H., Kilner, P. J., Birks, E. J., and Misfeld, M. (1999). The aortic outflow and root: a tale of dynamism and crosstalk. *Ann. Thorac. Surg.*, **68**(3 Suppl), S37–S43.

Yoshimoto, H., Shin, Y. M., Terai, H., and Vacanti, J. P. (2003). A biodegradable nanofiber scaffold by electrospinning and its potential for bone tissue engineering. *Biomaterials*, **24**(12), 2077–2082.

Zalewski, A., Shi, Y., and Johnson, A. G. (2002). Diverse origin of intimal cells: smooth muscle cells, myofibroblasts, fibroblasts, and beyond? *Circ. Res.*, **91**(8), 652–655.

Zhu, Y., Leong, M. F., Ong, W. F., Chan-Park, M. B., and Chian, K. S. (2007). Esophageal epithelium regeneration on fibronectin grafted poly(l-lactide-co-caprolactone) (pllc) nanofiber scaffold. *Biomaterials*, **28**(5), 861–868.

Zimmermann, W. H., Schneiderbanger, K., Schubert, P., Didie, M., Munzel, F., Heubach, J. F., Kostin, S., Neuhuber, W. L., and Eschenhagen, T. (2002). Tissue engineering of a differentiated cardiac muscle construct. *Circ. Res.*, **90**(2), 223–230.

Samenvatting

Een veelvoorkomende behandelmethode ter verbetering van de klepfunctie bij vergevorderde hartklepziekten, is een hartklepvervanging. Hoewel huidige klepvervangingen in de vorm van mechanische of biologische prothesen relatief goed functioneren, brengen deze kleppen aanzienlijke risico's en nadelen met zich mee. Een belangrijke tekortkoming van huidige hartklepprothesen, in het bijzonder voor kinderen, is dat deze niet meegroeien, zich aanpassen of repareren, zoals natuurlijk weefsel dat doet. Om deze reden wordt de multidisciplinaire aanpak van tissue engineering als veelbelovende techniek gezien voor een nieuwe generatie hartklepprothesen. Het concept van tissue engineering is gebaseerd op het zaaien van patiënt-eigen cellen op een biodegradeerbaar dragermateriaal, dat vervolgens wordt gestimuleerd om te groeien en ontwikkelen in een fysiologische kweekomgeving. Hiermee kan nieuw levend weefsel in de vorm van een hartklep worden gemaakt dat als vervanging kan dienen voor de zieke hartklep. Deze nieuwe prothese is lichaamseigen, en zal daarom geen afstotingsreacties met zich mee brengen. Bovendien is het levend weefsel dat mee kan groeien en dat zich kan aanpassen aan veranderingen. Hoewel succesvolle implantaties van gekweekte hartkleppen hebben plaatsgevonden in dierstudies aan de pulmonaire positie van het hart, waren deze kleppen nog niet voldoende sterk voor de aorta positie. Daarom is een belangrijke uitdaging in het kweken van functionele hartkleppen het nabootsen van de eigenschappen van natuurlijke hartkleppen, die het duurzaam functioneren in het lichaam waarborgen.

Een belangrijke vraag voor toekomstige klinische toepassingen bij patiënten is: Hoe goed is goed genoeg voor succesvolle implantatie van tissue-engineerde hartkleppen? Het eerste doel van dit werk was het definiëren van kwalitatieve en kwantitatieve criteria om te kunnen bepalen wanneer deze klepvervangingen geschikt zijn voor implantatie in patiënten. In dit proefschrift werden deze criteria gebaseerd op mechanische en structurele eigenschappen van gezonde humane volwassen aortakleppen. In natuurlijke kleppen is de collageenvezel architectuur de belangrijkste matrixcomponent die verantwoordelijk is voor het dragen van de hoge drukbelasting in de aorta. Derhalve is kennis over de functie van collageen in relatie met het mechanische gedrag van natuurlijk hartklepweefsel een belangrijke onderzoeksfocus geweest om criteria te kunnen definiëren voor tissue-engineerde hartkleppen.
De relatie tussen mechanische eigenschappen en collageen organisatie (hoeveelheid, mate van cross-linking, en fibril morfologie) werd bestudeerd in humane aortakleppen op globaal en locaal niveau. Vervolgens werden de mechanische eigenschap-

pen van de kleppen, verkregen door middel van trekproeven, gecorreleerd aan collageengerelateerde parameters (i.e., relatieve hoeveelheid en cross-link concentratie). Hieruit volgde dat collageen cross-links, in tegenstelling tot de hoeveelheid collageen, sterk gecorreleerd bleek aan de weefselstijfheid in de humane aortakleppen. Door deze bevindingen is het aandachtsgebied ter verbetering van de mechanische integriteit van gekweekte weefsels specifieker gericht op de relevantie van cross-links. Een andere kwestie die in het onderzoek aan de orde kwam was de vraag hoe en in welke mate mechanische belasten de collageen fibrilmorfologie benvloedt. Om te bepalen hoe locale spanningen de collageen fibril diameter, de diameterverdeling, en de fibrildichtheid benvloeden, werden deze parameters bestudeerd in humane aortakleppen met behulp van transmissie elektronen microscopie. Het mechanische gedrag van de kleppen werd gemplementeerd in een mathematisch model om de spanningsverdeling in de klepvliesjes te voorspellen tijdens maximale fysiologische belasting. De resultaten hiervan toonden aan dat hoge spanningen in het weefsel geassocieerd waren met dikkere fibrillen, een lagere fibrildichtheid en een grotere spreiding in fibrildiameter. Deze bevindingen brengen inzicht in het effect van mechanisch belasten op de collageen architectuur, en zijn derhalve waardevol voor het optimaliseren van mechanische conditioneringsprotocollen voor tissue engineering van hartkleppen.

Het tweede doel van dit proefschrift was het verbeteren van de mechanische eigenschappen van gekweekte weefsels richting de karakteristieken van natuurlijke humane aortakleppen. Deze karakteristieken werden beschouwd als objectieve criteria voor tissue-engineerde kleppen. Twee strategieën zijn toegepast in het tissue engineering protocol om dit te bereiken. De eerste aanpak had betrekking op een aanpassing van het scaffold design met als doel een langdurige mechanische ondersteuning in de gekweekte weefsels. Het scaffold materiaal wat op dit moment gebruikt wordt is een netwerk van een snel afbreekbaar polymeer (polyglycolic acid gecoat met poly-4-hydroxybutyrate - PGA-P4HB). Dit materiaal breekt binnen enkele weken af, en zal hierdoor geen mechanische steun geven na implantatie. Aangezien sommige tissue engineering toepassingen deze scaffold ondersteuning juist nodig hebben, is de geschiktheid van een langzaam degraderende polymeer scaffold- gemaakt van electrogesponnen poly-ε-caprolactone (PCL)- geëvalueerd voor cardiovasculaire tissue engineering, en vergeleken met de PGA-P4HB scaffold. Na optimalisatie van de electrogesponnen PCL scaffold bleek deze goede celingroei en biosynthese van extracellulaire matrix te vertonen, terwijl de elastische eigenschappen en mechanische integriteit behouden bleef. De electrogesponnen PCL scaffolds bleken veelbelovende alternatieven op PGA-P4HB scaffolds, in het bijzonder voor tissue-engineerde bloedvaten en de wand van een gekweekte aortaklep, alwaar mechanische ondersteuning voor langere duur gewenst is. De tweede aanpak ter verbetering van de mechanische sterkte van de gekweekte hartkleppen, was gericht op het stimuleren van weefselgroei en ontwikkeling door middel van biochemische impulsen. Na een evaluatie van biochemische factoren, bekend van hun stimulerende effect op eiwitsynthese in vivo of in vitro, zijn insuline en hypoxia gekozen voor lange termijn tissue engineering experimenten. Een fysiologisch relevante zuurstofspanning, aanzienlijk lager dan tot dan toe gebruikt in experimenten, en insuline supplementen werden gebruikt tijdens

de groei van hartklepweefsel om de sterkte hiervan te verbeteren. Zowel insuline als hypoxia waren verantwoordelijk voor meer matrixproductie en betere mechanische eigenschappen, maar een synergistisch effect werd niet waargenomen. Hoewel de hoeveelheid collageen en cross-links in de gekweekte weefsels nog lager waren dan in natuurlijke humane hartkleppen na vier weken kweken, bleken de weefsels gekweekt onder hypoxische condities de sterkte en stijfheid van natuurlijke kleppen geëvenaard te hebben. De hypoxisch gekweekte weefsels waren zelfs tweemaal zo sterk en stijf als de weefsels gekweekt met normale lucht. Deze resultaten impliceren dat zuurstofspanning een cruciale parameter is om de mechanische eigenschappen criteria van natuurlijke kleppen te behalen in tissue-engineerde hartkleppen. Gekweekte weefsels, gebaseerd op een snel degraderende scaffold, met deze sterkte waren tot nu toe niet behaald. Deze bevindingen brengen de toepassing van een gekweekte aortaklep dichterbij, en kunnen worden beschouwd als een belangrijke stap in hartklep tissue engineering.

Dankwoord

Hoewel promoveren een individuele prestatie is, is het niet iets wat je in je eentje volbrengt. Nu het er dan echt bijna op zit, wil ik graag een aantal mensen bedanken die hebben bijgedragen aan het ontstaan van dit boekje.
Allereerst wil ik hier mijn twee copromotoren bedanken; Carlijn, je enthousiasme en positief kritische houding ten opzichte van het onderzoek werkten aanstekelijk op mij. Ondanks je tijdelijke afwezigheid heb je me in de 'schrijffase' super geholpen. Zowel persoonlijk als in je rol als coach en begeleider heb ik je altijd enorm gewaardeerd. Anita, jij bent in de laatste fase van mijn promotie (enigszins uit nood) mijn begeleider geworden, waar ik erg blij mee was. Ik kon bij jou altijd binnenlopen, of dit nu voor advies, een kritische blik, of gewoon een gezellig gesprek was. Uiteraard wil ik hier ook mijn promotor noemen. Frank, ik haalde inspiratie uit je vele ideeën en je vooruitziende blik in het onderzoek. Bovendien liet je me vrij om mijn eigen weg te vinden in mijn project, dit vond ik erg prettig.
Er zijn ook een aantal mensen van buiten de universiteit die in mijn promotieonderzoek een belangrijke rol hebben gespeeld. Ruud Bank, ik wil je bedanken voor de mogelijkheid die je hebt geboden om een vruchtbare samenwerking op te zetten tussen de TU/e en jouw groep bij TNO. Je inbreng is erg waardevol geweest, niet alleen voor mijn promotiewerk, maar voor het gehele hartklep-onderzoek. Ik heb er vertrouwen in dat deze samenwerking een blijvende zal zijn. Ook Jessica Snabel van TNO, heel erg bedankt voor al het labwerk dat je voor me verricht hebt! Ad Bogers en Sjors van Kats van de Nederlandse hartkleppenbank in Rotterdam, het onderzoek naar natuurlijke hartkleppen is voor dit project een belangrijke stap geweest naar een toekomstige klinische toepassing van tissue-engineerde hartklep-prothesen. Ik wil jullie bedanken voor jullie vertrouwen en bereidwilligheid hieraan mee te werken. De initiator van deze samenwerking was Bas de Mol. Dank je wel! De electronenmicroscopische analyses waren niet mogelijk geweest zonder de intensieve hulp van Fons Verheijen van de Universiteit Maastricht. Veel dank hiervoor! My Swiss colleagues, I very much appreciated your critical but positive feedback on my research from a more clinical perspective. The annual trips to Switzerland were always a great success, both from a scientific as a personal point of view.
En dan mijn collegaatjes op vloer vier van w-hoog... Wat was het super om te werken met zo'n leuke club mensen! De collageen/hartkleppen-groep bestaande uit Mirjam, Martijn, Rolf, Ralf, Niels, Anita, Anita, Petra, Mieke, Moniek, Maria, Marjolein, Marijke en Jeroen, bedankt voor jullie gezelligheid en fijne samenwerking. Ik hoop nog

regelmatig een biertje met jullie te kunnen drinken! Patrick, Leo, Marleen, Yvon en Alice, bedankt dat jullie altijd klaarstonden voor hulp. Tijdens mijn promotie heb ik meerdere studenten mogen begeleiden tijdens hun stage, studentassistentschap of afstuderen. Joep, Mieke, Renate en Nicole: bedankt voor jullie bijdrage aan dit werk! Karlien, Julienne, Lisette, Mirjam en Debbie, onze 'meidenavonden' waren altijd supergezellig, en in de laatste periode vooral een hele fijne afwisseling van de stressvolle momenten. Maartje, Yvonne, en eigenlijk ook een beetje Sjoerd ;), jullie waren fijne kamergenoten, bedankt voor de leuke tijd!
Jeroen, Deb, Bart, Willie, Eef, Eef, Lex, Bram, Roos, Lars, Marielle, Sas, Jean, Tibi, Inge, Peer en Doreen, als oudste en dus de enige echte BMT-groep brengen jullie de nodige ontspanning en lol. Ik ben echt superblij dat we elkaar nog zo vaak zien, en de weekendjes, etentjes en ski-vakanties zijn altijd top!
Deb, al sinds de eerste dag van mijn studie zijn we de beste maatjes. Ook tijdens onze promotie was je er altijd om lief en leed mee te delen. Ik ga het missen om overdag met je te kletsen, maar dat moeten we dan maar in de avonden en weekenden inhalen! En dan mijn vriendinnetjes van de middelbare school, Vivian, Danielle en Lonneke, ondanks het minder frequente contact in vergelijking met vroeger blijft het altijd zo vertrouwd als ik jullie zie. Ik waardeer onze vriendschap ontzettend! Annie, Hans, Ad, Mirjam, Michiel, Jessica en Paul, steeds bleven jullie geïnteresseerd in de laatste vorderingen van mijn werk. Dank jullie wel hiervoor!
Syl, dank je wel voor al je steun, enthousiasme en positivisme. Een lievere zus kan ik me niet wensen. Pap en mam, jullie hebben mij altijd onvoorwaardelijk gesteund. Jullie hebben mij het perfecte voorbeeld gegeven om het beste uit mezelf te halen. Door jullie ben ik geworden wie ik ben.
Tot slot, lieve Jeroen, samen met jou kan ik de wereld aan. Zowel letterlijk tijdens een van onze exotische avonturen, als figuurlijk. Het was heel bijzonder en fijn om jou ook werk-gerelateerd zo dichtbij te hebben tijdens onze studie en promotie. Ik ben zo blij met jou!

Angelique Balguid,
Eindhoven, November 2007

Curriculum Vitae

Angelique Balguid is geboren op 13 juli 1979 in Berkel en Rodenrijs. In 1997 behaalde zij haar VWO diploma aan het Stedelijk College Den Hulster in Venlo. Aansluitend studeerde zij Biomedische Technologie aan de Technische Universiteit Eindhoven. Als onderdeel van deze studie heeft zij stage gelopen aan de University of California in San Francisco (USA). Hier deed ze onderzoek op het gebied van hartmechanica en -modellering, waarvoor zij de Dr. E. Dekker beurs van de Nederlandse Hartstichting heeft ontvangen. Haar afstudeerwerk richtte zich op het in kaart brengen van de schade die optreedt in kransslagaders tijdens een dotterbehandeling. In 2003 besloot zij promotieonderzoek te doen aan de faculteit Biomedische Technologie van de Technische Universiteit Eindhoven, resulterend in dit proefschrift.